NASA TECHNICAL MEMORANDUM

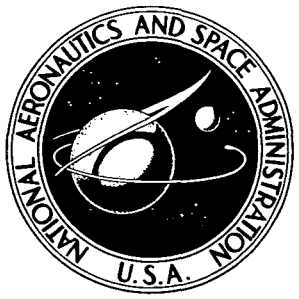

NASA TM X-3103

NASA TM X-3103

EFFECT OF ROTOR-TO-STATOR SPACING ON ACOUSTIC PERFORMANCE OF A FULL-SCALE FAN (QF-5) FOR TURBOFAN ENGINES

by Joseph R. Balombin and Edward G. Stakolich

Lewis Research Center
Cleveland, Ohio 44135

NATIONAL AERONAUTICS AND SPACE ADMINISTRATION • WASHINGTON, D. C. • SEPTEMBER 1974

1. Report No.	2. Government Accession No.	3. Recipient's Catalog No.
NASA TM X-3103		

4. Title and Subtitle	5. Report Date
EFFECT OF ROTOR-TO-STATOR SPACING ON ACOUSTIC PERFORMANCE OF A FULL-SCALE FAN (QF-5) FOR TURBOFAN ENGINES	SEPTEMBER 1974
	6. Performing Organization Code

7. Author(s)	8. Performing Organization Report No.
Joseph R. Balombin and Edward G. Stakolich	E-7879
	10. Work Unit No. 501-24

9. Performing Organization Name and Address	11. Contract or Grant No.
Lewis Research Center National Aeronautics and Space Administration Cleveland, Ohio 44135	

12. Sponsoring Agency Name and Address	13. Type of Report and Period Covered
National Aeronautics and Space Administration Washington, D.C. 20546	Technical Memorandum
	14. Sponsoring Agency Code

15. Supplementary Notes

16. Abstract

A study was made of the effect of increasing the fan rotor-to-stator spacing on the noise level of a full-scale, single-stage, 1.6-pressure-ratio fan. Noise data were obtained with axial spacings of 1.14, 1.65, and 2.27 rotor chord lengths. Over this spacing range, data indicate a reduction of 1.5 PNdB. Apparently, rotor-alone noise at the frequency at which the rotor-stator interaction noise was cut off limited the noise reduction for the QF-5 fan. It seems, however, that the reduction in sound power level with increases in spacing is potentially about 6 dB over the range of spacings tested.

17. Key Words (Suggested by Author(s))

Fan noise
Rotor-to-stator spacing
Noise reduction

18. Distribution Statement

Unclassified - unlimited
Category 01

19. Security Classif. (of this report)	20. Security Classif. (of this page)	21. No. of Pages	22. Price*
Unclassified	Unclassified	70	$3.75

* For sale by the National Technical Information Service, Springfield, Virginia 22151

EFFECT OF ROTOR-TO-STATOR SPACING ON ACOUSTIC PERFORMANCE OF A FULL-SCALE FAN (QF-5) FOR TURBOFAN ENGINES

by Joseph R. Balombin and Edward G. Stakolich

Lewis Research Center

SUMMARY

A study was conducted of the noise generation effects of the rotor-to-stator spacing on a 1.83-meter- (6-ft-) diameter fan suitable for turbofan engine application. This 1.6-pressure-ratio fan was run without inlet guide vanes, and the axial spacing between fan rotor and stator was varied between approximately 1 and 2 rotor chord lengths. Design values of tip speed and thrust are 332.5 meters per second (1090 ft/sec), and 84 500 newtons (19 000 lb), respectively. Changes in sound level and in radiation characteristics were compared for the fan fundamental tone and for higher harmonics. In the case of the fan fundamental tone, which was theoretically cut off, no reduction in noise level was observed. The remaining discrete-frequency power levels generally decreased at a rate of approximately 6 decibels per doubling of the axial separation between rotor and stator over the range of spacings tested, at constant tip speed. The actual reduction varied from tone to tone. The level of a "haystack" in the noise spectrum decreased at the same rate as did the higher fan harmonics. Overall sound power levels and maximum perceived noise levels were reduced by approximately 1.5 decibels at 85-percent speed.

Some measurements of the fan aerodynamic performance were made to check its performance in regards to pressure ratio and weight flow.

INTRODUCTION

In designing quiet engines for commercial aircraft, the most pressing acoustic objective has been to reduce the noise from the fan. Several techniques are being used and refined, while others are being researched. One of these partially exploited techniques has been to increase the spacing between the rotor and stator of a single-stage fan. Some studies (e.g., ref. 1) of the effects of spacing have been made, and reductions of

several decibels in the sound level of the blade-passage frequency tone have been demonstrated. Some uncertainty, though, remains as to the exact amount of the sound reduction with increases in spacing. A more complete knowledge of this relation for turbofans would be helpful in making the necessary trade-off between the lower noise and the weight or performance penalties that result from increasing the rotor-to-stator spacing.

A single-stage fan without inlet guide vanes was tested at the NASA Lewis Research Center to evaluate the effects of the spacing between rotor and stator. The following are some of the characteristics of this fan: diameter, 1.83 meters (6 ft); bypass ratio, 5.4; tip speed, 333 meters per second (1090 ft/sec); total pressure ratio, 1.6. Provision was made in the design to allow the fan (bypass) stator to be moved to obtain three axial separations; these separations allowed a doubling of rotor-to-stator spacing from approximately 1 to 2 rotor chord lengths. Also, the relative numbers of rotor blades and stator vanes were selected in accordance with the Tyler and Sofrin cutoff theory (ref. 2) so as to reduce the level of the fundamental tone propagated to the far field.

In the program described in this report, a study was made of the effect on fan noise of varying the fan rotor-to-stator spacing. The results were examined for the effects of the spacing on the total noise output of the fan and on the basic constituents of the fan noise. In this fan, the basic constituents of fan noise were the fan discrete tones, the broadband noise, and a broadband hump, or "haystack"; no multiple pure tones were observed. In operating this fan, an apparent change in bypass pressure ratio was observed; consequently, the results of a comparison at constant tip speed may include effects of a change in pressure ratio.

APPARATUS

Test Facility

The full-scale fan acoustic test facility is located in the open area adjacent to the main compressor and drive building of the 10- by 10-Foot Supersonic Wind Tunnel at the NASA Lewis Research Center. Figure 1(a) is a plan view of the area. The main drive motors of the 10- by 10-Foot Supersonic Wind Tunnel are used to drive the test fan through a speed-increasing gearbox, a reversing gearbox, and a series of drive-shaft extensions.

The main drive system consists of four 28 000-kilowatt (37 500-hp), wound-rotor induction motors in tandem for a total of 112 000 kilowatts (150 000 hp). The drive system has been modified by means of transfer switches which select one motor for driving the fan and allow two other motors to provide dynamic braking. Presently, a semiautomatic speed control is provided that holds fan speed to within 3 to 5 rpm over the operating speed range of 1750 to 3719 rpm.

The test fan is located on a concrete foundation, 33.5 meters (110 ft) from the wall of the building, and 5.8 meters (19 ft) above the ground level (fig. 1(b)). A concrete viaduct extends from the building wall to just short of the test-fan foundation and serves as a support for the drive-shaft bearing struts, the 4.25:1 speed-increasing gearbox, and the reversing gearbox. The drive shaft is enclosed in a 0.63-centimeter (0.25-in.) thick steel cover to reduce drive-shaft noise. The fan is positioned to exhaust away from the building to allow for unobstructed air discharge from the fan nacelle. Sixteen microphones mounted on poles at the elevation of the fan axis provide the far-field sound-sensing capability. All instrumentation equipment for the fan test facility is housed in the control room, which is located in the main drive building.

The noise characteristics of the fan test facility are described in appendix A.

Test Fan

The QF-5 fan is a full-scale fan originally intended for possible use in a 97 860-newton- (22 000-lb-) thrust, research turbofan aircraft engine. This 1.83-meter-(6-ft-) diameter, single-stage fan was designed without inlet guide vanes, to avoid wakes on the rotor and thus avoid a source of noise (ref. 3). The fan consists of a rotor with midspan dampers, a fan (bypass) stator, and a core stator. Both core and bypass flows are provided for in this fan. The most important performance design features for operation at cruise design conditions are listed in table I.

The three rotor-to-stator (bypass) spacings at which measurements were made were 1.14, 1.65, and 2.27 rotor chord lengths. The fan was designed to operate with the smallest spacing; the other two spacings were obtained as illustrated in figure 2, which shows the rotor-and-stator section of the fan assembly. To increase the spacing, the bypass stator was moved back from its design position, and spacers were added at the tip leading edge and removed from the hub trailing edge to maintain a similar flow passageway. Both the rotor and the core stator were unchanged in axial position. The reference rotor chord length of 0.19 meter (7.65 in.) was measured as the shortest distance between leading and trailing edges at midspan. The separation between rotor and stator was measured as the distance at midspan between the rotor trailing edge and the stator leading edge. An effective rotor-to-stator spacing can also be calculated. To do this, the projected distance along the rotor flow direction from rotor to stator is used instead of the axial separation between rotor and stator. For the QF-5 fan, the rotor-outlet relative air angle at the tip is 35°; with this value, the effective rotor-to-stator spacing corresponding to the quoted axial spacings of 1.14, 1.65, and 2.27 chords are 1.39, 2.01, and 2.77 chords, respectively. While provision had been made to locate the core stator at both 0.69 and 1.26 axial chords downstream of the rotor, only the closer position was used.

Some of the physical characteristics of the rotor and stators are given in table II. Figure 3 shows the fan rotor and stator. The fan velocity triangles at the entrances to and exits from the rotor blade and stator vanes at 80 and 100 percent, respectively, of cruise design corrected speed are specified in table III. This fan (designed by Pratt & Whitney Aircraft) incorporated a multiple circular arc airfoil for the fan rotor, and double circular arc airfoils for the bypass stator and the core stator.

Instrumentation

Aerodynamic measurements. - Some aerodynamic measurements were made of weight flow and pressure ratio in order to check the fan performance. The cutaway drawing of the fan installation (fig. 4) shows the relative size of the flow passageways and the locations of the instrumentation stations relative to the fan rotor and stators. Both the bypass-flow and the core-flow ducts are identified. Bypass performance data were obtained from station 3 instrumentation, and core performance data from station 4 instrumentation. Table IV lists the type of instrumentation located at each station. The actual arrangement of the taps is illustrated in figure 5.

In obtaining the aerodynamic data, each pressure and temperature value was, in turn, digitized and recorded on magnetic tape; from these taped data, calculations were later made. For each speed at which the fan was run, two samples of aerodynamic data were taken; each sample of data consisted of the average of the data from eight complete scans of the instrumentation located at each station.

Acoustic measurements. - Acoustic measurements were made outdoors on the horizontal centerline of the fan - 5.8 meters (19 ft) above ground. The 16 microphones were located 30.5 meters (100 ft) away from the fan, from 10° to 160°, in 10° increments (fig. 1); angles were measured from the fan inlet axis. In making the measurements, 1.3-centimeter- (1/2-in.-) diameter condenser microphones were used; these microphones have sensitivities of -60 decibels relative to 1 volt per 0.1 newton per square meter (1 volt per microbar). Frequency response of the system, as a whole, was uniform from 50 hertz to 20 kilohertz. The only known errors are those due to ground reflection; the 1/3 octave data were corrected for these errors.

Data reduction was accomplished in two ways. The first was the reduction on-line, during testing, of the noise signals into 1/3 octaves. This analysis was performed for each speed at which the fan was tested, and generally three samples of noise data were taken for each speed. The resulting 1/3 octave data were sequential 4-second rms linear time averages of the microphone signals. A block diagram of this system appears in figure 6. This diagram includes everything except the on-line analog magnetic tape recording of each microphone signal.

The second method of acoustic data reduction made use of a fine-resolution,

constant-bandwidth analyzer. This analysis was done off-line and was accomplished by playing back the analog noise tapes produced at the time of the test into the narrow-band analyzer and plotting the resulting spectra on an x-y recorder. The plots that were made generally present examinations of the noise data from 0 to 10 kilohertz, with a nominal 20-hertz resolution. In a few instances, analyses of a 2-kilohertz portion of the frequency spectrum, with a nominal resolution of 4 hertz, were also made. The analyzer used speed-up techniques to provide real-time analysis. In obtaining the data used in this report, linear time averages of about 50 seconds were used.

TEST PROCEDURE

The fan was operated over a range of speeds, and data were taken at several repeat speed points. The percent design corrected speed points at which the fan was tested were 60, 70, 80, and 85. A single point at 90 percent was taken, although fan operation over 85 percent speed was avoided to avoid the effect of a flow separation that occurred in the core duct at higher speeds. The fan was first cycled through these points three separate times, and acoustic data were taken at each point. After the acoustic data were taken, the three station 5 rakes were mounted in their positions at the nozzle exit (the other rakes were always mounted). Then the fan was twice cycled through its speed range, and 100 seconds of aerodynamic data were taken at each point.

One factor having an effect on the operation of this fan is what appears to have been flow separation in the fan core duct. Total pressure readings taken from one of the station 4 rakes in the core stream near the fan support pylon were about 7000 newtons per square meter (1 psi) less than ambient pressure, which indicated a local area of no flow or reverse flow. One problem with operating the fan in this condition was the damage to the sheet-metal divider between the bypass and core flows. The lifting of some of the panel edges in the area of the separated core flow was ascribed to the static-pressure differences existing between the two ducts at that point.

The flow separation was apparently the result of the nonaxial core-stator discharge airflow striking the fan support pylon. The fan was originally designed as part of an engine to be considered in the NASA-Lewis Quiet Engine Program. On the engine, to reduce the loading on the core stator vanes and to eliminate inlet guide vanes at the core compressor, the airflow was not turned completely axially by the stator, but instead, the airflow left the core stator at an angle of 30° from the axis. For the investigation reported herein, the fan alone was used, but it was used as designed for the engine. In this fan application, small struts supporting the flow divider were placed at this same 30° angle. However, the main support strut, or pylon, beneath the fan was still oriented axially. This support strut was a 20 percent thick section airfoil in shape, and it had caused no noticeable turbulence in previous fan testing or in simulated scale tests when

the approach airflow was axial. However, the nonaxial flow of the QF-5 fan created a separated flow region at one side of this strut, apparently due to the attainment of the critical Mach number.

To reduce the possibility of any extensive damage to the fan casing from the aforementioned core performance, the maximum-speed test point was lowered from 90 percent of design to 85 percent of design. Any damage to the flow divider was repaired after each test. Because of this problem of core flow, core aerodynamic measurements were inconsistent. Consequently, those results will not be presented.

RESULTS AND DISCUSSION

Aerodynamic Results

Figure 7 shows the operating-line data (design nozzle) obtained from the fan tests with the smallest rotor-to-stator spacing superimposed on the fan bypass-stream design performance map. Comparison of the actual results with the design predicted operating line indicates fair agreement over the speed range covered.

Measurements of two fan characteristics are presented to describe the fan operation. Figure 8 presents the bypass pressure ratio as a function of fan speed; also shown are the design values for 90 and 100 percent corrected speeds. For this fan, the measured pressure ratio is slightly less than design, and apparently the 100 percent design value for pressure ratio would not have been reached. Figure 9 presents the bypass pressure ratio as a function of rotor-to-stator spacing. The figure shows that the pressure ratio increased slightly with spacing as speed increased. Whether this small, but consistent, behavior is a function of the small changes in the bypass flow duct geometry with spacing changes is not known.

The curves (fig. 10) of the bypass mass flow as a function of fan speed for three spacings are similar to the pressure-ratio curves. There is an increase in mass flow with increased spacing between rotor and stator.

Difficulty was experienced in determining an accurate and consistent temperature in the fan inlet, and this difficulty consequently led to errors in ratios and efficiencies. Because of the uncertainty in the inlet temperature measurements, fan efficiency data are not presented.

Acoustic Results

The main objective of this study was to determine the effects of varying the axial separation between rotor and stator on the acoustic performance of the fan. To accomplish this end, comparisons were made of measured sound pressure levels of the components making up the fan noise spectrum. Thus, in addition to comparisons of overall

power spectra and perceived noise, comparisons were made between the levels of the fundamental blade passage tone, the higher-order harmonics of the blade passage frequency, the fan broadband noise, and the broadband "haystacks."

General considerations. - A sample noise spectrum for the QF-5 fan is presented in figure 11 to illustrate the appearance of these noise components. Each component presented in figure 11 will first be covered individually, and later in combination as overall noise levels. It is to be noted that the amplitude of the second harmonic of blade passage frequency (BPF) is greater in the far field than that of the fundamental, or first harmonic. Although this situation of the second harmonic being greater than the first is generally true only in the rear quadrant, the effect is extensive enough that the level of the second harmonic tone determines the overall sound pressure level (OASPL). An extremely important consideration in this study is the fact that because the fundamental blade passage frequency tone was designed to be cut off (so that interaction between the fan rotor and stator would not give rise to this frequency tone), changes in sound level due to changes in the interaction between rotor and stator would be expected to affect only the overtones, or higher order harmonics. This fact makes it necessary to examine several of the fan tone harmonics as well as the fundamental blade passage frequency tone to determine the relation between rotor-to-stator spacing and the reduced fan noise.

Figure 12 compares the maximum, 1/3 octave sound pressure levels of the second harmonic from 60, 70, 80, and 85 percent fan speeds for the various rotor-to-stator spacings. It is clear that the reduction in sound level caused by increasing the rotor-to-stator spacing is not a function of fan speed. For this reason, and for the sake of simplicity, the sound data presented and the conclusions that are drawn from this point on will be generally only from 85 percent speed data.

Fundamental tone. - Although the fan was designed so that the fundamental fan tone, or first harmonic, would be theoretically cut off, a fundamental tone (e.g., fig. 11) does propagate into the far field. There is (ref. 2) a criterion for determining whether or not an interaction tone or multiple of the blade passage frequency will propagate from the fan. This criterion is

$$\frac{U}{U_T} = \frac{mB}{mB + nV} \tag{1}$$

in which

U rotating speed of a mode

U_T blade tip speed

m multiple, or harmonic, of the blade passage frequency

B number of rotor blades (36 for the QF-5 fan)

n negative integer

V number of stator blades (88 for the QF-5 fan)

Depending on whether $|U/U_T|$ is greater or less than 1, a particular tone will or will not be propagated to the far field. In the case of the first harmonic, or fundamental, $U/U_T = 36/(36 + 88n)$. Since for no value of n will the expression be greater than 1, noise caused by interaction at the blade passage frequency should not be detected by the microphones. However, for the second harmonic, $U/U_T = 72/(72 + 88n)$, and for this tone, $|U/U_T|$ can be greater than 1 (e.g., for $n = -1$). Similarly, higher order harmonics satisfy the criterion, and, in fact, are present.

The observed blade passage frequency tone (e.g., fig. 11) is believed to result from free atmospheric turbulence (ref. 4) and the fixed-spot distortion of the facility (ref. 5); consequently, this tone is not affected by cutoff or changes in spacing. Furthermore, under flight conditions the blade passage frequency tone as caused by these phenomena may disappear (ref. 6).

The effect of changes in spacing on the fundamental is shown in figure 13. The fact that the blade passage frequency tone level does increase slightly with increases in spacing may be due to inaccuracies in measurement or to a change in fan aerodynamics (e.g., figs. 8 and 10) from one stator position to another.

Overtone noise. - The reduction in sound level that resulted when the rotor-to-stator spacing was increased was calculated by combining the reductions of the second, third, fourth, and fifth harmonics of the blade passage frequency. Figure 14 shows how the overtone sound pressure level is reduced by increases in rotor-to-stator spacing. Overtone sound pressure level is defined herein as the sound level calculated by adding only the contributions from the second, third, fourth, and fifth harmonics, and it is basically a measure of the noise generated by the interaction between the fan rotor and stator. This level is obtained by adding the sound pressure levels obtained from narrow-band spectrum (20-Hz bandwidth resolution) analyses of the far-field microphone data. The contribution from the blade passage frequency tone was omitted from the calculation because the fundamental itself was not affected by changes in the rotor-to-stator spacing.

In calculating power levels from the QF-5 fan, the computation was performed in a way similar to the computation of overtone sound pressure level. Power contributions from the second to fifth harmonics of the blade passage frequency were added together, and any contribution from the fundamental tone was left out. Table V presents the overtone power level and the power levels from the individual QF-5 fan tones for each rotor-to-stator spacing. As can be seen from the table, the sound power level differences associated with doubling the spacing are, for the second to fifth harmonics, 6.3, 4.4, 4.9, and 5.2 decibels, respectively. The result of these individual reductions is an overtone reduction of 5.9 decibels.

Some studies of the effects of the rotor-to-stator spacing have been conducted by

others - in particular, Lowson (ref. 1); Smith and House (ref. 7); and Silverstein, Katzoff, and Bullivant (ref. 8). Reference 1 showed a 2-decibel reduction of sound per doubling of spacing over 1- to 2-chord spacings. Reference 7 showed a 6-decibel reduction of sound per doubling of spacing; that is, a reduction with the square of the ratio of spacing to rotor chord, $(s/c)^2$.

These first two functions present results of differences of the total sound power level as the spacing between fan rotor and stator, presumably of a single-stage fan, was changed. These results should be comparable to the changes in overtone sound power level found in the present program. The omission of the noise contribution of the unaffected cutoff fundamental tone from the present program results should place the present results on the same standing as those of the reference studies, since those studies (as far as can be determined) did not involve any cutoff tones.

Reference 8, which was a study of wakes downstream of an airfoil, provided an expression for the maximum velocity defect in the wake of $(2.42\ C_D/s/c + 0.3)$, in which C_D is the drag coefficient. According to the modeling of reference 6, in which fan stator blades respond to the changes in incoming flow angles and velocities created by the rotor wakes and generate a varying lift force, the relative level of the noise resulting from this fluctuating force is assumed to be represented as $20 \log (2.42\ C_D/s/c + 0.3)$. The rate of reduction of this level would be about 5 decibels per doubling of spacing.

A comparison of the sound reduction measured in this investigation with the results from the first two studies (refs. 1 and 7) and the extension (ref. 9) of the wake defect study (ref. 8) is presented in figure 15. As can be seen, the overtone reduction of the QF-5 fan agrees well with the relation of reference 7 and with the wake dissipation results.

Individual higher order harmonics. - Figures 16 to 19 illustrate the sound radiation patterns of the second to fifth harmonics, respectively, for each of the three rotor-to-stator spacings. Figure 16 shows that for the second harmonic, increased rotor-to-stator spacing resulted in a small decrease in the sound pressure level ahead of the fan and a much greater decrease to the rear of the fan. Figure 17 shows that for the third harmonic, the reduction in sound pressure level with increased rotor-to-stator spacing tended to be more constant at all radial locations. For the fourth and fifth harmonics, figures 18 and 19 show that, with the exception of the variation in the intermediate spacing data of the fifth harmonic, the reduction in sound pressure level with increased spacing was uniform at all radial locations.

Table VI presents sound power level values for the higher order harmonics in the front and rear quadrants and the value of reduction for the doubling of the spacing between rotor and stator. The division between front and rear quadrants was made at 70° because examination of the polar plots of the sound pressure levels of the harmonics showed this angle generally to be between lobes.

Examination of the values of sound power displayed in table VI and of the sound pres-

sure levels as plotted in figures 13 and 16 to 19 suggest several hypotheses about the characteristics of fan discrete tone noise. One such hypothesis is that there are two sources of tone noise present in a fan, or at least in the QF-5 fan. One source of fan tone noise is affected by changes in rotor-to-stator spacing, and the other is not. This consequence results if the assumption is made that the blade number design criterion of reference 2 as applied to the QF-5 fan was successful in eliminating the propagation of first harmonic noise caused by the rotor-and-stator interaction. There are a number of differences between the first and other harmonics to indicate basic differences in tone generation.

In addition to the relative constancy of the amplitude of the fan fundamental, or first harmonic, in contrast to the several-decibel magnitude reduction of the higher harmonics with spacing increases, there are differences in directivity. Comparison of figure 13 with figures 16 to 19 indicates that the peak magnitude of the cutoff fundamental tone occurs in the front quadrant (around 50°), whereas the peak magnitudes of the other harmonics (which, since they are not cut off, should be a function of the rotor-and-stator interaction) all appear in the rear quadrant (between 110° and 130°). These differences between the characteristics of the fundamental tone, which should not be a function of rotor-and-stator interaction, and the other tones, which should be a function of rotor-and-stator interaction, are quite marked.

A second source of tone generation in the QF-5 fan is very likely an interaction between the fan rotor and nonuniformities in the inlet airflow, perhaps as described in reference 10. A previous study (ref. 5) of what was called inflow distortion has been made at the fan test facility of the Lewis Research Center. It appears that noise from this inflow distortion occurred at the same frequencies as the QF-5 fan noise caused by the rotor-and-stator interaction but differed by peaking in the inlet quadrant. This second means of noise production thus seems to operate independently of the rotor-and-stator interaction. Since this noise from inflow distortion propagates at multiples of the blade passage frequency, it simply adds to the rotor-and-stator interaction noise to produce the measured sound pressure level. In the case of the fundamental blade passage frequency tone, this second source is the only source of the sound pressure level. In the case of other harmonics, the contribution varies.

An attempt can be made to separate the rotor-and-stator interaction noise from what may be termed rotor-alone noise if the sound power level values of table VI are thought of as being made up of two components. One component is due to rotor-and-stator interaction and decreases by 2.5 to 3 decibels from one spacing to another; the other component is due to inflow distortion (interacting with the rotor alone) and is unchanged by spacing. This interaction of the inflow distortion with the rotor alone generated relatively smaller harmonics than did the rotor-and-stator interaction, judging by the changes in propagation of inlet noise at higher frequencies. Examination of figures 18 and 19 shows the front quadrant noise to be reduced by about the same amplitude as

was the rear quadrant noise. This would indicate that at these multiples of the fan fundamental tone, only the rotor-and-stator interaction component of noise is significant. At smaller multiples of the fundamental tone, that is, the second and third harmonics, the amplitudes of both noise sources are comparable. It may be that there is sufficient noise propagating into the front quadrant at low multiples of blade passage frequency to produce a noise floor so that the reduction in sound level from increases in spacing is not fully realized.

"Haystack". - Another component of the QF-5 fan noise spectrum that was affected by changes in rotor-to-stator spacing is what could be described as a "haystack." The amplitude of this component was small enough that its level had no effect on the overall sound pressure level or perceived noise rating of this fan. However, it seems useful to consider it, because, although not a discrete tone, it was affected by changes in rotor-to-stator spacing, just as would be a fan tone whose level was determined entirely by rotor-and-stator interaction. This component, present at all speeds, was only observed in the rear quadrant. Spectrally, it is a broadband hump of a few-hundred-hertz bandwidth, near in frequency to some of the harmonics of the blade passage frequency. Reference may be made to figure 11 for a sample spectrum with a "haystack." Several "haystacks" occur in the spectrum, but, as they are similar, only one will be discussed in any detail - the one with a center frequency close to the frequency of the second harmonic.

In order to define some of the terms and quantities which will be used, reference will be made to figures 20 and 21. A comparison of these two figures illustrates how the spectrum of this noise component differs from the blade passage frequency tone of the QF-5 fan and from fan tones in general. Figure 20 is a typical analysis of the 85 percent speed noise between about 1 and 3 kilohertz, which shows the blade passage frequency tone and a number of shaft passage frequency (SPF) tones. Figure 21 is an analysis at the same resolution (4 Hz) of the noise around the second harmonic between about 3 and 5 kilohertz. While some shaft passage frequency tones do appear in figure 21, there is an additional feature, a large nondiscrete-frequency noise component, or "haystack." To facilitate study of the "haystack," the comparison will be made on the basis of center frequency and peak level. In figure 20, the sound pressure level base on which the various tones rest is rather constant in amplitude. In figure 21, this base increases by about 10 decibels near the frequency of the fan harmonic. To rate the amplitude of the "haystack," a smoothed value of the maximum level (disregarding the shaft passage frequency tones) was chosen. To characterize the frequency of the "haystack," the value of frequency which appeared to be the center of the maximum "haystack" level was chosen. As is apparent from the sample figures, neither the peak amplitude level nor the center frequency value could be determined very precisely.

One characteristic of the "haystack" that was unaffected by changes in rotor-to-stator spacing was the variation of the "haystack" center frequency with the angular

location of the microphone from the fan. Examination of rear quadrant narrowband spectra indicate that the center frequency of the second-harmonic "haystack" changes with regard to the frequency of the second harmonic. Figure 22 shows the frequency of the "haystack" normalized to the frequency of the second harmonic. At angles closer to or farther from the fan inlet, there is a slight decrease or increase, respectively, in the normalized center frequency.

Figure 23 presents the peak value of the sound pressure level of the "haystack" at each one of the three rotor-to-stator spacings. A consistent reduction in level is apparent as the stator is moved away from the rotor. The amount of this reduction, an average of approximately 6 decibels per doubling of the spacing, is nearly the same as that for the second harmonic, which suggests a possible close relation between the "haystack" and the second harmonic.

The similarities between the reduction in amplitude of the "haystack" with changes in spacing and also the angle at which the "haystack" peak amplitude occurs, and the amplitude reduction and peak angle of the second harmonic seem unlikely to be a coincidence. One may, perhaps, speculate that the QF-5 fan "haystack" is the result of an interaction between some turbulence in the exit airflow and the fan harmonic tone. Both phenomena are based on fluctuations in air pressure, and a modulation process by which the discrete tone combines with a random airflow variation to create a noise component is conceivable.

Broadband noise. - An indication of the variation in fan broadband noise with fan spacing was obtained by examining the narrowband data at 3 kilohertz. The sound pressure level at a frequency of 3 kilohertz (see fig. 11) was chosen rather than an integrated value of estimated broadband noise on the basis of ease of reduction. This was made with the assumption that because this frequency was at a broadband portion of the spectrum, any changes in the fan broadband noise level would be similarly exhibited by changes in the 3-kilohertz level. Figure 24 presents the variation in level of this fan broadband noise with changes in spacing. The figure shows that any reduction of broadband noise at this frequency with increased rotor-to-stator spacing was insignificant. Some differences did occur at other frequencies, but no consistent trend was evident. For example, at 5 and 7 kilohertz, there was no change in broadband level between the data for the smallest and the intermediate rotor-to-stator spacing, and there was a 2-decibel reduction between the data for the intermediate and the largest spacing. Apparently, only the "haystack" and those blade passage frequency harmonics that have not been cut off are affected by spacing changes between the fan rotor and stator.

Overall acoustic performance of QF-5 fan. - Power levels and perceived noise calculated from 1/3 octave data reflect the reductions in overall noise that resulted from changes in the rotor-to-stator spacing. The calculations of power and perceived noise levels used corrected sound pressure levels. The higher frequencies were corrected for atmospheric attenuation by amounts dependent on the conditions of ambient tempera-

ture, pressure, and humidity; the lower frequencies (up to 1250 Hz) were corrected by taking into account the imperfect sound reflection off the test-site pavement. Figures of 1/3 octave sound pressure and sound power spectra, as well as sideline perceived noise, are presented in appendix B.

The curves (fig. 25) of sound power level as a function of frequency for 60- and 85-percent speed illustrate that the reductions in noise from one spacing to another occurred primarily at the harmonics of the blade passage frequency. As recorded in table V, the blade passage frequency sound power level obtained with the smallest spacing was about 5 decibels below the overtone sound power level. With increases in spacing, the overtone sound power level decreased by about 6 decibels, but the blade passage frequency sound power level increased slightly. The consequence of these offsetting noise changes is that over the 1- to 2-chord range of rotor-to-stator spacing, the sound power level for the QF-5 fan at 85 percent speed decreased by only about 1.5 decibels, as illustrated in figure 26. As could be seen in figure 9, changing the rotor-to-stator spacing brought about a change in operating pressure ratio. Figure 27 shows that a 2.5 decibel reduction in sound power level could be obtained if the fan were operated in such a way as to maintain a constant pressure ratio.

The figure of sound power level as a function of pressure ratio (fig. 27) illustrates the strong dependence of noise on fan pressure ratio (essentially specific work output). It is evident that both pressure ratio and rotor-to-stator spacing have a major effect on fan noise.

The perceived noise level curves (fig. 28) for 60 percent and 85 percent speeds also reflect the changes in sound pressure level from increasing the rotor-to-stator spacing. As expected, the closest spacing caused the most annoyance, and the farthest spacing, the least. The difference in maximum perceived noise level between the closest rotor-to-stator spacing of 1.14 rotor chords and the farthest spacing of 2.27 chords varied from 1 to 3 decibels at 60 and 85 percent speeds. Figure 29 shows that the reduction in the value of the maximum sideline perceived noise level with spacing ratio was about 1.5 decibels at 85 percent speed.

CONCLUDING REMARKS

Tests were conducted on a full-scale, single-stage, high-pressure-ratio fan to determine the effect of increasing the rotor-to-stator spacing on the noise from the fan. A comparison was made of the sound levels of the different noise components over a range of spacing of approximately 1 to 2 rotor chords. Changes in spacing had a pronounced effect on the levels of those noise components caused by the flow interaction between rotor and stator. The reduction in noise levels over this range of spacing was 5 to 6 decibels for all tones except that of the fundamental blade passage frequency. The

latter tone appeared sufficiently reduced in amplitude (cut off) by the relative numbers of rotor and stator blades that its level was controlled by what appears to have been rotor-alone noise. The net result of these effects was that the noise produced at the 2.27-chord spacing was about 2 decibels less than the noise at the 1.14-chord spacing.

Some implications of the results of this study concern the effectiveness of cutoff and of increased rotor-to-stator spacing in reducing fan noise. For the QF-5 fan, both techniques were used, but fairly small perceived noise reductions were obtained. The choice of more than twice as many stator blades as rotor blades was intended to cut off the propagation of the fundamental blade passage frequency tone so that it would be completely eliminated, and only the overtones, or higher frequency fan tones would be heard. Then, moving the bypass stator row farther and farther away from the rotor would reduce the sound level of the overtones because the strength of the rotor wakes at the stator would have been reduced. Strictly speaking, it would appear that both design objectives were met - the fundamental blade passage frequency tone as caused by rotor-and-stator interaction was eliminated, and the level of the overtones was reduced. However, a tone at the fundamental blade passage frequency was generated. This tone occurred at a sensitive Noy area of frequency and was large enough in amplitude so that the reduction of other fan tones was not effective in reducing total sound power noise. The fact that the directivity, or polar pattern, of the fundamental tone sound pressure level was radically different from that of the higher order harmonics and that the level of the fundamental was not affected by changes in rotor-to-stator spacing (as were the other harmonics) strongly suggests that the fundamental tone heard is generated by the rotor alone, not by a rotor-and-stator interaction. This fan noise was probably an effect of an interaction between the fan rotor and inflow nonuniformities.

It would seem that increasing the distance between the fan rotor and stator is an effective way of reducing the fan noise caused by rotor-and-stator interaction. However, for fan noise caused by an interaction between the fan rotor and nonuniformities in the incoming airflow, other design techniques for quieting the fan are necessary. Perhaps a smaller number of rotor blades would be useful in reducing the amount of rotor-alone noise. This approach would have a second advantage if the number of rotor blades were small enough that the blade passage frequency would occur at less than a Noy sensitive frequency (less than 1 kHz). Then, by using four times as many stator blades as rotor blades, the second harmonic tone as well as the first (fundamental) would be cut off.

Lewis Research Center,
National Aeronautics and Space Administration,
Cleveland, Ohio, April 23, 1974,
501-24.

APPENDIX A

NOISE CHARACTERISTICS OF FAN TEST FACILITY

Because of the proximity of the fan test facility to the main compressor and drive building of the 10- by 10-Foot Supersonic Wind Tunnel, the possibility of measurement errors caused by reflections from the building to the microphones was considered. To reduce this possibility, the wall of the building facing the fan apparatus and microphones was covered to a height of 9.1 meters (30 ft) by a 15.2-centimeter- (6-in.-) thick layer of acoustic damping material (fig. 1(b)). The material chosen was an open-cell polyurethane ether foam which is weather resistant and has very good sound absorptive properties above 400 hertz.

Tests were performed, at a distance of 15.2 meters (50 ft) out from the wall, in which a 3.492-centimeter- (1.375-in.-) diameter converging nozzle was mounted on the concrete viaduct in place of the fan and with the insulation installed on the building wall. The sound produced by a nitrogen jet expanding supersonically from the nozzle was measured by an array of microphones centered on the nozzle (the 10° microphone was not used). The nozzle was oriented to exhaust directly towards the building wall. Supply pressure on the nozzle was held constant at 34.3 newtons per square centimeter (35 psia) throughout the test. This acoustic source was highly directional. The sound field had a peak decibel level approximately 20° from the flow discharge axis. At 90°, the level was 10 decibels below the peak, and it remained at this level from 90° to 180°. The test provided a comparison between the sound field of the jet exhausting towards the absorptive wall and the relatively free sound field of the jet exhausting away from the wall.

Comparison of 1/3 octave band sound pressure spectra for the two jet configurations at comparable locations showed differences of the order of 4 decibels below 200 hertz. Agreement was consistently good above 1000 hertz. The differences in sound pressure were random in nature. Differences from one azimuthal location to another showed no pattern, and no pattern was found which could be attributed to the nearness of the building wall.

The sound power spectra are presented in figure 30, which shows good agreement down to 400 hertz. The high point at 60 hertz, where the two curves are coincident, is probably the result of 60-hertz electronic noise. At low frequencies (below 400 Hz), there is a consistent difference of the order of 4 decibels. Results of the test indicate that above 400 hertz the treated wall satisfactorily represents (within 1 dB) a free field.

Tests were also run to determine the sound level caused by the drive machinery and the shaft turning without a fan coupled to it. Figure 31 indicates the noise power level generated at 3120 rpm. The effect of placing a shroud or cover around the drive shaft is also shown; at frequencies above 400 hertz, a fairly uniform reduction of the order of

8 decibels was observed. For purposes of comparison, the facility background noise level, without any machinery running, is also presented. It indicates that the shaft noise, although lowered by the cover, is still 10 to 15 decibels greater than the background noise. These levels were considerably less than the noise levels generated by the QF-5 fan.

APPENDIX B

ONE-THIRD OCTAVE DATA

The results of the 1/3 octave analyses of the QF-5 fan noise at 60, 70, 80, and 85 percent of design speed with rotor-to-stator spacings of 1.14, 1.65, and 2.27 rotor chords are presented in figures 32 to 88. These data are corrected for ground reflection and atmospheric attenuation. The table below gives the breakdown of the data as they are presented in the figures.

Data	Rotor-to-stator spacing, rotor chords	Figures
Sound power level	1.14	32
	1.65	33
	2.27	34
Sound pressure level at angular locations from 10° to 160° relative to inlet axis	1.14	35 to 50
	1.65	51 to 66
	2.27	67 to 82
Perceived noise level on 114.3-meter (375-ft) sideline at 60 percent of design speed	1.14	83
	1.65	84
	2.27	85
Perceived noise level on 304.8-meter (1000-ft) sideline at 85 percent of design speed	1.14	86
	1.65	87
	2.27	88

REFERENCES

1. Lowson, M. V.: Reduction of Compressor Noise Radiation. Jour. Acoust. Soc. Am., vol. 43, no. 1, Jan. 1968, pp. 37-50.

2. Tyler, J. M.; and Sofrin, T. G.: Axial Flow Compressor Noise Studies. Trans. SAE, vol. 70, 1962, pp. 309-332.

3. Crigler, John L.; and Copeland, W. Latham: Noise Studies of Inlet-Guide-Vane-Rotor Interaction of a Single-Stage Axial Flow Compressor. NASA TN D-2962, 1965.

4. Hanson, Donald B.: The Spectrum of Rotor Noise Caused by Atmospheric Turbulence. Presented at the Spring Meeting of the Acoustical Society of America, New York City, April 23-26, 1974.

5. Povinelli, Frederick P.; Dittmar, James H.; and Woodward, Richard P.: Effects of Installation Caused Flow Distortion on Noise from a Fan Designed for Turbofan Engines. NASA TN D-7076, 1972.

6. Feiler, C. E.; and Merriman, J. E.: Effects of Forward Velocity and Acoustic Treatment on Inlet Fan Noise. Paper 74-946, AIAA, Aug. 1974.

7. Smith, M. J. T.; and House, M. E.: Internally Generated Noise from Gas Turbine Engines. Measurement and Prediction. Jour. Eng. Power, vol. 89, no. 2, Apr. 1967, pp. 177-190.

8. Silverstein, Abe; Katzoff, S.; and Bullivant, W. Kenneth: Downwash and Wake Behind Plain and Flapped Airfoils. NACA TR-651, 1939.

9. Dittmar, James H.: Methods for Reducing Blade Passing Frequency Noise Generated by Rotor-Wake-Stator Interaction. NASA TM X-2669, 1972.

10. Metzger, F. B.: Progress in Source Noise Suppression of Subsonic Tip Speed Fans. Paper 73-1032, AIAA, Oct. 1973.

TABLE I. - DESIGN CHARACTERISTICS OF QF-5 FAN

Corrected flow, kg/sec (lb/sec)	385.9 (850)
Corrected fan speed, rpm	3630
Corrected tip speed, m/sec (ft/sec)	332.5 (1090)
Bypass pressure ratio	1.60
Core pressure ratio	1.45
Predicted bypass efficiency	0.870
Predicted core efficiency	0.872
Bypass ratio	5.40

TABLE II. - PHYSICAL CHARACTERISTICS OF QF-5 FAN

Blade parameter	Rotor	Fan stator	Core stator
Number	36	88	88
Chord, m (in.):			
Hub	0.17 (6.65)	0.10 (4.0)	0.08 (3.0)
Midspan	.19 (7.65)	.10 (4.0)	.08 (3.0)
Tip	.21 (8.12)	.10 (4.0)	.08 (3.0)
Aspect ratio:			
Hub	2.65	2.74	1.12
Tip	2.17	2.74	1.12
Span, m (in.):			
Leading edge	0.49 (19.02)	0.29 (10.95)	0.09 (3.35)
Trailing edge	.41 (16.17)	.28 (10.95)	.09 (3.35)
Hub-to-tip ratio:			
Leading edge	0.445	0.679	0.821
Trailing edge	.512	.715	.835
Solidity:			
Hub	2.36	2.35	2.35
Tip	1.38	1.63	1.95

TABLE III. - FAN VELOCITY DESIGN PARAMETERS

(a) At 80 percent of cruise design corrected speed

Fan rotor					
Diameter, cm (in.):					
At rotor leading-edge station	92.48 (36.41)	119.15 (46.91)	134.85 (53.09)	155.32 (61.15)	167.84 (66.08)
At rotor trailing-edge station	98.96 (38.96)	122.48 (48.22)	135.86 (53.49)	153.59 (60.47)	163.25 (64.27)
Relative Mach number (rotor):					
At rotor leading-edge station	0.595	0.699	0.759	0.833	0.873
At rotor trailing-edge station	.415	.436	.479	.561	.594
Meridional velocity, m/sec (ft/sec):					
At rotor leading-edge station	141.0 (462.2)	147.2 (482.6)	148.9 (488.2)	147.4 (483.2)	141.9 (465.2)
At rotor trailing-edge station	141.7 (464.5)	145.7 (477.6)	153.4 (503.0)	164.9 (540.8)	168.7 (553.1)
Relative air angle (rotor), deg:					
At rotor leading-edge station	45.06	39.07	35.97	31.95	29.06
At rotor trailing-edge station	90.73	75.97	68.16	58.37	55.16
Wheel speed, m/sec (ft/sec):					
At rotor leading-edge station	140.7 (461.3)	181.3 (594.4)	205.2 (672.7)	236.3 (774.9)	255.4 (837.3)
At rotor trailing-edge station	150.5 (493.6)	186.4 (611.0)	206.7 (677.8)	233.7 (766.2)	248.4 (814.4)
Diffusion factor:	0.501	0.541	0.525	0.464	0.452
Bypass stator					
Diameter, cm (in.):					
At stator leading-edge station	125.10 (49.25)	137.59 (54.17)	148.34 (58.40)	158.06 (62.23)	167.46 (65.93)
At stator trailing-edge station	131.55 (51.79)	142.44 (56.08)	151.89 (59.80)	160.66 (63.25)	169.16 (66.60)
Absolute Mach number (stator):					
At stator leading-edge station	0.627	0.644	0.644	0.624	0.589
At stator trailing-edge station	.499	.509	.503	.485	.457
Meridional velocity, m/sec (ft/sec):					
At stator leading-edge station	162.0 (531.2)	172.2 (564.6)	175.9 (576.7)	172.8 (566.4)	159.8 (523.8)
At stator trailing-edge station	173.5 (568.7)	177.2 (580.9)	175.7 (576.1)	169.7 (556.3)	160.9 (527.6)
Absolute air angle (stator), deg:					
At stator leading-edge station	48.97	51.20	52.52	53.39	51.37
At stator trailing-edge station	90.00	90.00	90.00	90.00	90.00
Diffusion factor:	0.334	0.348	0.365	0.378	0.396
Core stator					
Diameter, cm (in.):					
At stator leading-edge station	92.58 (36.45)	96.65 (38.05)	100.43 (39.54)	104.09 (40.98)	107.67 (42.39)
At stator trailing-edge station	93.88 (36.96)	97.59 (38.42)	101.12 (39.81)	104.52 (41.15)	107.80 (42.44)
Absolute Mach number (stator):					
At stator leading-edge station	0.643	0.597	0.577	0.571	0.573
At stator trailing-edge station	.426	.430	.430	.432	.436
Meridional velocity, m/sec (ft/sec):					
At stator leading-edge station	125.3 (411.3)	131.1 (429.7)	130.5 (427.8)	128.1 (419.9)	125.6 (411.7)
At stator trailing-edge station	132.7 (435.2)	132.1 (433.2)	130.5 (427.9)	129.8 (425.5)	130.0 (426.1)
Absolute air angle (stator), deg:					
At stator leading-edge station	34.84	39.94	41.31	40.84	39.63
At stator trailing-edge station	63.36	62.10	60.91	59.78	58.75
Diffusion factor:	0.436	0.364	0.335	0.324	0.321

TABLE III. - Concluded. FAN VELOCITY DESIGN PARAMETERS

(b) At 100 percent of cruise design corrected speed

Fan rotor					
Diameter, cm (in.):					
At rotor leading-edge station	92.89 (36.57)	119.48 (47.04)	135.03 (53.16)	155.50 (61.22)	167.97 (66.13)
At rotor trailing-edge station	99.52 (39.18)	122.38 (48.18)	135.59 (53.38)	153.11 (60.28)	163.09 (64.21)
Relative Mach number (rotor):					
At rotor leading-edge station	0.800	0.933	1.007	1.094	1.135
At rotor trailing-edge station	.513	.524	.574	.681	.733
Meridional velocity, m/sec (ft/sec):					
At rotor leading-edge station	195.3 (640.3)	205.1 (672.3)	207.5 (680.4)	203.5 (667.1)	194.3 (636.9)
At rotor trailing-edge station	175.4 (575.0)	176.3 (577.9)	185.9 (609.5)	202.6 (664.4)	210.4 (689.8)
Relative air angle (rotor), deg:					
At rotor leading-edge station	47.87	42.07	38.94	34.53	31.30
At rotor trailing-edge station	90.26	76.01	68.30	58.56	55.23
Wheel speed, m/sec (ft/sec):					
At rotor leading-edge station	176.7 (579.3)	227.2 (745.0)	256.8 (842.0)	295.7 (969.6)	319.5 (1047.4)
At rotor trailing-edge station	189.3 (620.5)	232.8 (763.2)	257.9 (845.5)	291.2 (954.8)	310.2 (1017.0)
Diffusion factor:	0.535	0.583	0.566	0.495	0.467
Bypass stator					
Diameter, cm (in.):					
At stator leading-edge station	124.64 (49.07)	136.93 (53.91)	147.83 (58.20)	157.89 (62.16)	167.46 (65.93)
At stator trailing-edge station	130.81 (51.50)	141.45 (55.69)	151.13 (59.50)	133.20 (52.44)	128.24 (50.49)
Absolute Mach number (stator):					
At stator leading-edge station	0.773	0.798	0.797	0.765	0.714
At stator trailing-edge station	.555	.580	.578	.558	.526
Meridional velocity, m/sec (ft/sec):					
At stator leading-edge station	198.5 (650.7)	212.3 (696.1)	216.6 (710.1)	211.1 (692.0)	193.8 (635.5)
At stator trailing-edge station	196.3 (643.7)	205.5 (673.9)	205.9 (675.1)	199.2 (653.0)	188.9 (619.4)
Absolute air angle (stator), deg:					
At stator leading-edge station	48.17	50.44	51.64	52.44	50.49
At stator trailing-edge station	90.00	90.00	90.00	90.00	90.00
Diffusion factor:	0.404	0.404	0.414	0.420	0.435
Core stator					
Diameter, cm (in.):					
At stator leading-edge station	92.56 (36.44)	96.60 (38.03)	100.43 (39.54)	104.11 (40.99)	107.70 (42.40)
At stator trailing-edge station	93.83 (36.94)	97.51 (38.39)	101.07 (39.79)	104.50 (41.14)	107.80 (42.44)
Absolute Mach number (stator):					
At stator leading-edge station	0.800	0.743	0.721	0.716	0.720
At stator trailing-edge station	.501	.504	.506	.513	.521
Meridional velocity, m/sec (ft/sec):					
At stator leading-edge station	156.3 (512.6)	163.8 (536.9)	163.3 (535.3)	160.7 (527.0)	158.6 (519.9)
At stator trailing-edge station	158.6 (520.1)	156.8 (514.0)	155.6 (510.3)	156.3 (512.4)	157.5 (516.3)
Absolute air angle (stator), deg:					
At stator leading-edge station	34.86	40.01	41.27	40.68	39.61
At stator trailing-edge station	63.38	62.12	60.92	59.79	58.75
Diffusion factor:	0.465	0.402	0.375	0.361	0.357

TABLE IV. - AERODYNAMIC INSTRUMENTATION

Station	Number of sensors				
	Static pressure		Total pressure	Temperature	
	Wall	Stream		Wall	Stream
1	--	--	--	6	--
8	8	--	--	--	--
3	6	--	40	--	36
4	6	--	20	--	16
5	--	6	48	--	--

TABLE V. - FAN TONE POWER LEVELS

Harmonic	Rotor-to-stator spacing, rotor chords			Total change in tone power level with increase in spacing from 1.14 chords to 2.27 chords, dB
	1.14	1.65	2.27	
	Tone power level, dB (relative to 10^{-13} W)			
1	147.4	148.7	149.1	+1.7
2	152.5	149.7	146.2	-6.3
3	139.7	137.4	135.3	-4.4
4	140.3	138.4	135.4	-4.9
5	137.7	136.9	132.5	-5.2
Overtone	152.9	150.4	147.0	-5.9

TABLE VI. - FAN TONE POWER LEVELS BY RADIAL LOCATION

Blade passage frequency harmonic	Radial location	Rotor-to-stator spacing, rotor chords			Total decrease in power level with increase in spacing from 1.14 chords to 2.27 chords, dB
		1.14	1.65	2.27	
		Tone power level, dB (relative to 10^{-13} W)			
2	Front quadrant	142.7	141.0	140.2	2.5
	Rear quadrant	151.0	148.1	144.0	7.0
3	Front quadrant	133.8	133.7	131.2	3.0
	Rear quadrant	138.4	135.0	133.2	5.2
4	Front quadrant	132.1	130.0	127.3	4.8
	Rear quadrant	139.6	137.6	135.0	4.7
5	Front quadrant	127.8	125.3	122.8	5.1
	Rear quadrant	137.2	136.4	132.0	5.4

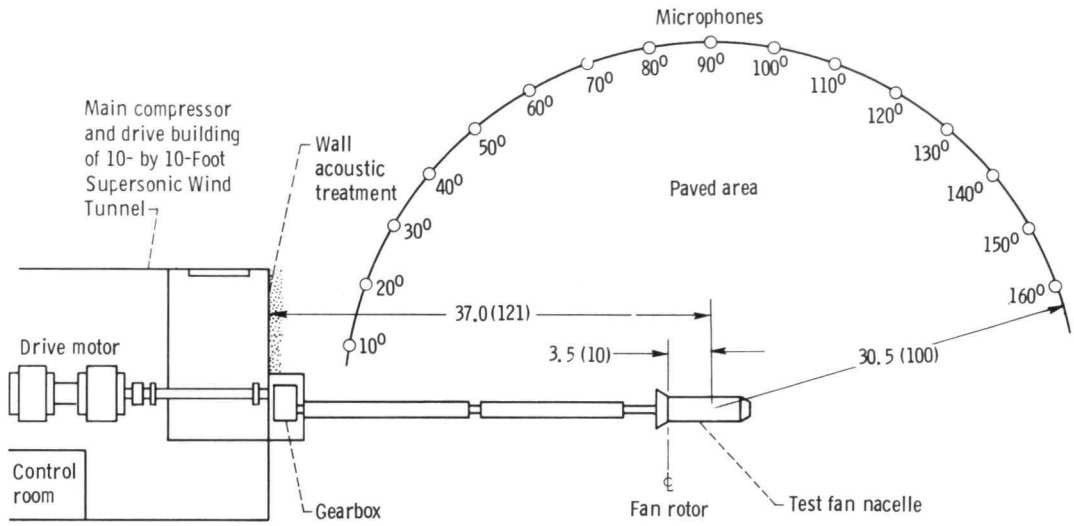

(a) Plan view. All dimensions are in meters (ft).

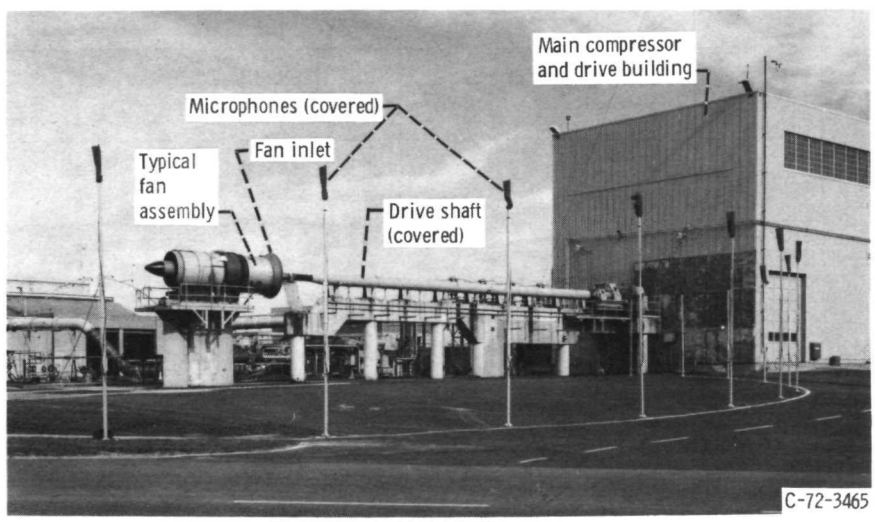

(b) Elevation view of facility.

Figure 1. - Full-scale fan acoustic test facility.

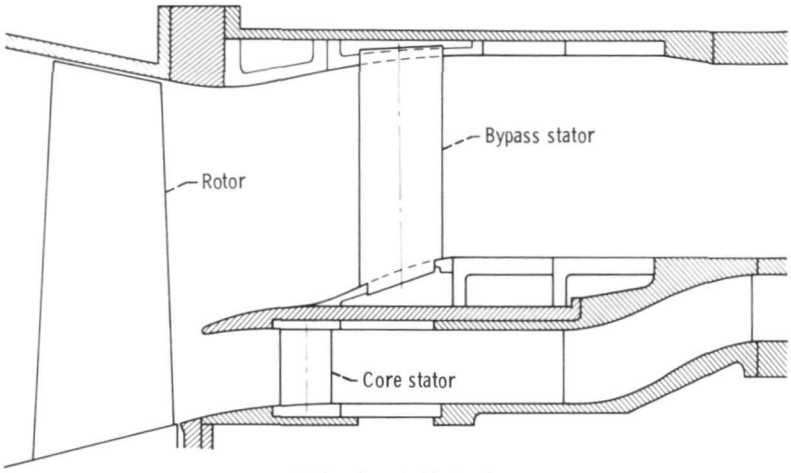

(a) Spacing, 1.14 chords.

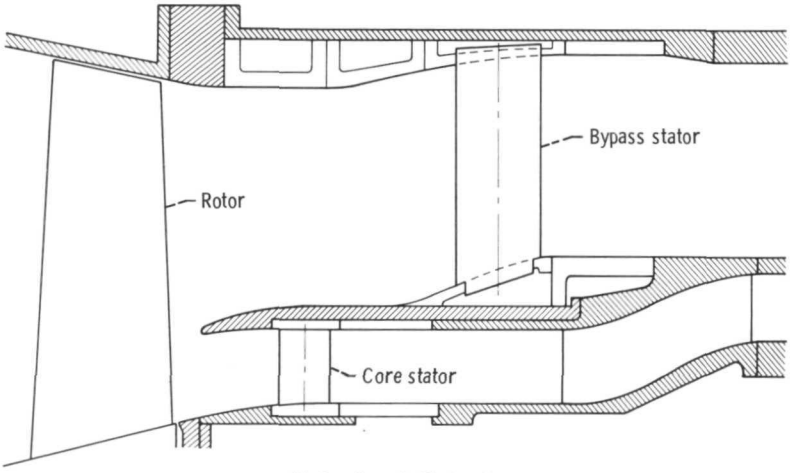

(b) Spacing, 1.65 chords.

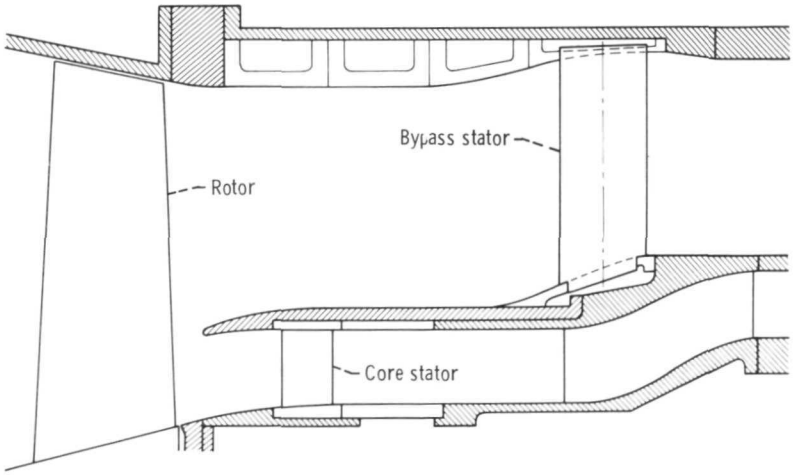

(c) Spacing, 2.27 chords.

Figure 2. - Fan rotor-to-stator spacing configurations.

(a) Rotor assembly.

(b) Stator assembly.

Figure 3. - Fan stage.

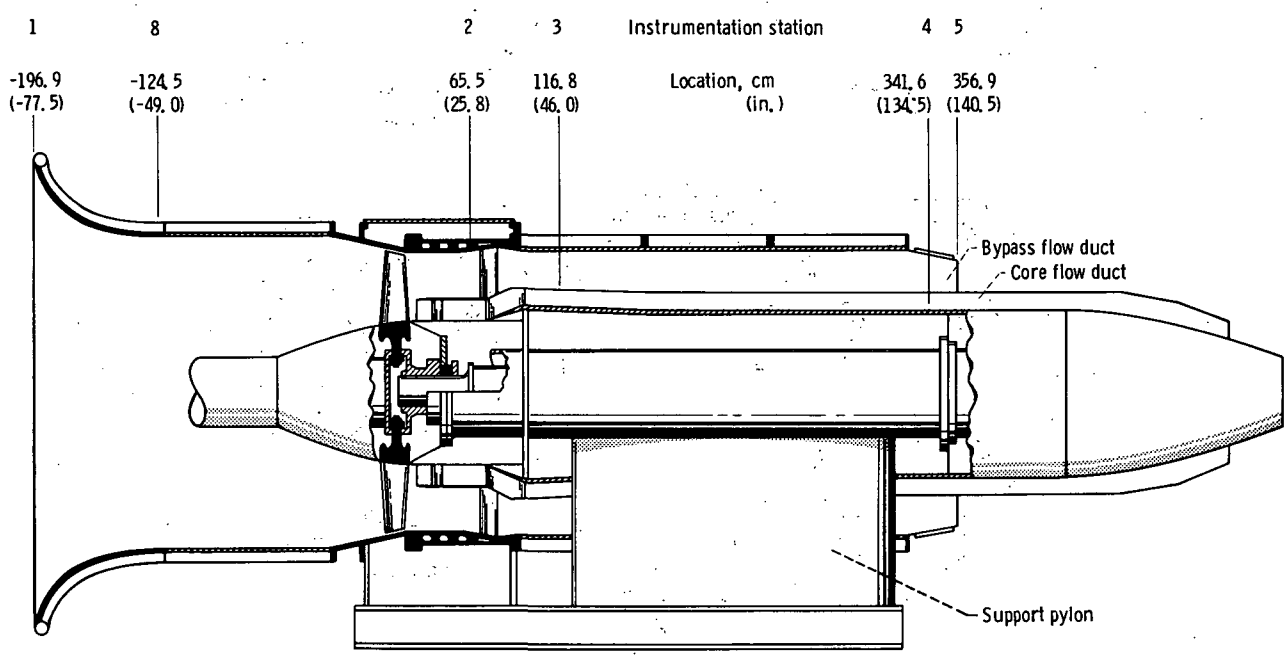

Figure 4. - Cutaway view of QF-5 fan installation, and axial locations of aerodynamic instrumentation stations.

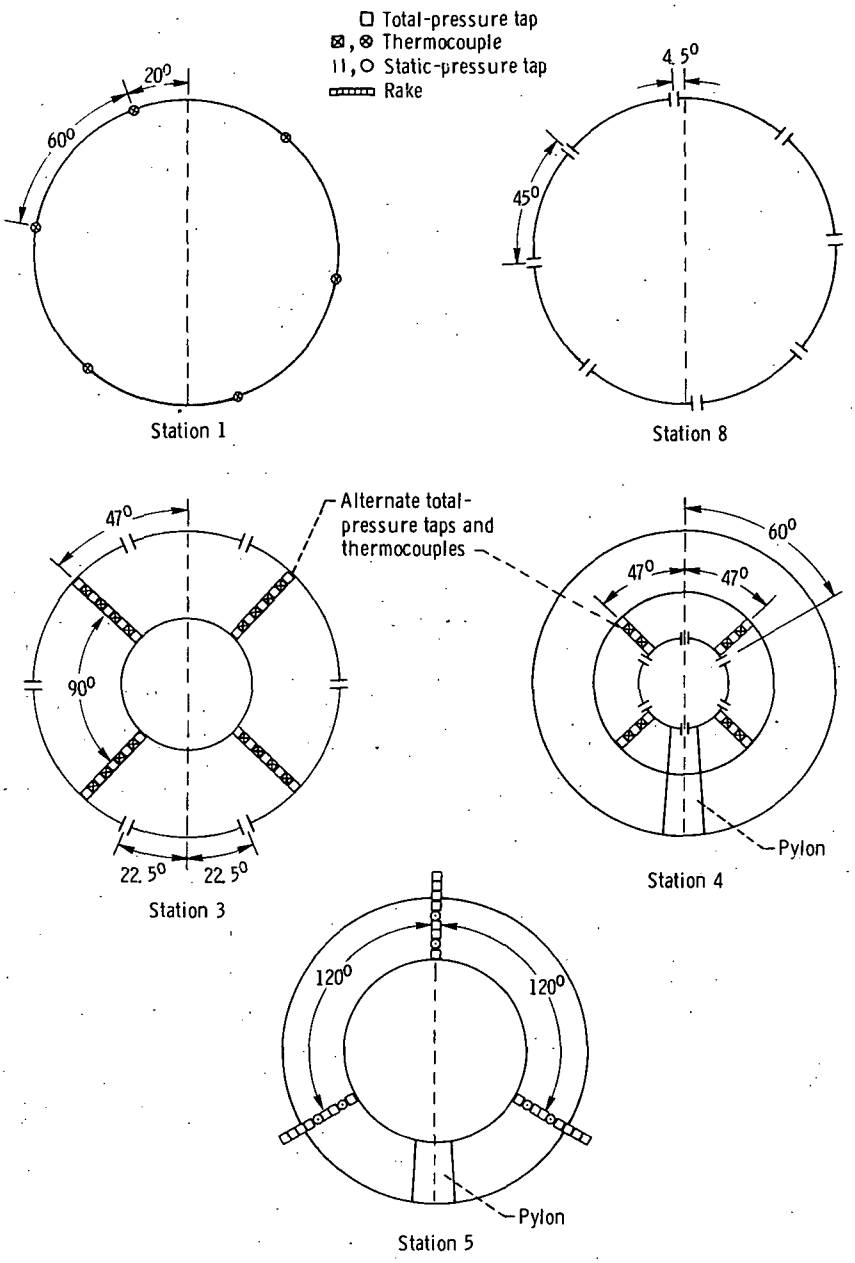

Figure 5. - Radial locations of fan aerodynamic instrumentation at numbered axial instrumentation stations. (Sketches not to scale; see table IV for correct number of rake elements at each station.)

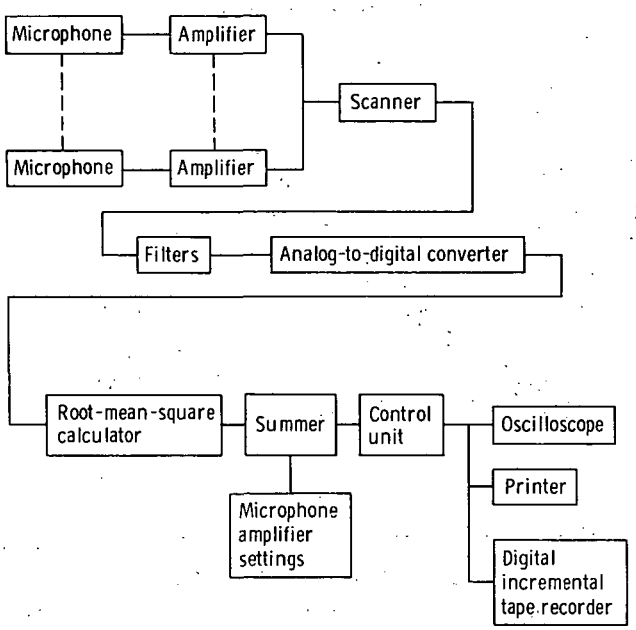

Figure 6. - Block diagram of acoustic data system.

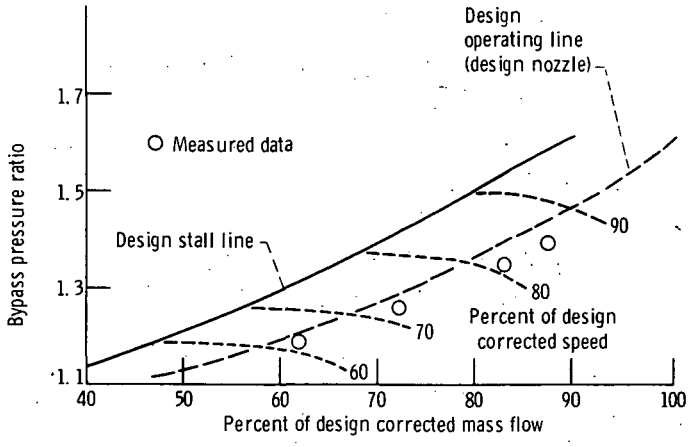

Figure 7. - Operating line of QF-5 fan with rotor-to-stator spacing of 1.14 rotor chords. One-hundred percent mass flow, 385.9 kilograms per second (850 lb/sec).

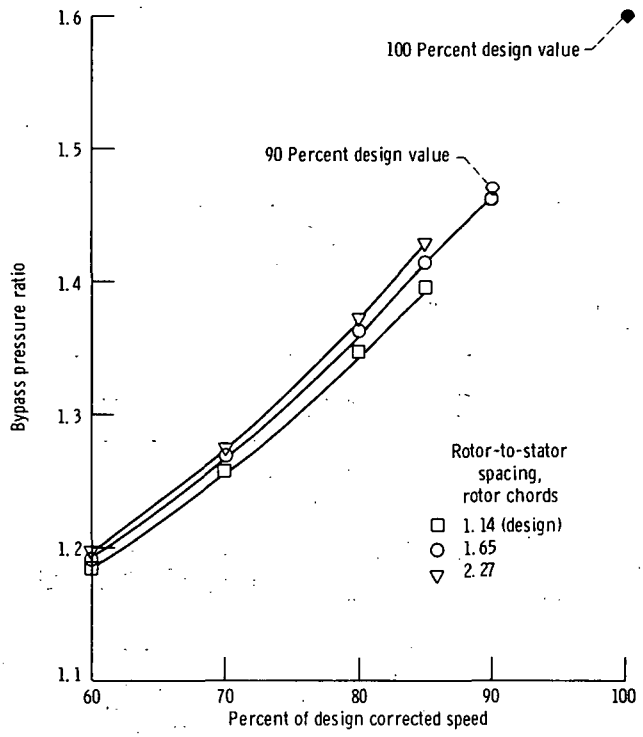

Figure 8. - Bypass pressure ratio as function of percent of corrected fan speed.

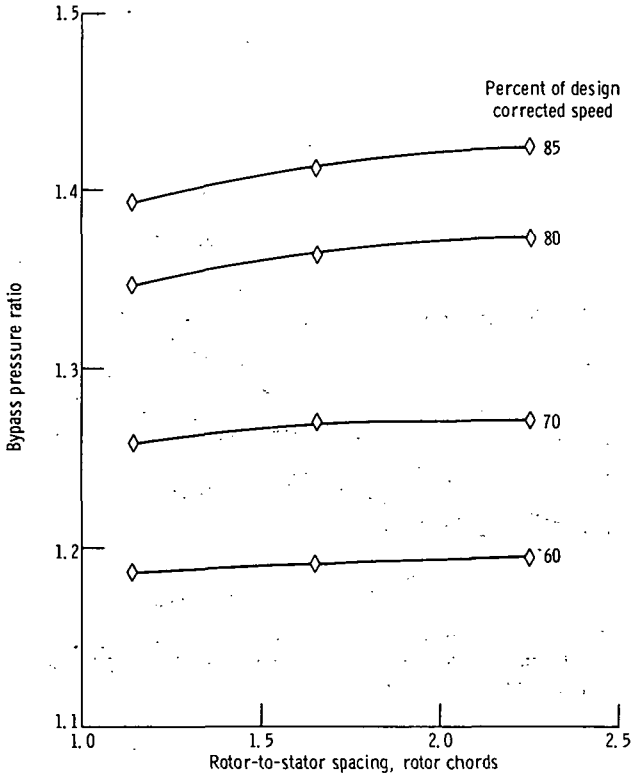

Figure 9. - Bypass pressure ratio as function of rotor-to-stator spacing.

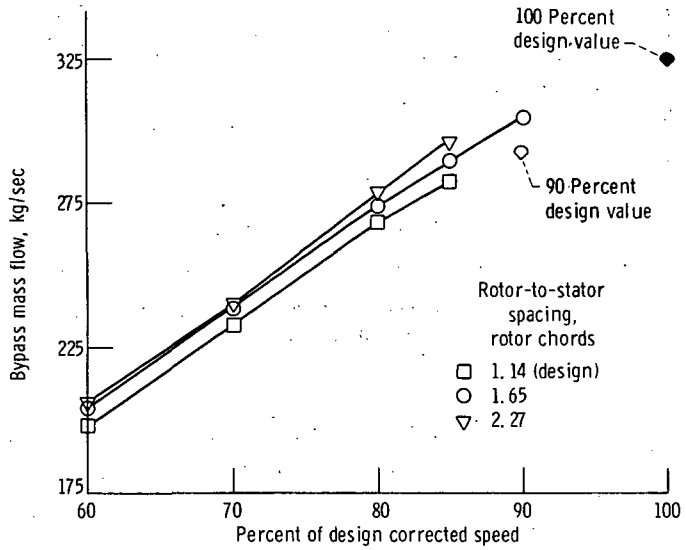

Figure 10. - Bypass mass flow as function of percent of corrected fan speed.

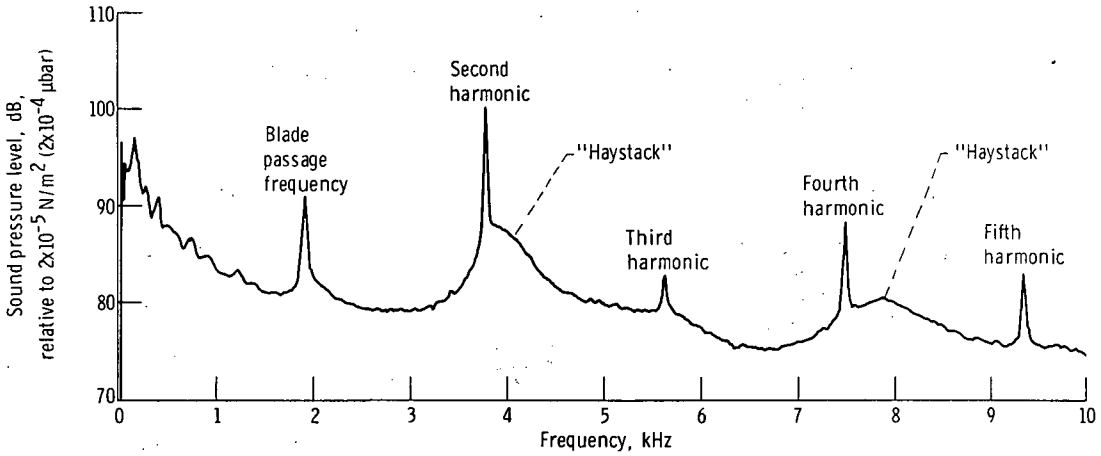

Figure 11. - Sample narrow-band spectra. Rotor-to-stator spacing, 1.65 rotor chords; fan speed, 85 percent of design corrected speed; microphone location, 140° from inlet axis.

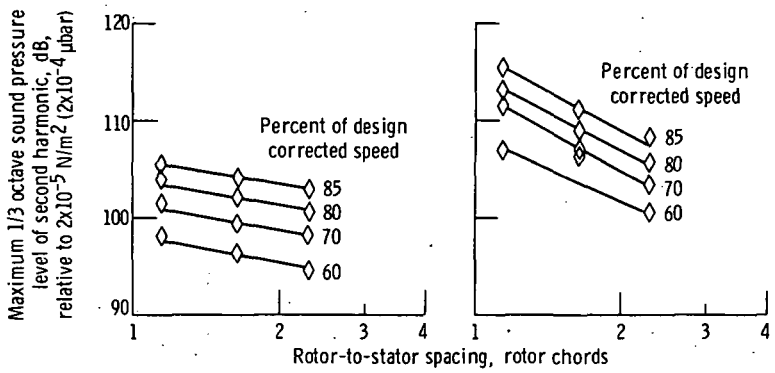

Figure 12. - Maximum sound pressure level of second harmonic as function of rotor-to-stator spacing.

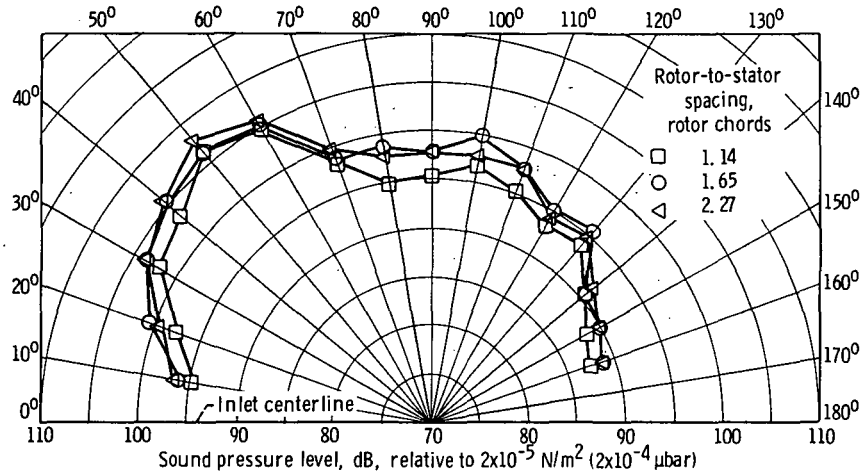

Figure 13. - Radiation pattern of blade passage frequency sound pressure level.

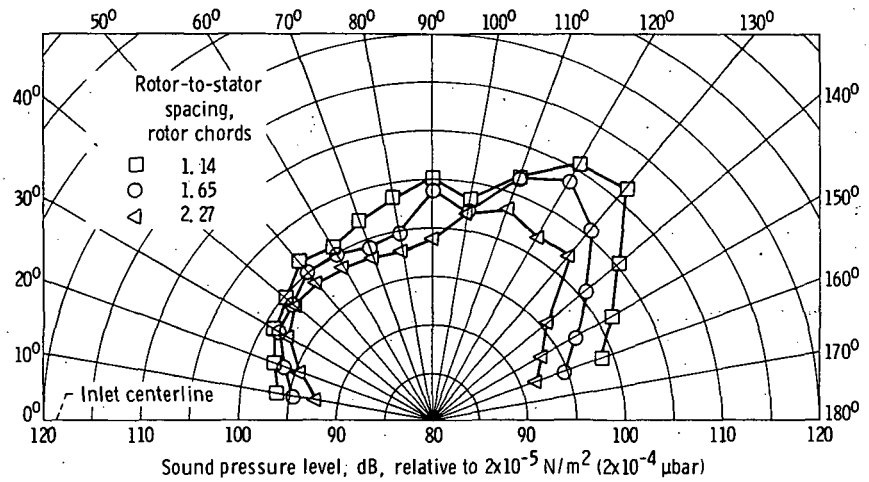

Figure 14. - Radiation pattern of overtone sound pressure level.

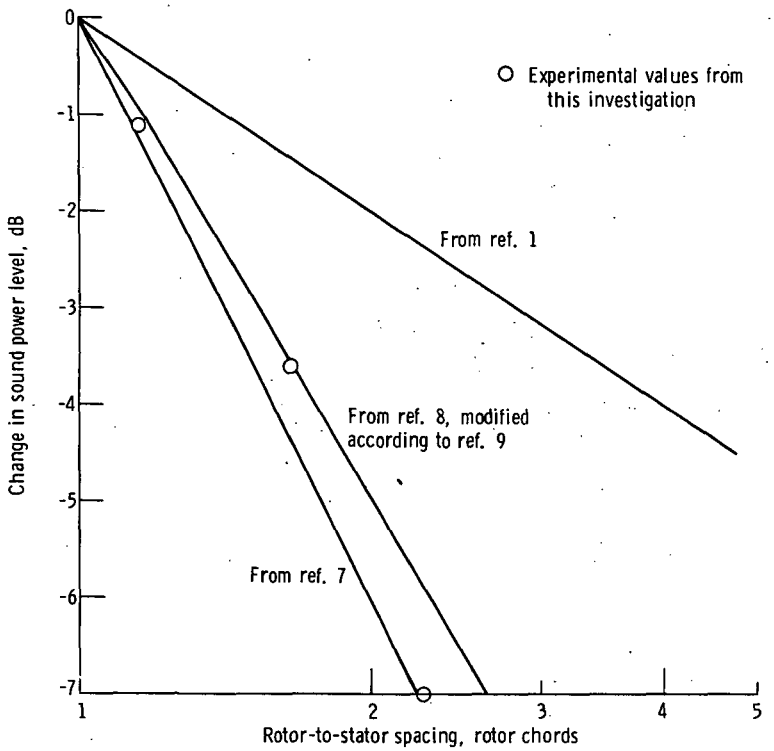

Figure 15. - Reduction in overtone sound power level with increase in rotor-to-stator spacing. (Sound power level at spacing of 1 rotor chord extrapolated to be 154 dB.)

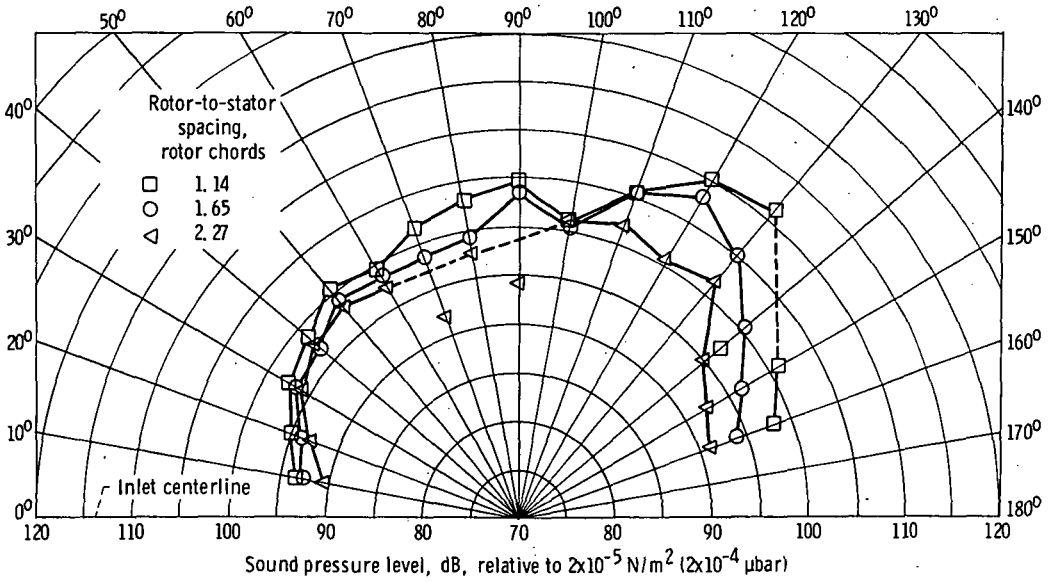

Figure 16. - Radiation pattern of second harmonic sound pressure level.

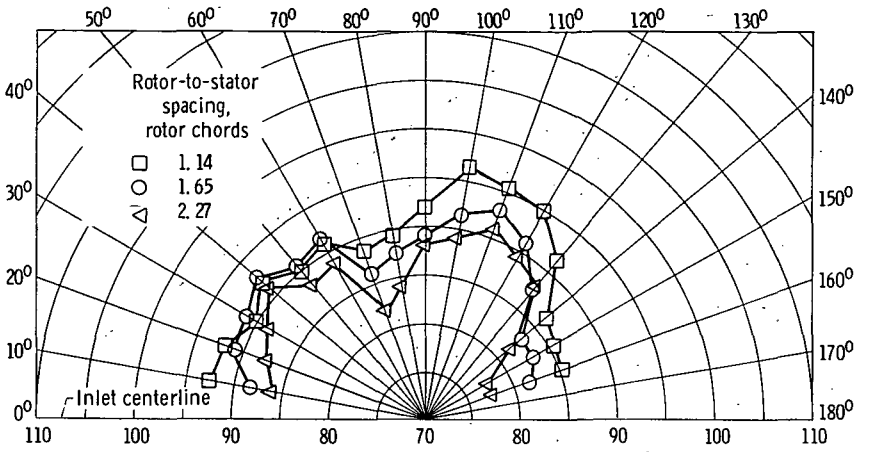

Figure 17. - Radiation pattern of third harmonic sound pressure level.

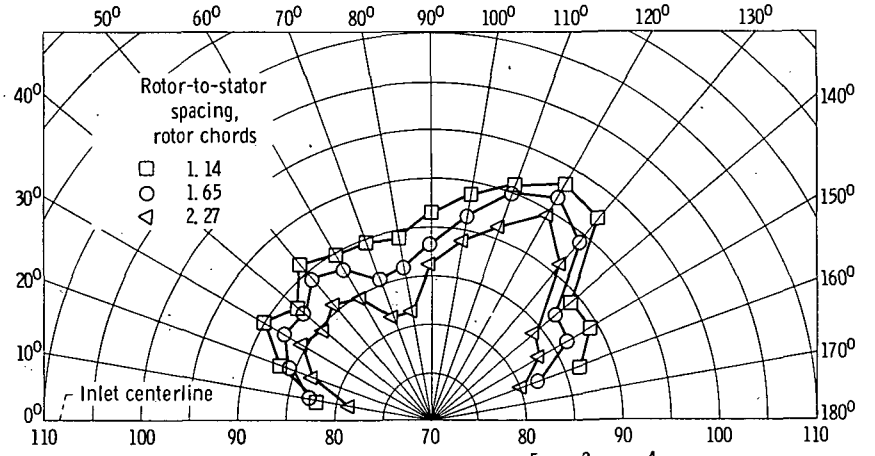

Figure 18. - Radiation pattern of fourth harmonic sound pressure level.

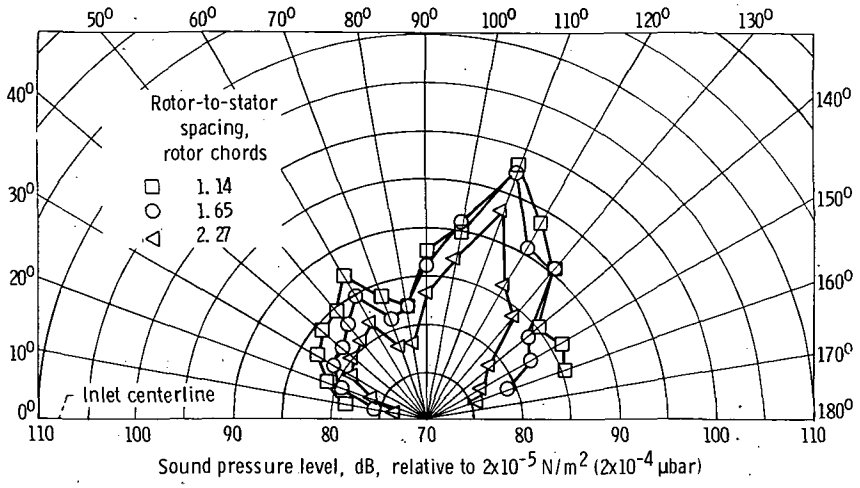

Figure 19. - Radiation pattern of fifth harmonic sound pressure level.

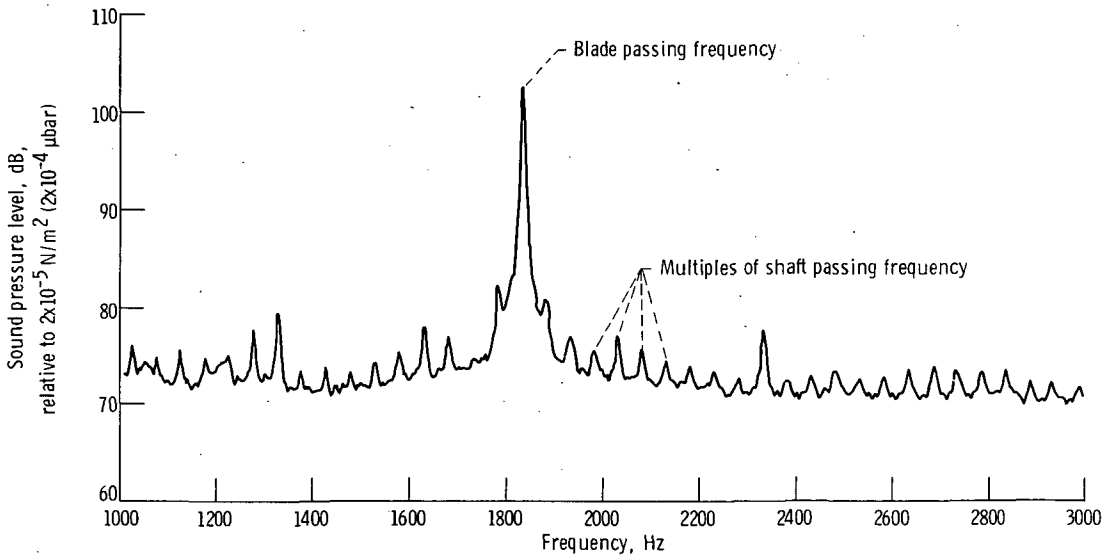

Figure 20. - Typical sound pressure level spectrum around fan tone.

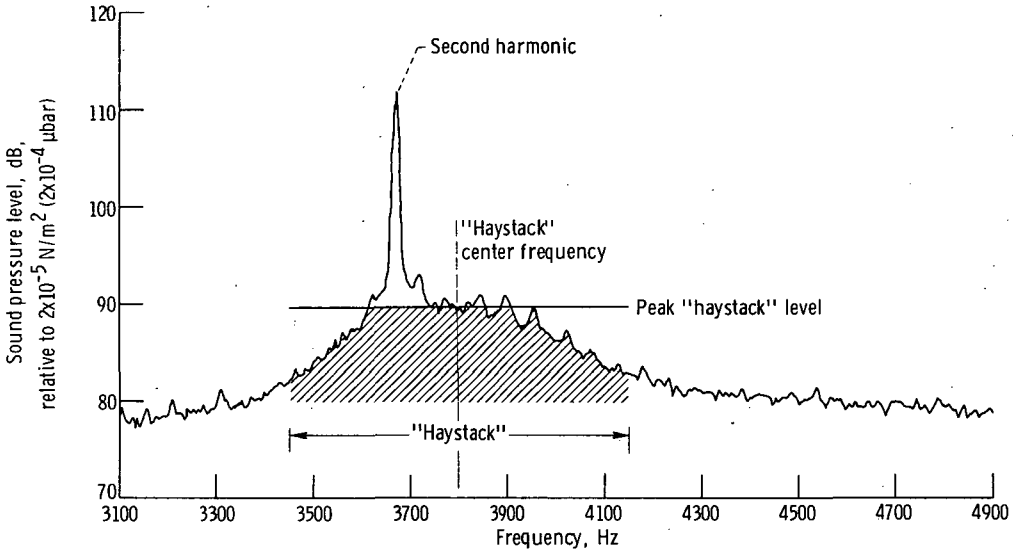

Figure 21. - Typical "haystack" spectrum.

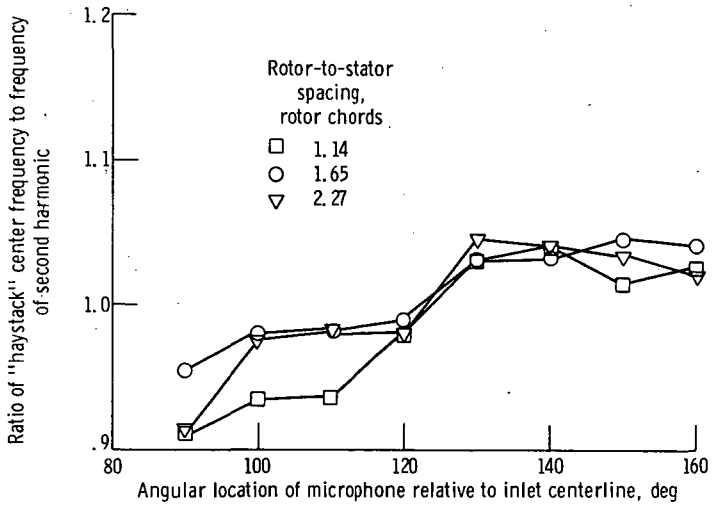

Figure 22. - Normalized center frequency of "haystack" as function of angular location of microphone.

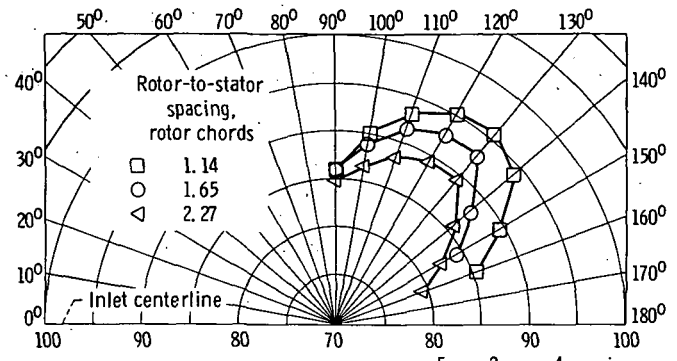

Figure 23. - Variation of peak amplitude of "haystack" with angle.

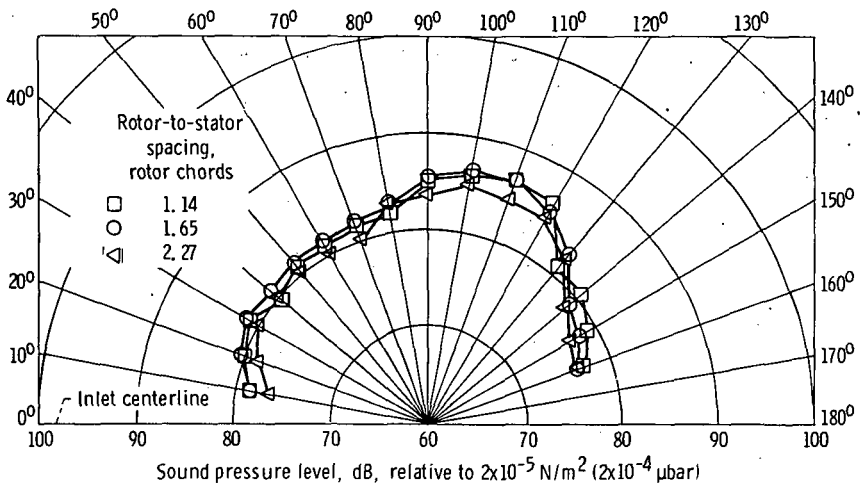

Figure 24. - Radiation pattern of fan broadband sound pressure level (30-Hz bandwidth at 3-kHz frequency).

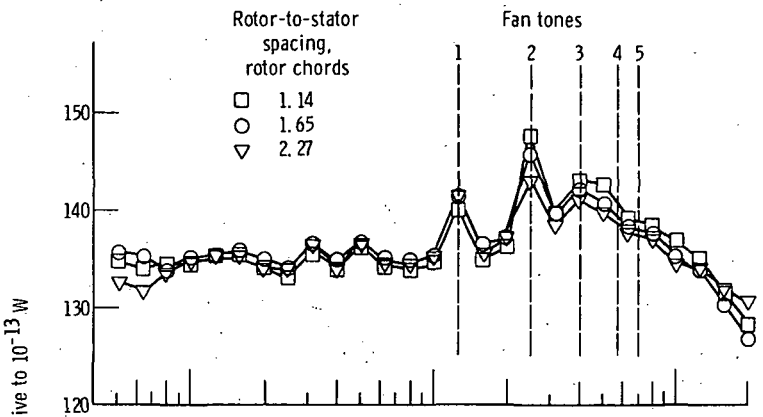

(a) Fan speed, 60 percent of design corrected speed.

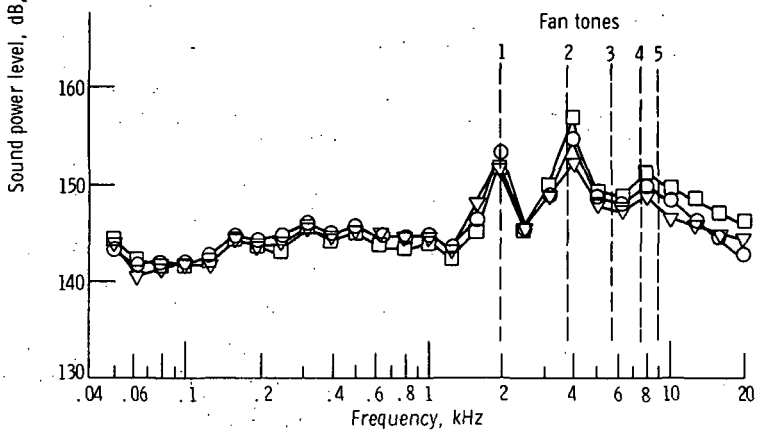

(b) Fan speed, 85 percent of design corrected speed.

Figure 25. - Sound power level spectra.

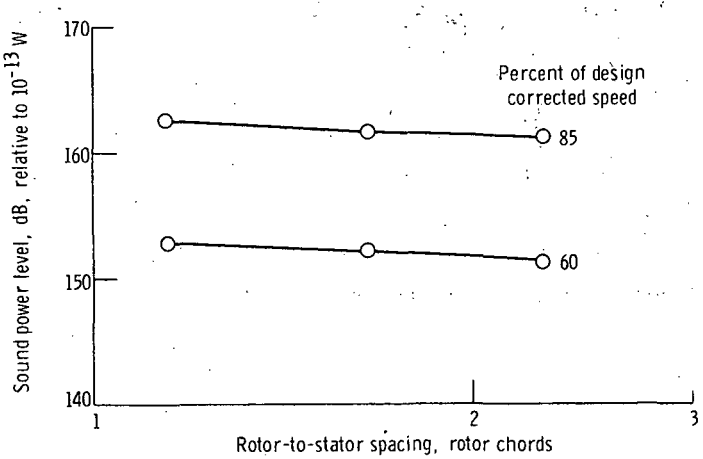

Figure 26. - Variation of total sound power level with rotor-to-stator spacing at constant speed.

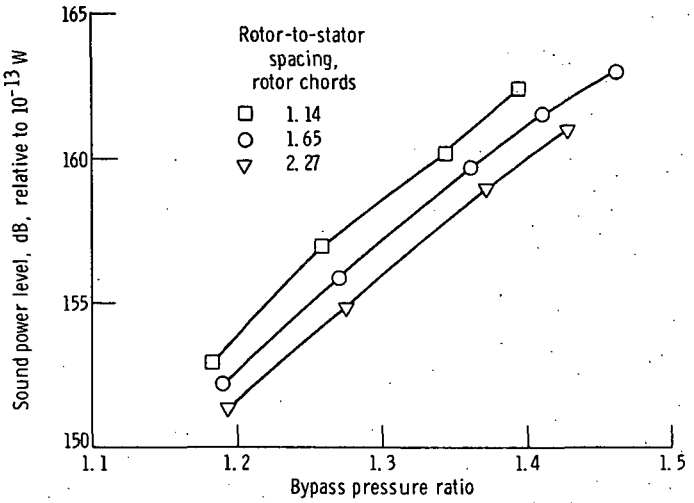

Figure 27. - Variation of sound power level with bypass pressure ratio.

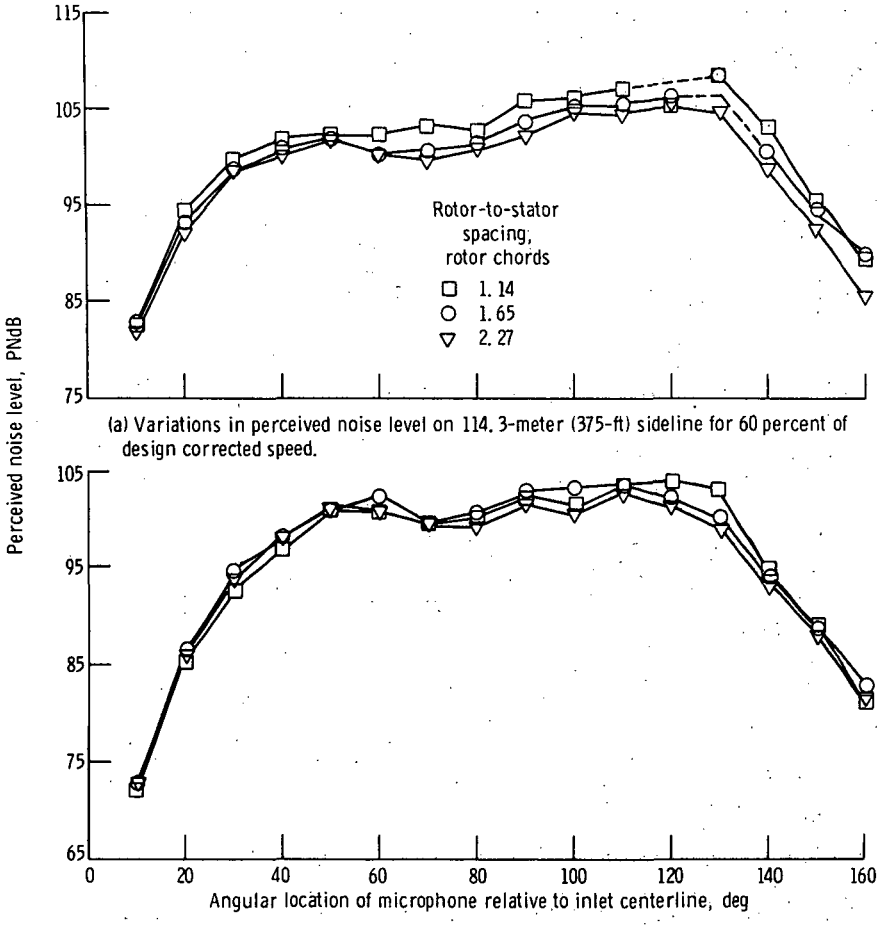

(a) Variations in perceived noise level on 114.3-meter (375-ft) sideline for 60 percent of design corrected speed.

(b) Variations in perceived noise level on 304.8-meter (1000-ft) sideline for 85 percent of design corrected speed.

Figure 28. - Directivity of perceived noise.

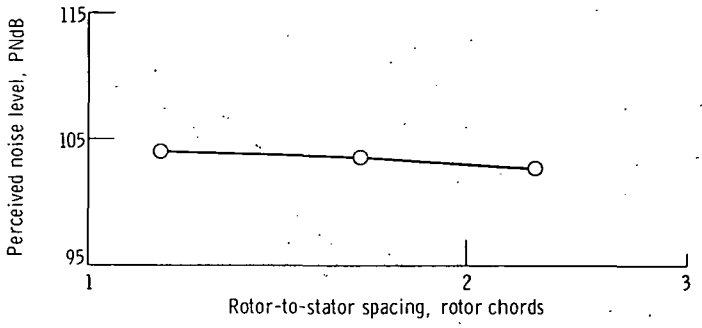

Figure 29. - Effect of rotor-to-stator spacing on perceived noise level on 304.8-meter (1000-ft) sideline at 85 percent speed.

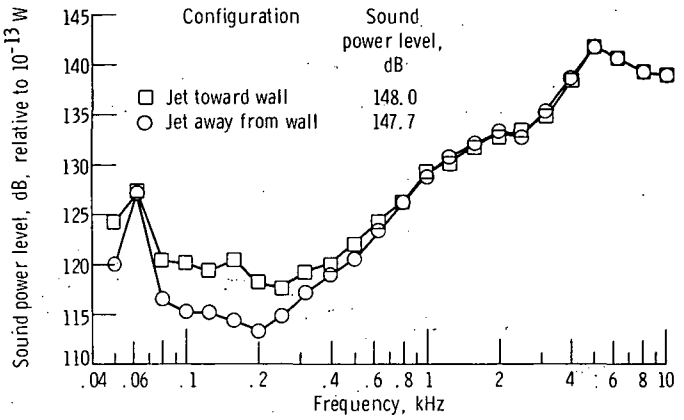

Figure 30. - Comparison of noise reflecting from treated building wall with free-field noise. Soft-wall calibration; nitrogen jet.

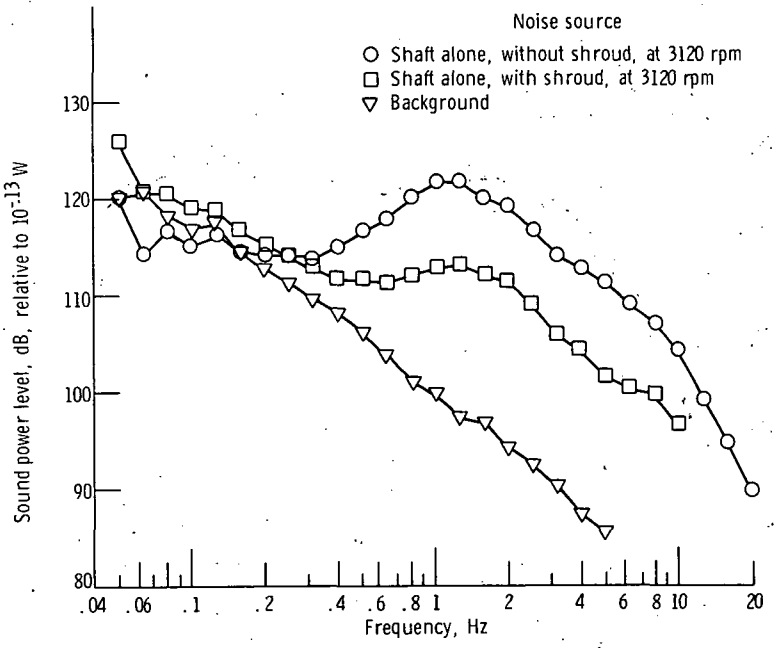

Figure 31. - Comparison of facility background noise levels without fan noise.

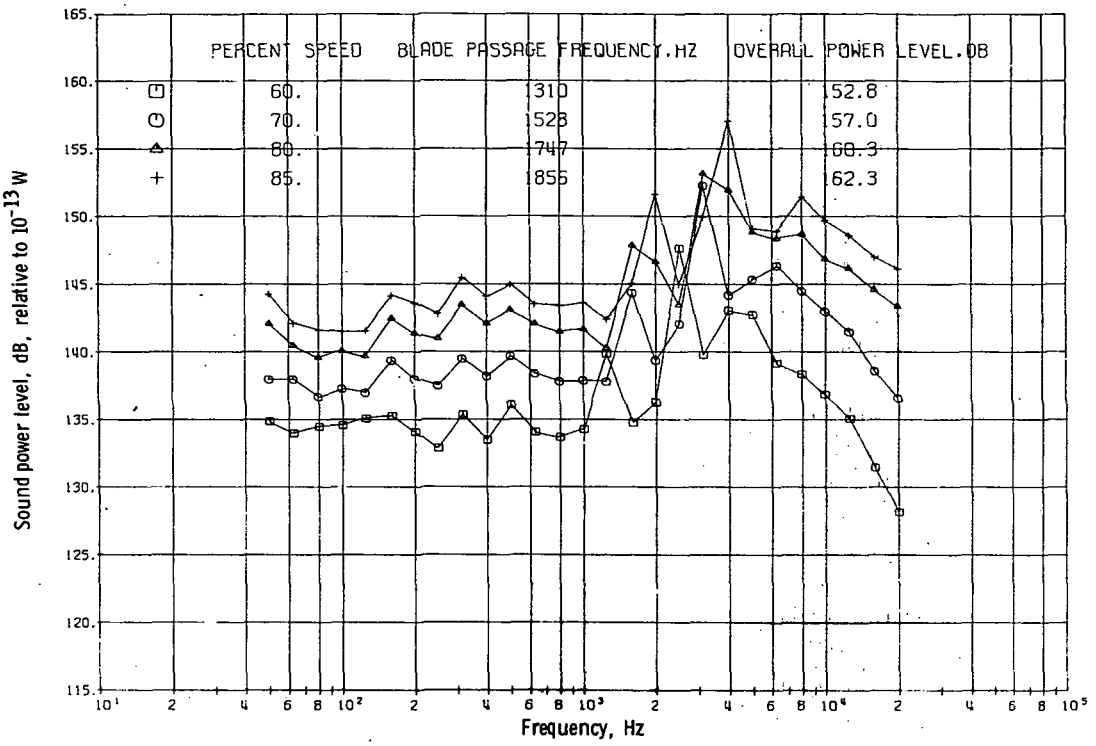

Figure 32. - Sound power levels with rotor-to-stator spacing of 1.14 chords.

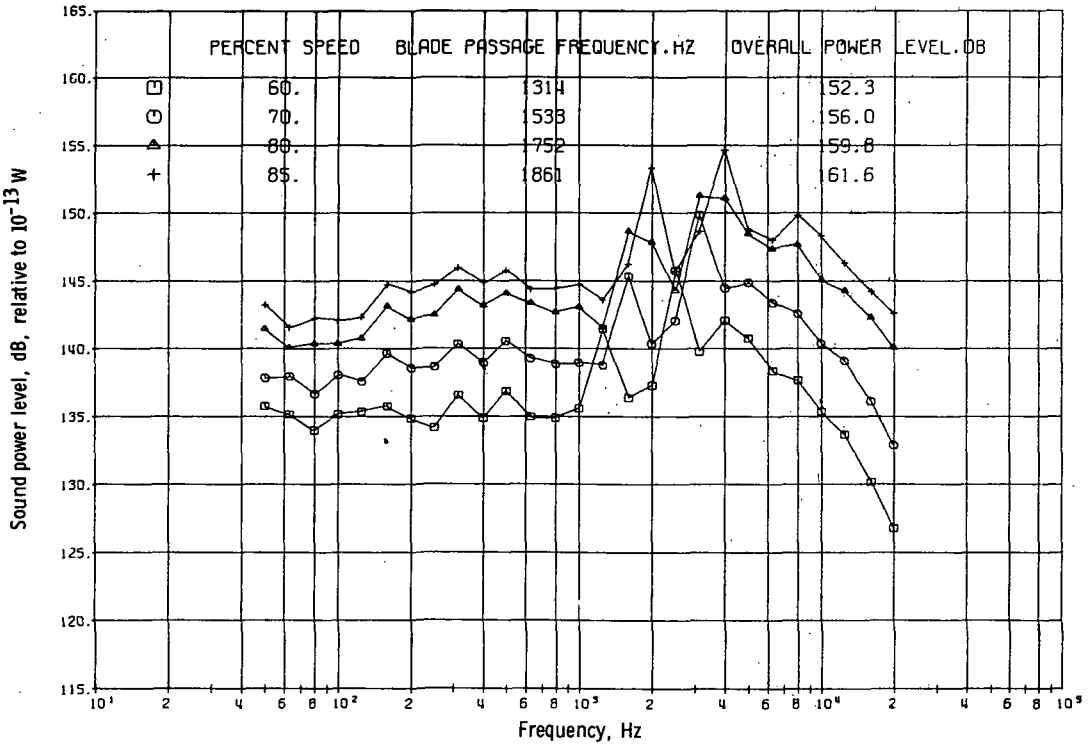

Figure 33. - Sound power levels with rotor-to-stator spacing of 1.65 chords.

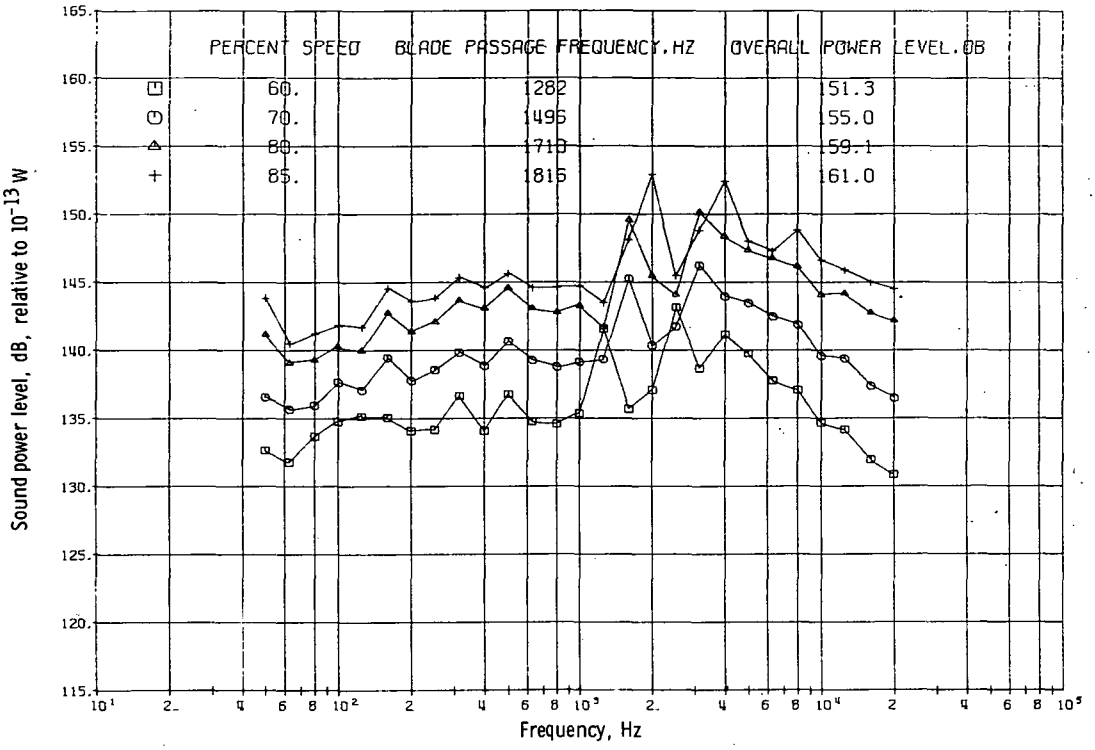

Figure 34. - Sound power levels with rotor-to-stator spacing of 2.27 chords.

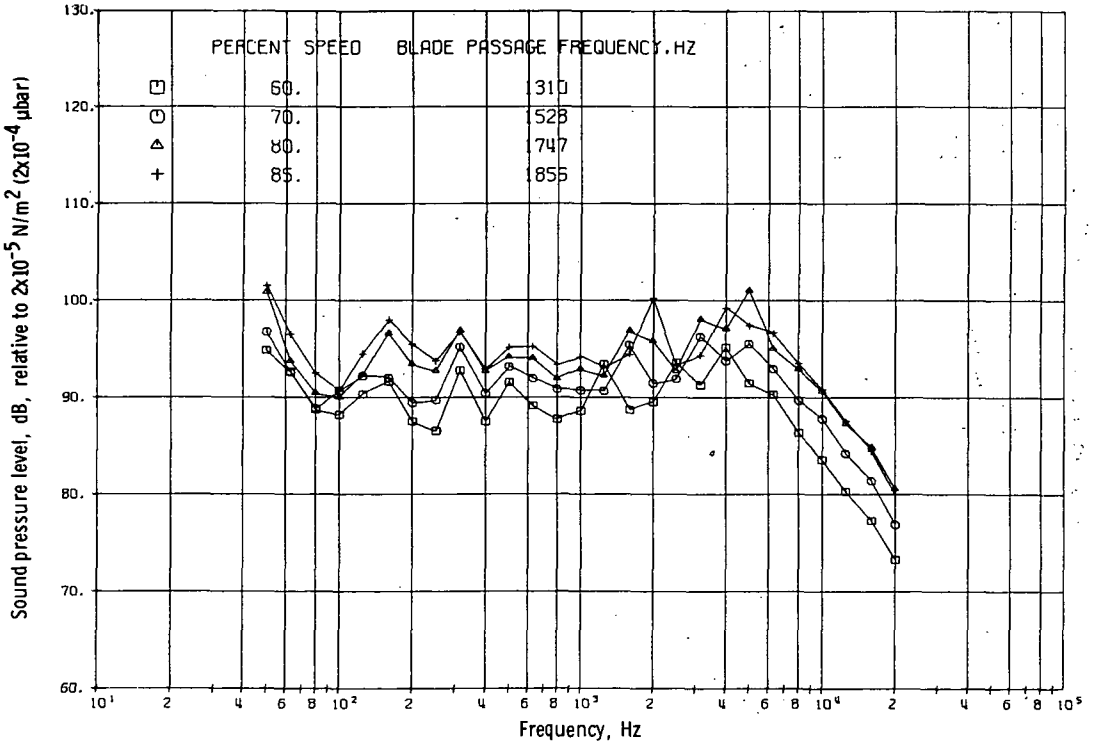

Figure 35. - Sound pressure levels with rotor-to-stator spacing of 1.14 chords, at 30.48-meter (100-ft) radius and 10^0 angular location.

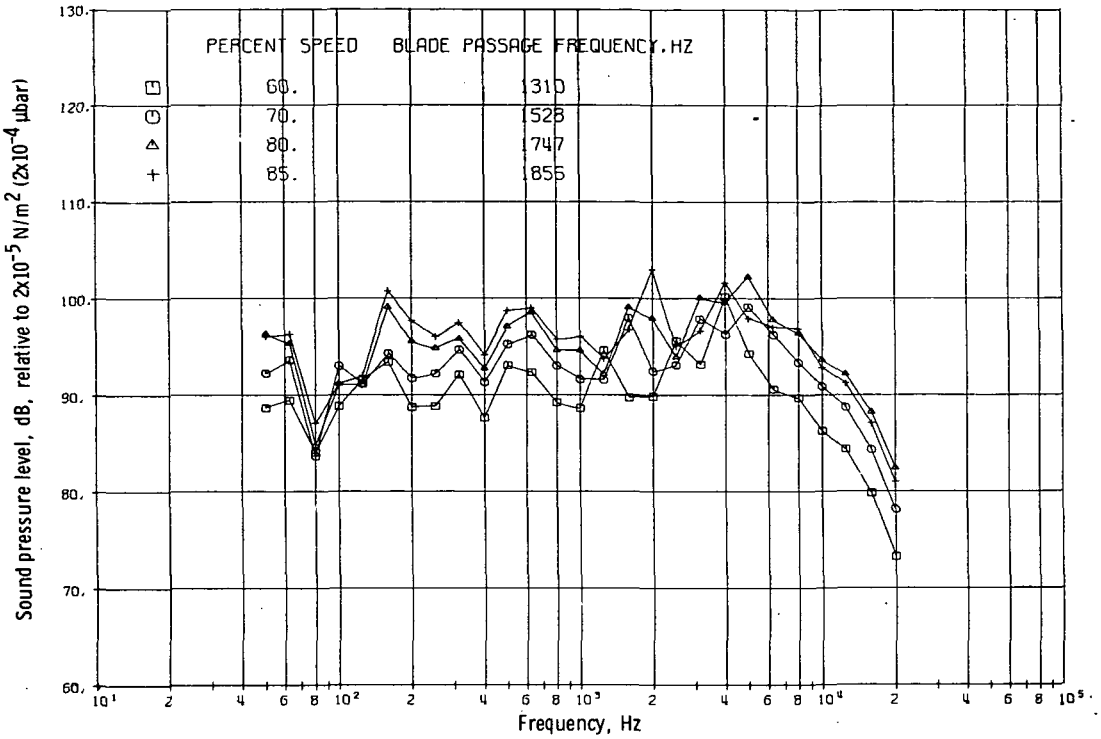

Figure 36. - Sound pressure levels with rotor-to-stator spacing of 1.14 chords, at 30.48-meter (100-ft) radius and 20^0 angular location.

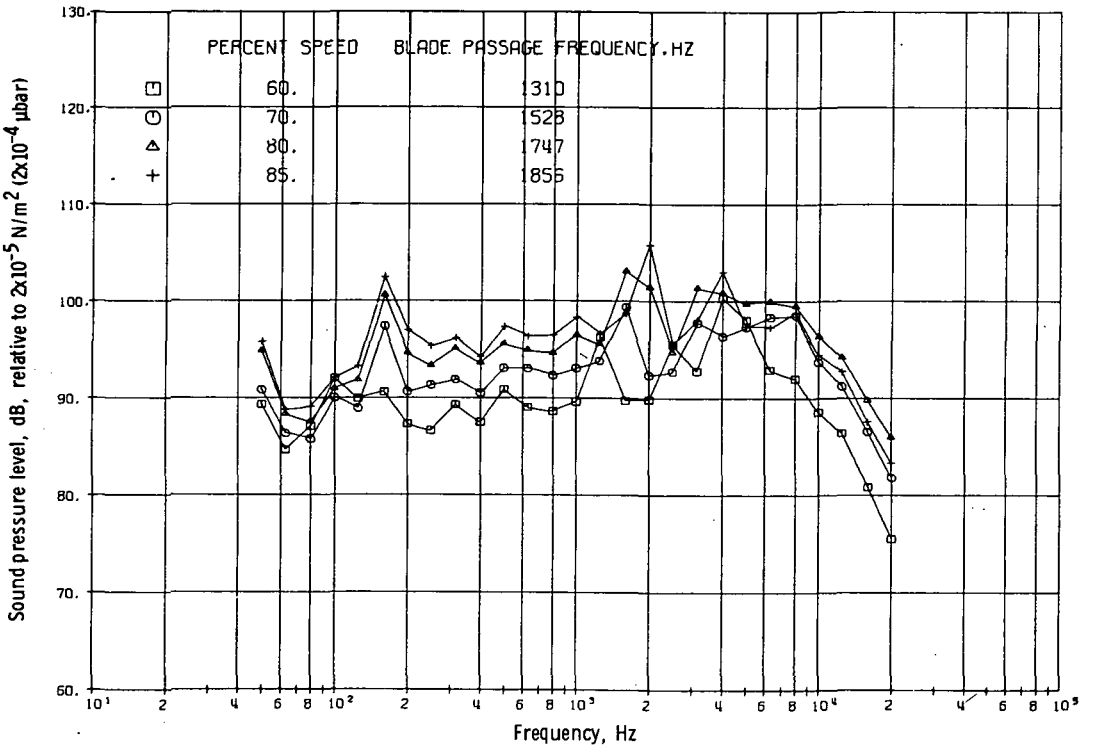

Figure 37. - Sound pressure levels with rotor-to-stator spacing of 1.14 chords, at 30.48-meter (100-ft) radius and 30^0 angular location.

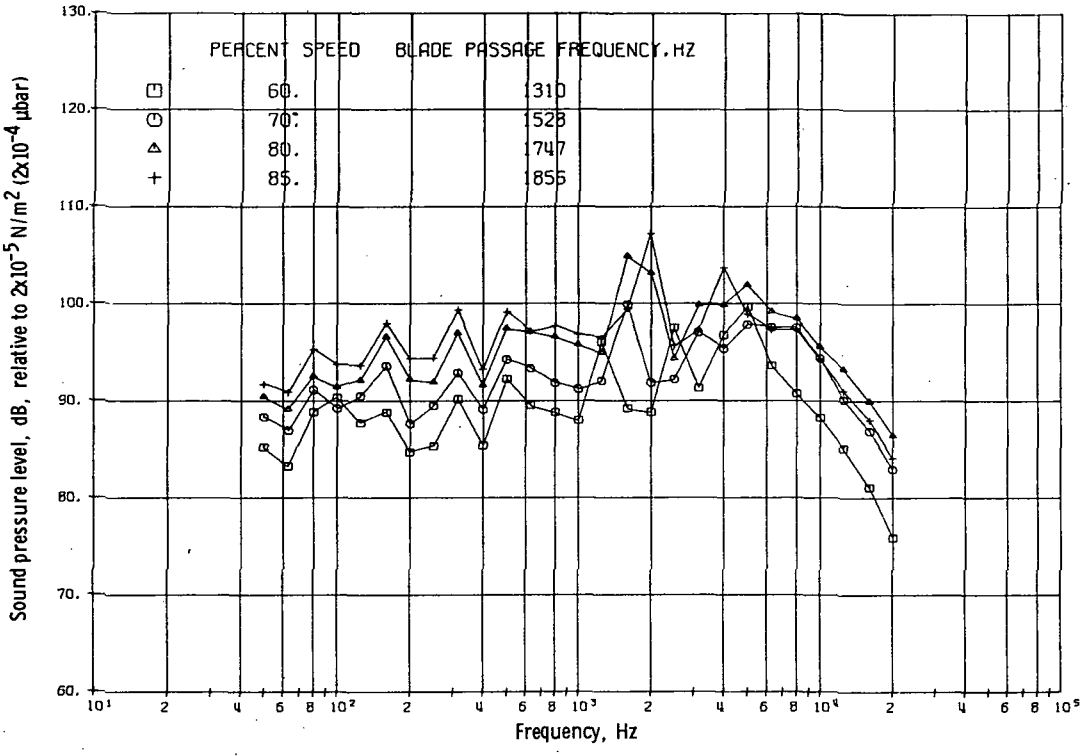

Figure 38. - Sound pressure levels with rotor-to-stator spacing of 1.14 chords, at 30.48-meter (100-ft) radius and 40^0 angular location.

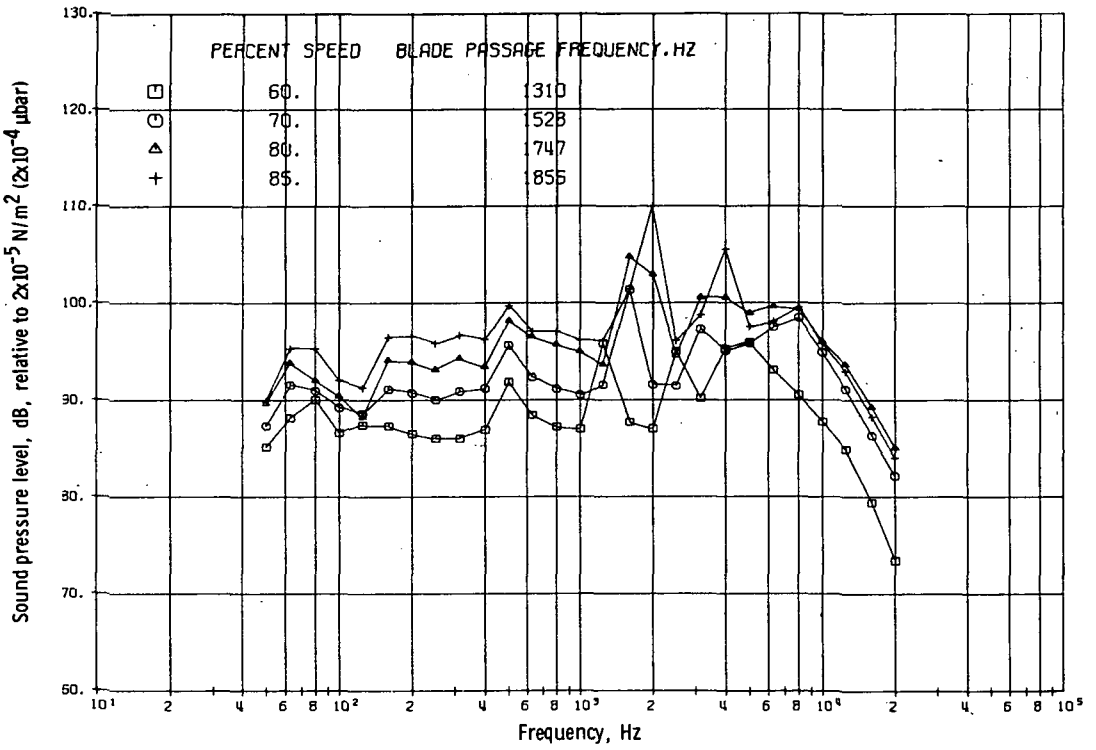

Figure 39. - Sound pressure levels with rotor-to-stator spacing of 1.14 chords, at 30.48-meter (100-ft) radius and 50^0 angular location.

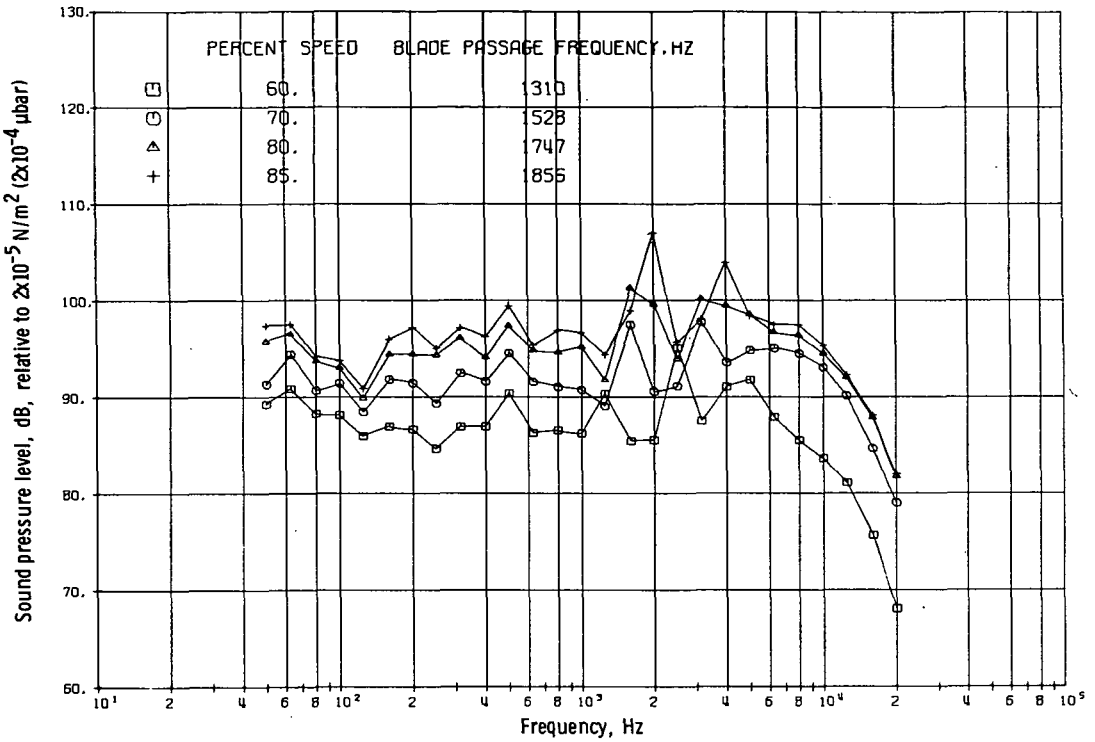

Figure 40. - Sound pressure levels with rotor-to-stator spacing of 1.14 chords, at 30.48-meter (100-ft) radius and 60^0 angular location.

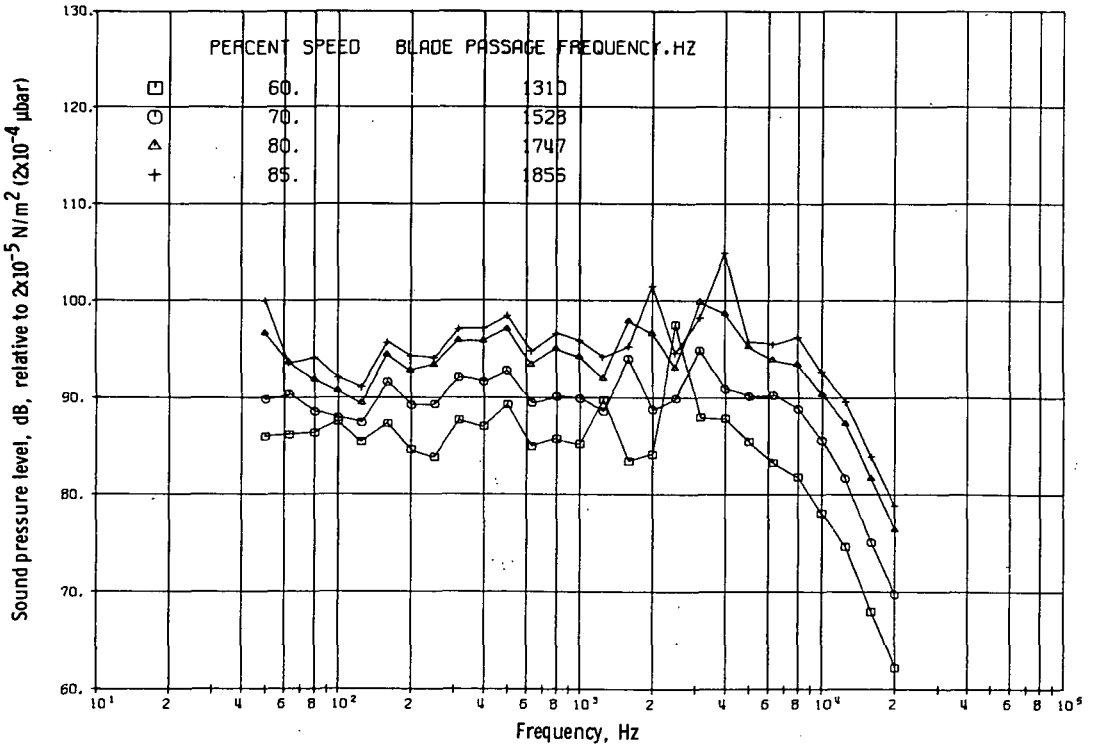

Figure 41. - Sound pressure levels with rotor-to-stator spacing of 1.14 chords, at 30.48-meter (100-ft) radius and 70^0 angular location.

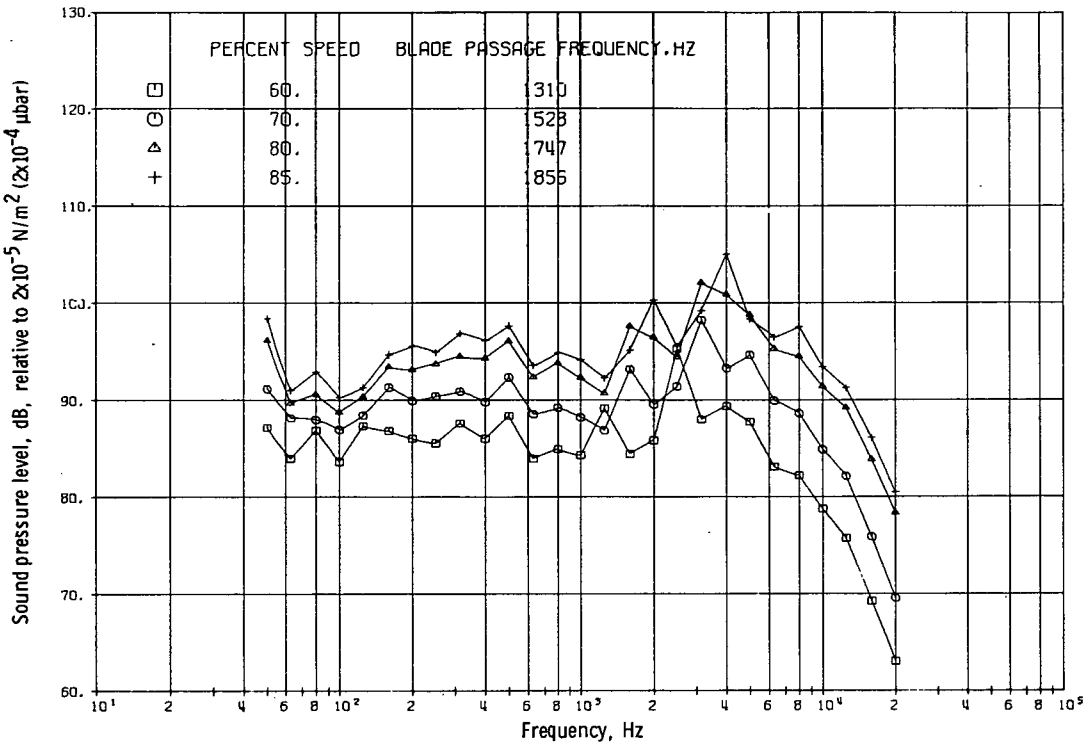

Figure 42. - Sound pressure levels with rotor-to-stator spacing of 1.14 chords, at 30.48-meter (100-ft) radius and 80^0 angular location.

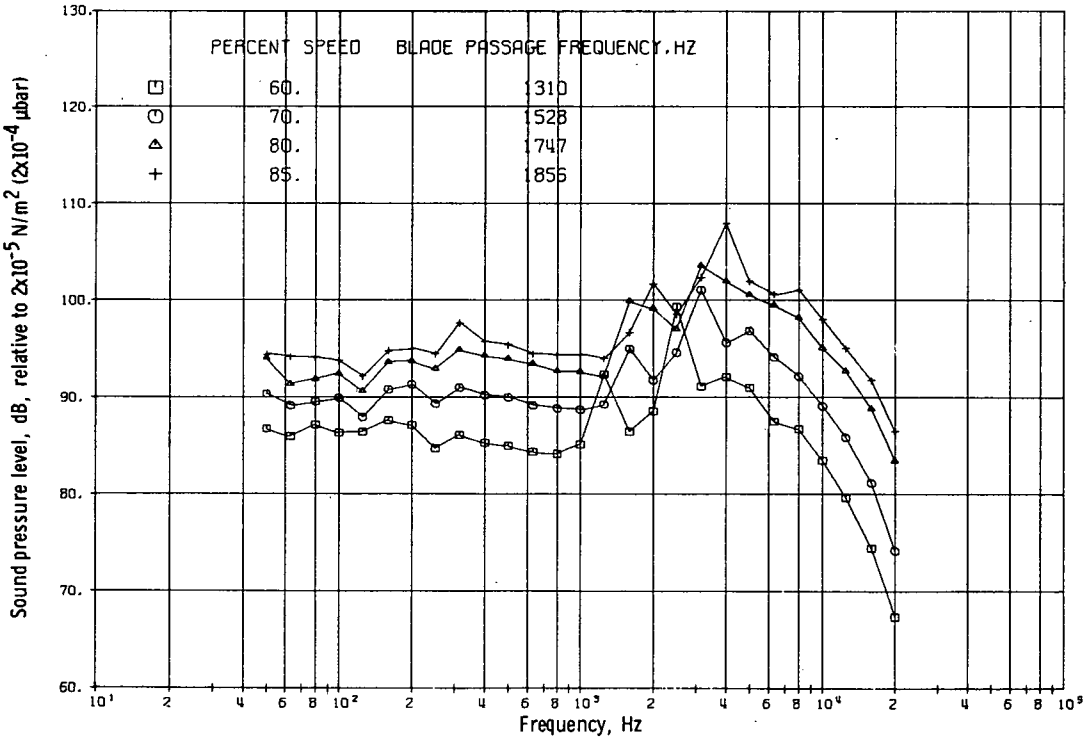

Figure 43. - Sound pressure levels with rotor-to-stator spacing of 1.14 chords, at 30.48-meter (100-ft) radius and 90^0 angular location.

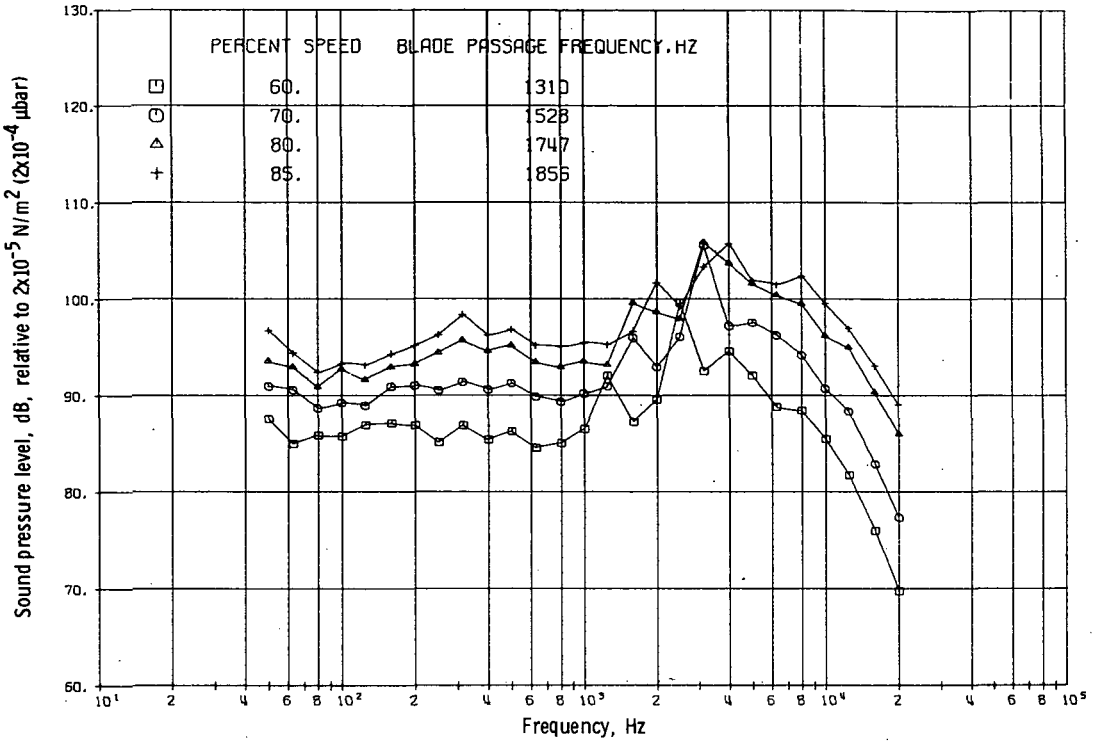

Figure 44. - Sound pressure levels with rotor-to-stator spacing of 1.14 chords, at 30.48-meter (100-ft) radius and 100^{0} angular location.

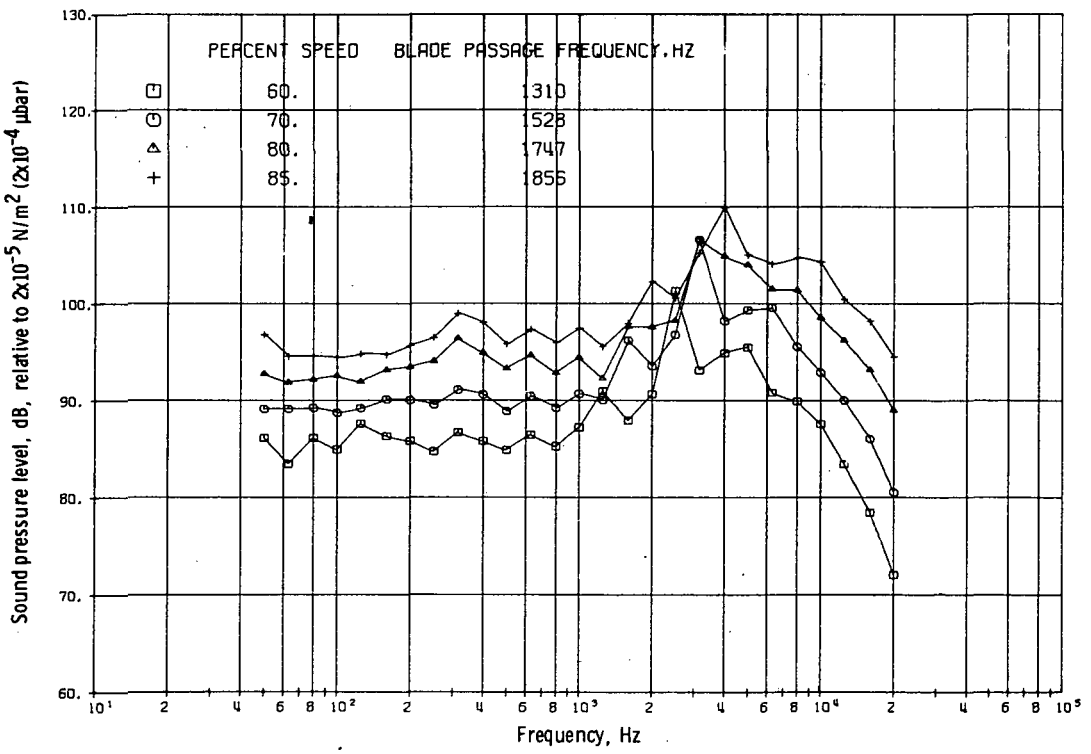

Figure 45. - Sound pressure levels with rotor-to-stator spacing of 1.14 chords, at 30.48-meter (100-ft) radius and 110^{0} angular location.

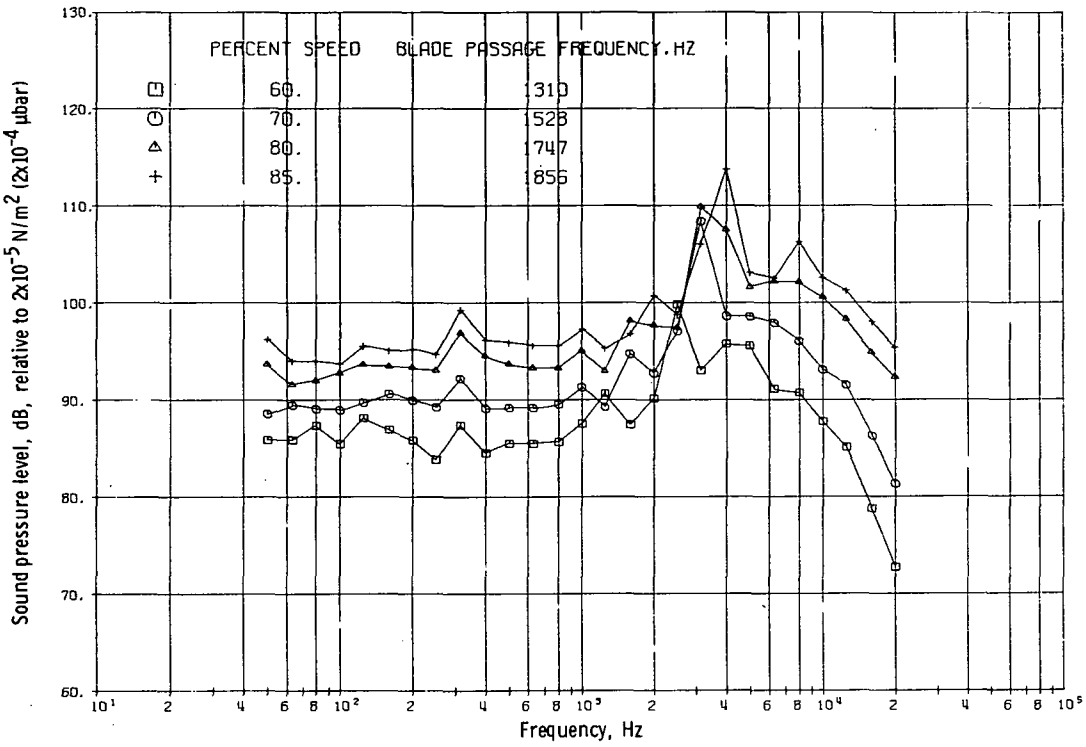

Figure 46. - Sound pressure levels with rotor-to-stator spacing of 1.14 chords, at 30.48-meter (100-ft) radius and 120^0 angular location.

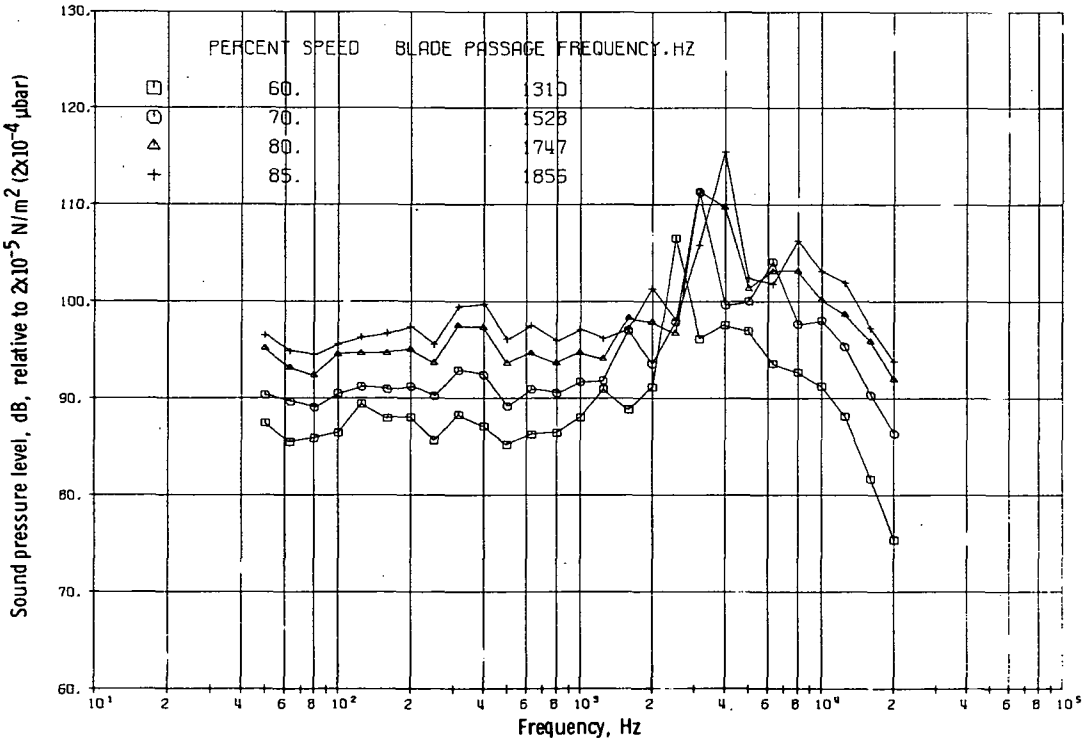

Figure 47. - Sound pressure levels with rotor-to-stator spacing of 1.14 chords, at 30.48-meter (100-ft) radius and 130^0 angular location.

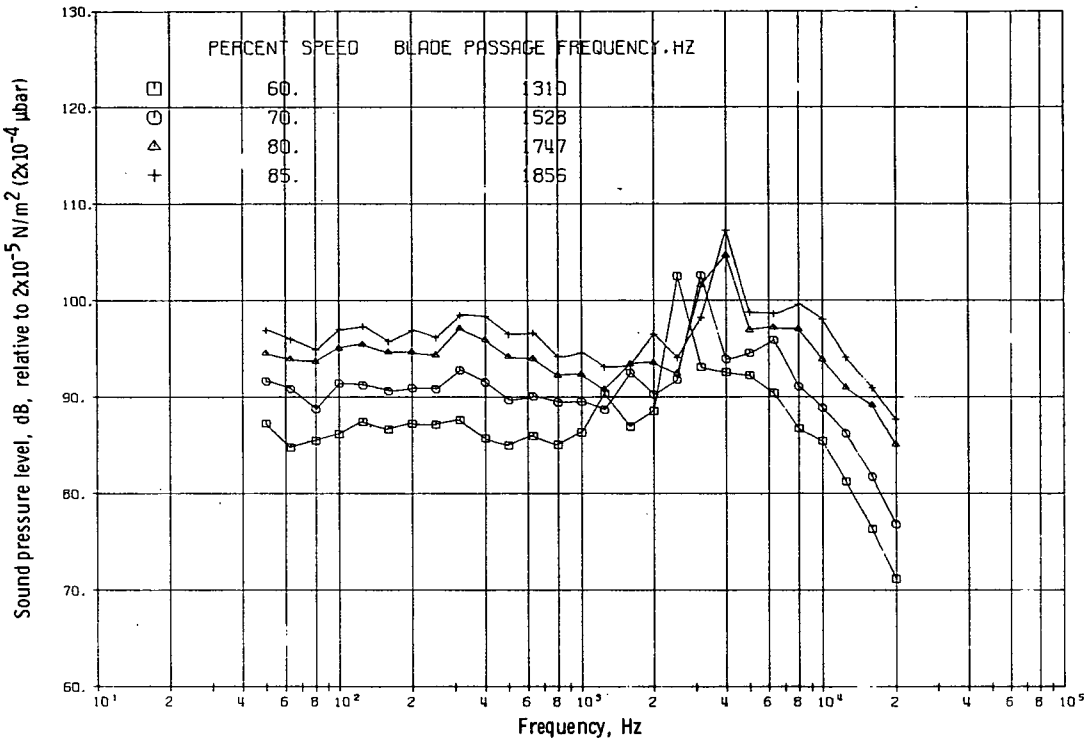

Figure 48. - Sound pressure levels with rotor-to-stator spacing of 1.14 chords, at 30.48-meter (100-ft) radius and 140^0 angular location.

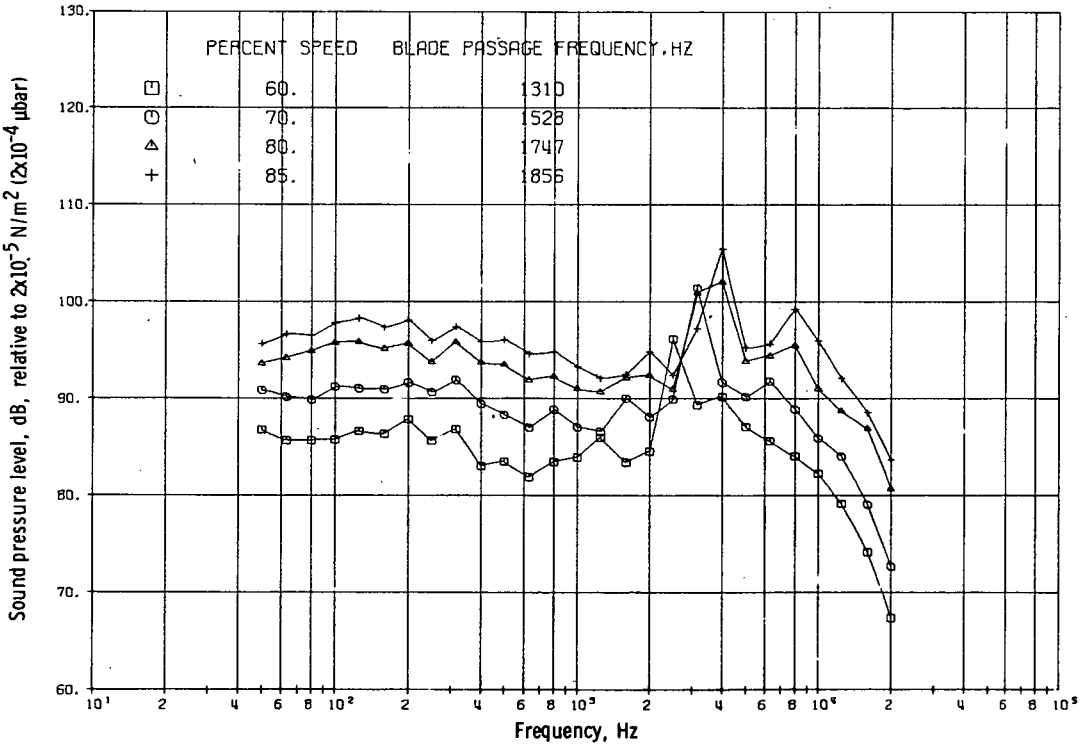

Figure 49. - Sound pressure levels with rotor-to-stator spacing of 1.14 chords, at 30.48-meter (100-ft) radius and 150^0 angular location.

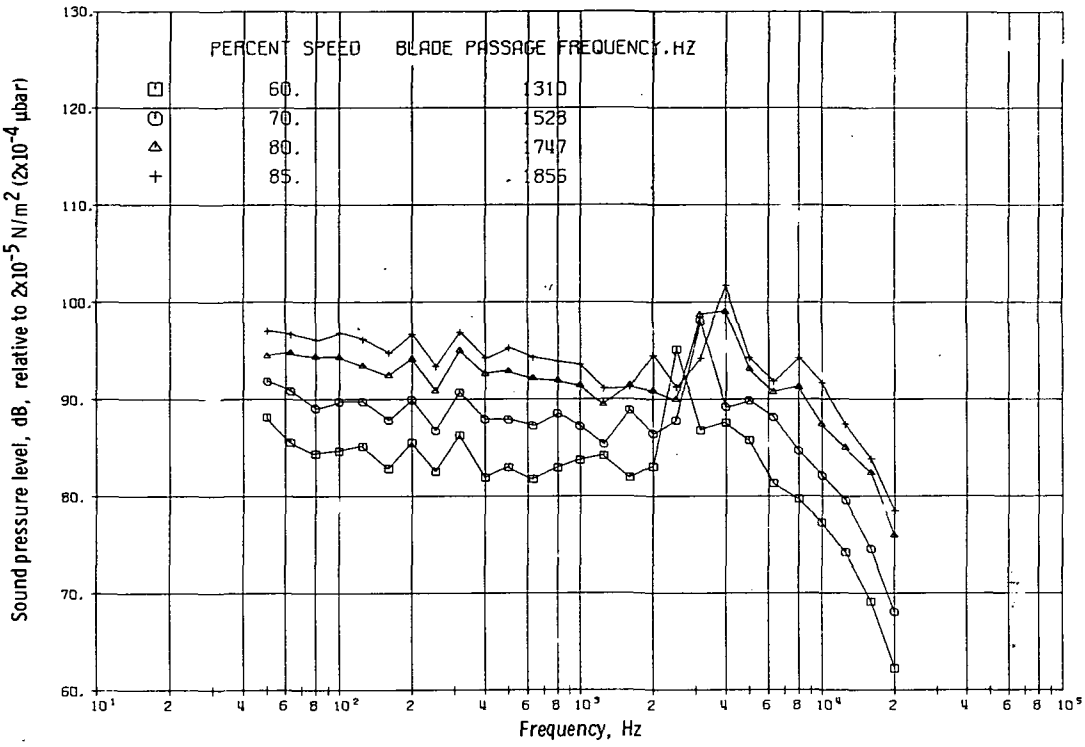

Figure 50. - Sound pressure levels with rotor-to-stator spacing of 1.14 chords, at 30.48-meter (100-ft) radius and 160^0 angular location.

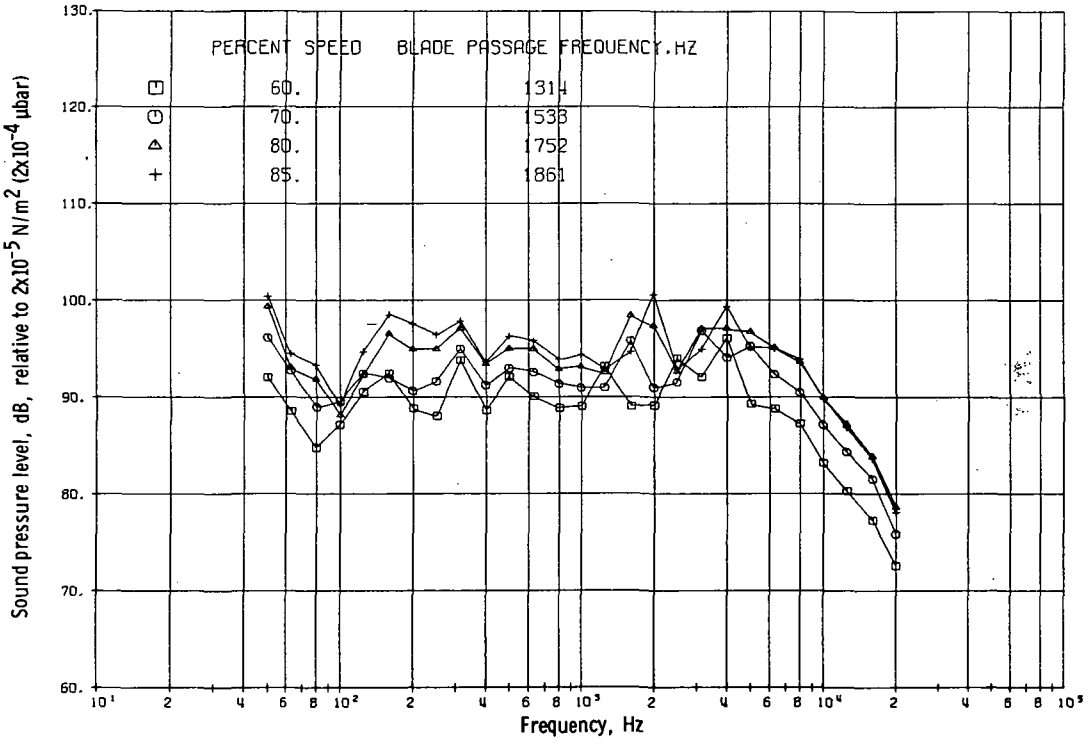

Figure 51. - Sound pressure levels with rotor-to-stator spacing of 1.65 chords, at 30.48-meter (100-ft) radius and 10^0 angular location.

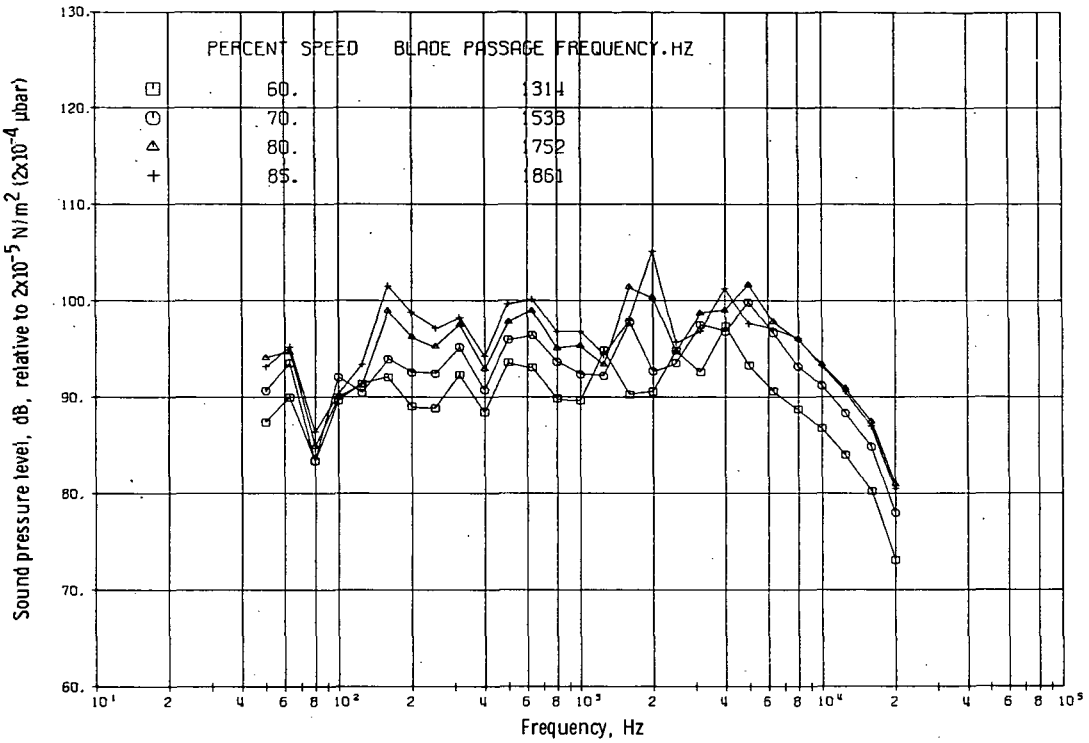

Figure 52. - Sound pressure levels with rotor-to-stator spacing of 1.65 chords, at 30.48-meter (100-ft) radius and 20^0 angular location.

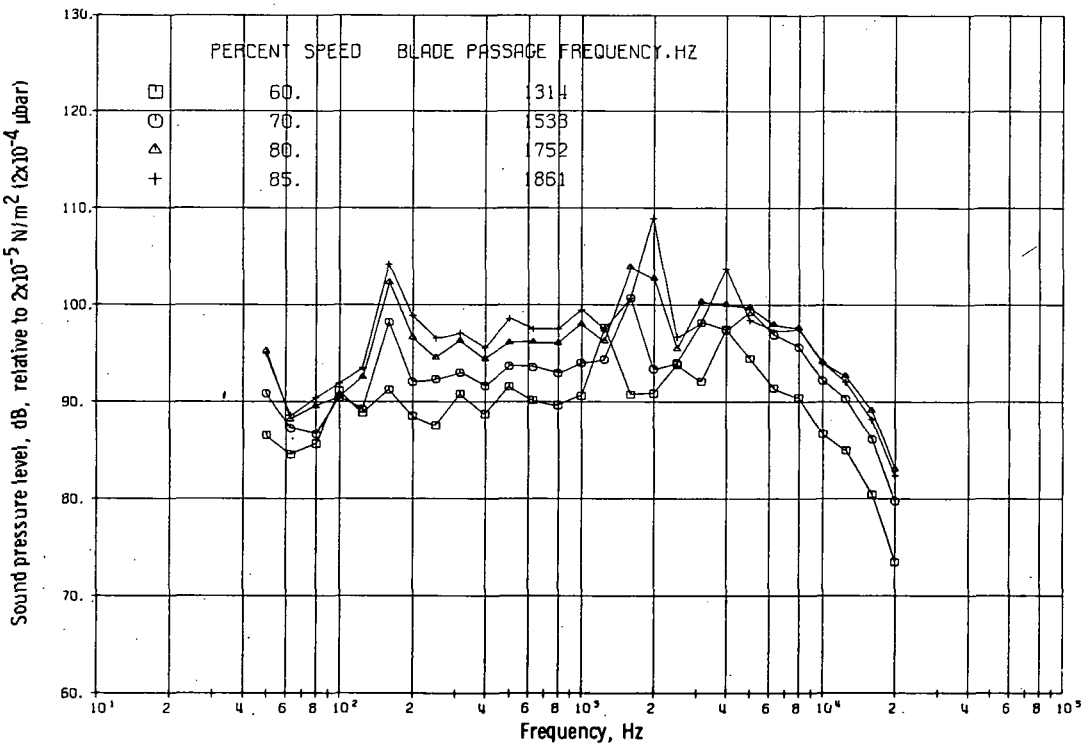

Figure 53. - Sound pressure levels with rotor-to-stator spacing of 1.65 chords, at 30.48-meter (100-ft) radius and 30^0 angular location.

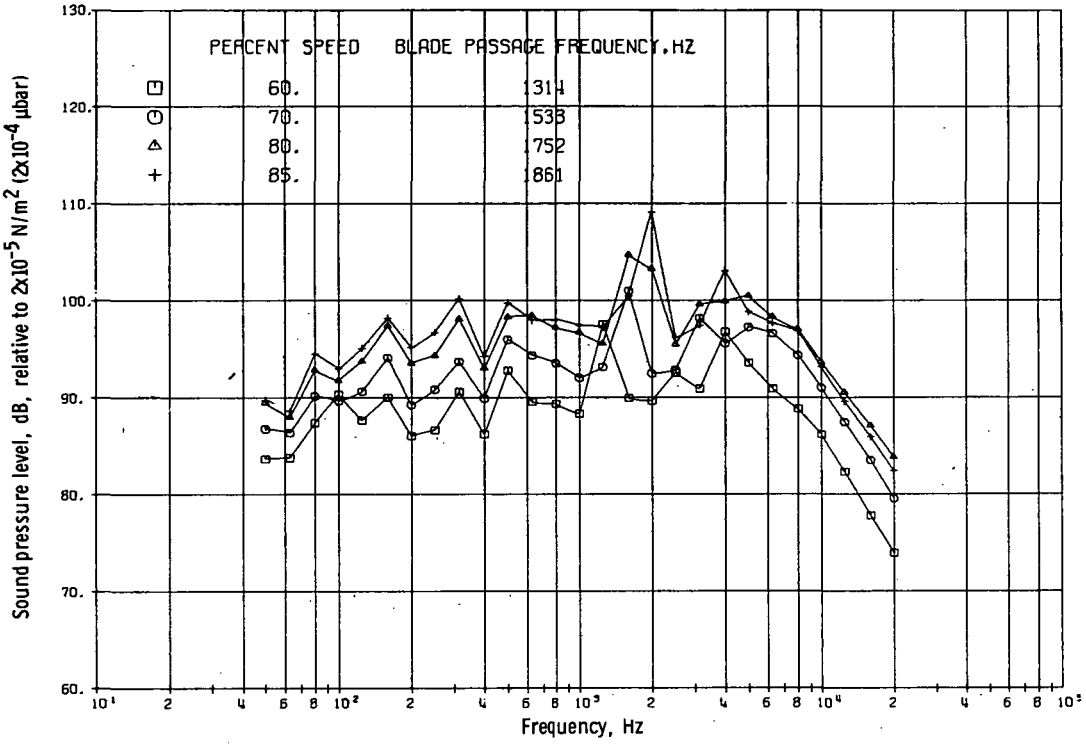

Figure 54. - Sound pressure levels with rotor-to-stator spacing of 1.65 chords, at 30.48-meter (100-ft) radius and 40^0 angular location.

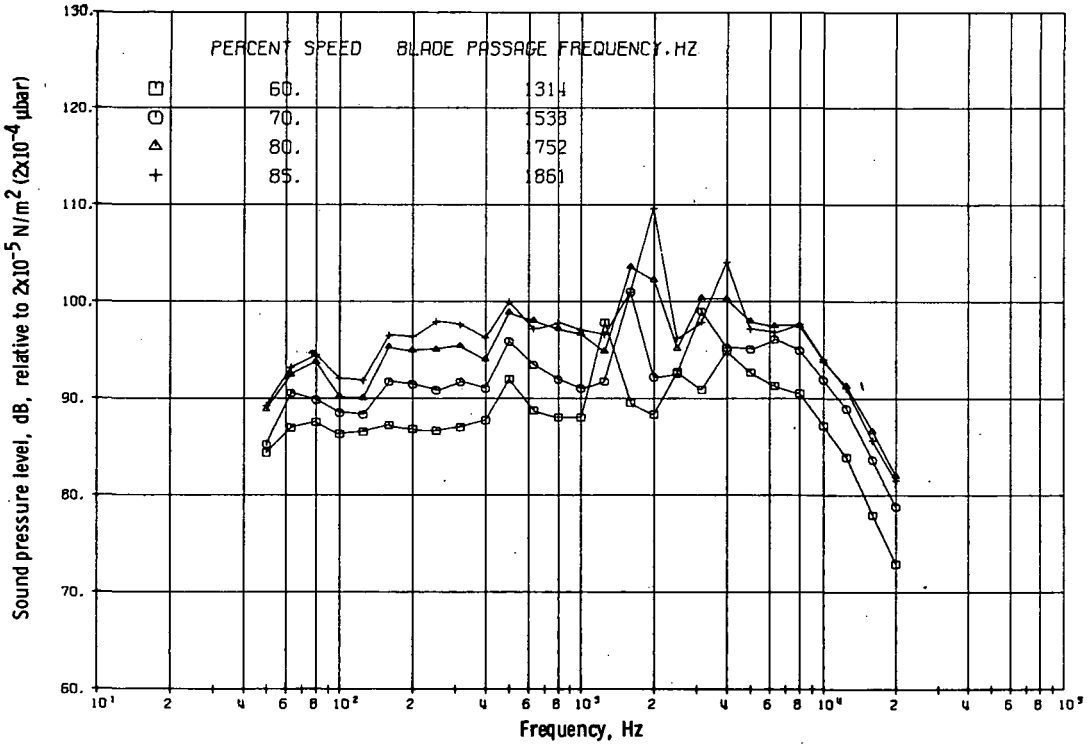

Figure 55. - Sound pressure levels with rotor-to-stator spacing of 1.65 chords, at 30.48-meter (100-ft) radius and 50^0 angular location.

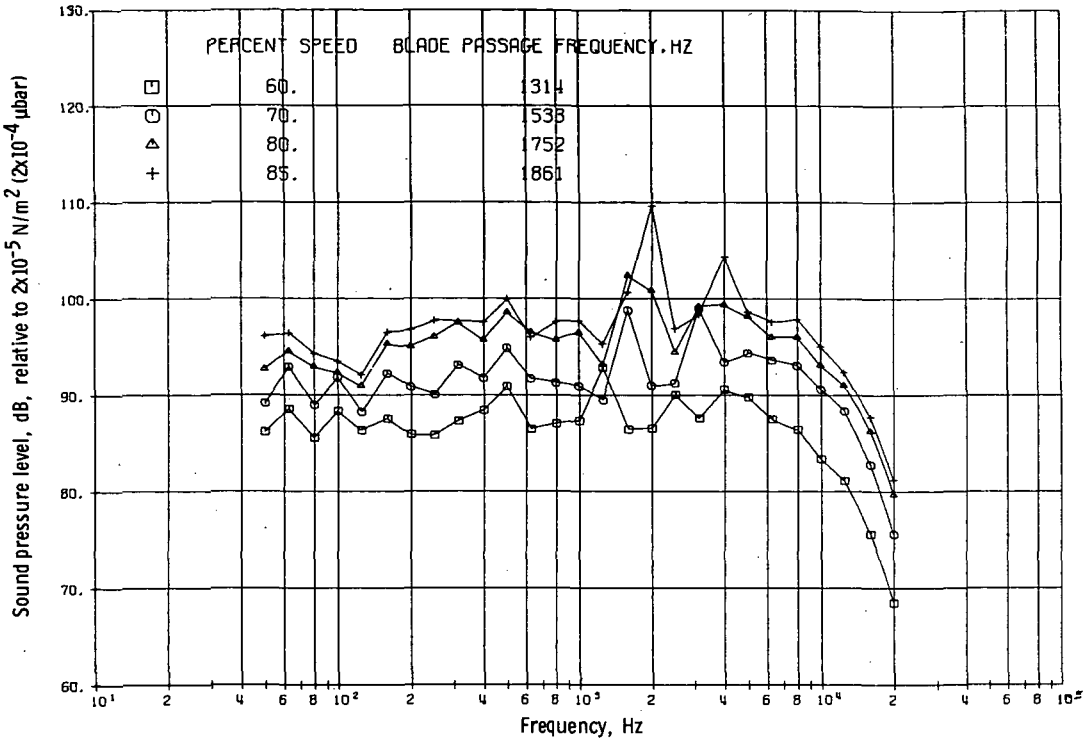

Figure 56. - Sound pressure levels with rotor-to-stator spacing of 1.65 chords, at 30.48-meter (100-ft) radius and 60^0 angular location.

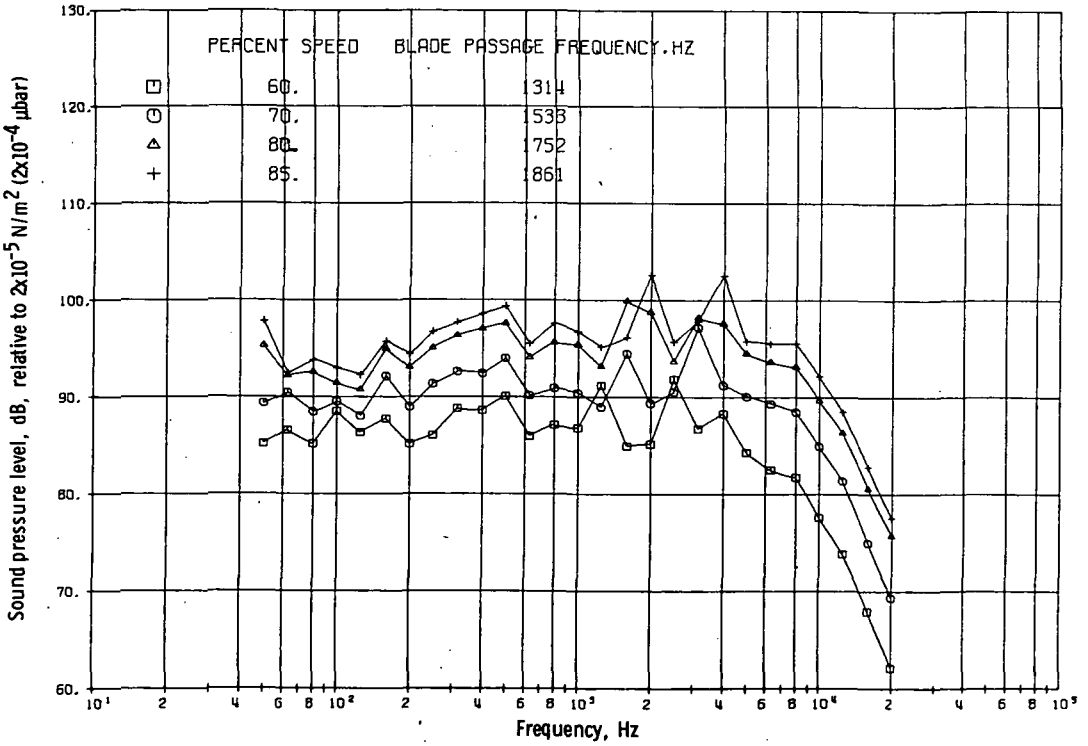

Figure 57. - Sound pressure levels with rotor-to-stator spacing of 1.65 chords, at 30.48-meter (100-ft) radius and 70^0 angular location.

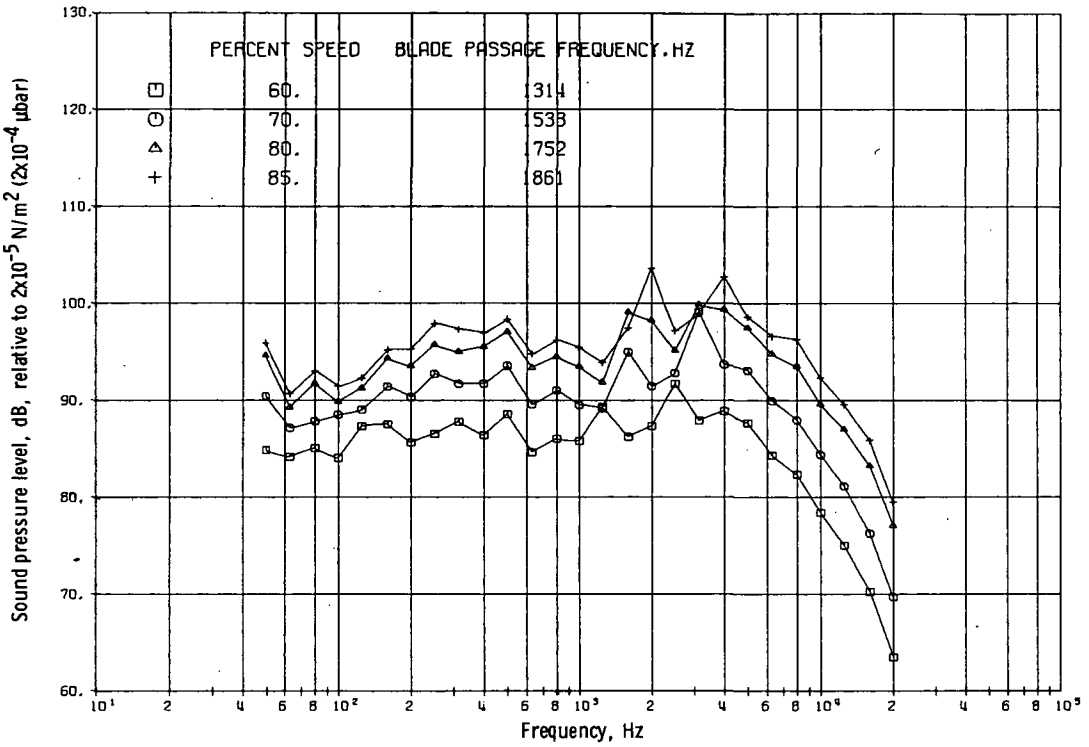

Figure 58. - Sound pressure levels with rotor-to-stator spacing of 1.65 chords, at 30.48-meter (100-ft) radius and 80° angular location.

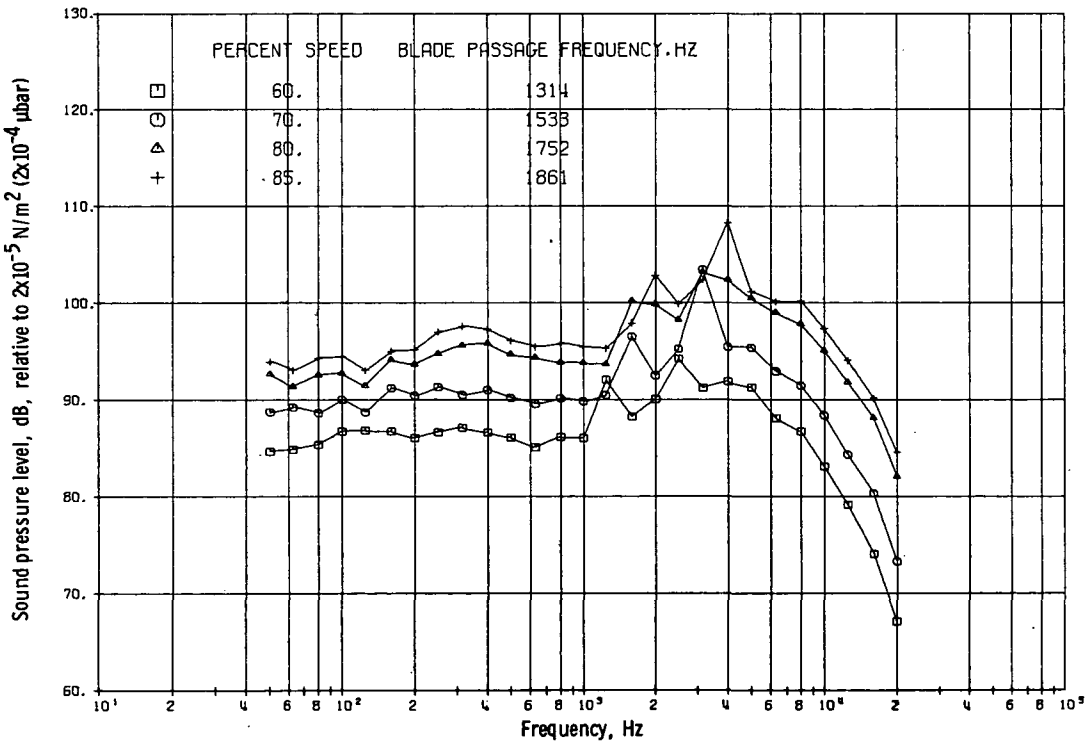

Figure 59. - Sound pressure levels with rotor-to-stator spacing of 1.65 chords, at 30.48-meter (100-ft) radius and 90° angular location.

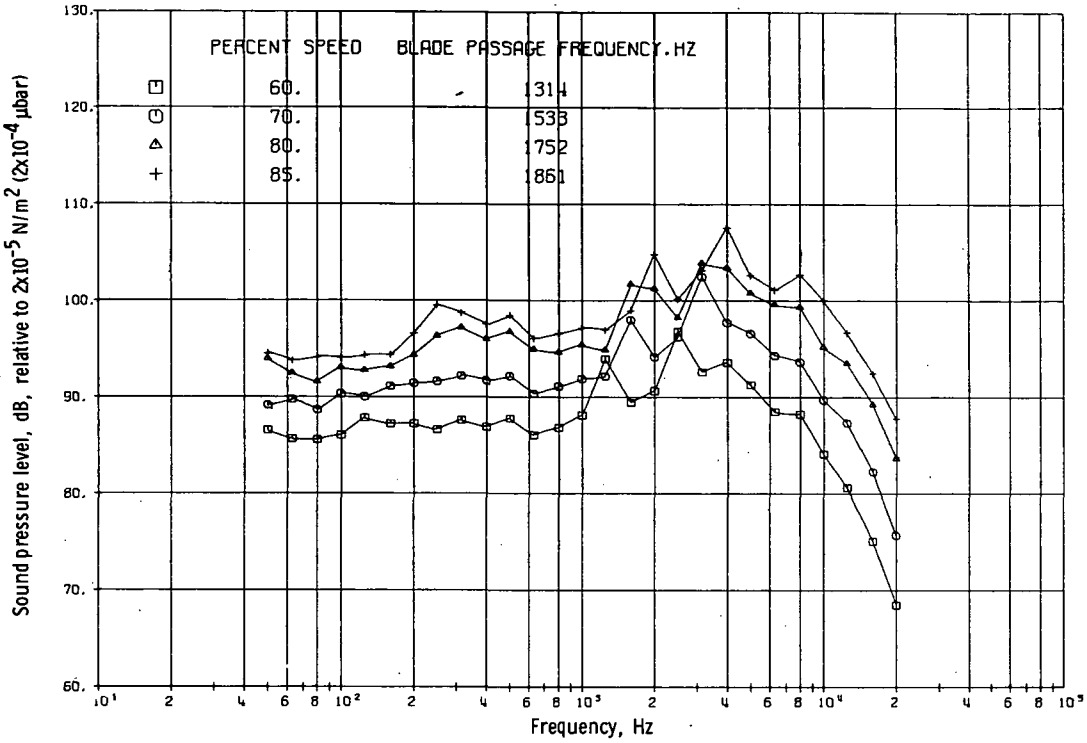

Figure 60. - Sound pressure levels with rotor-to-stator spacing of 1.65 chords, at 30.48-meter (100-ft) radius and 100^0 angular location.

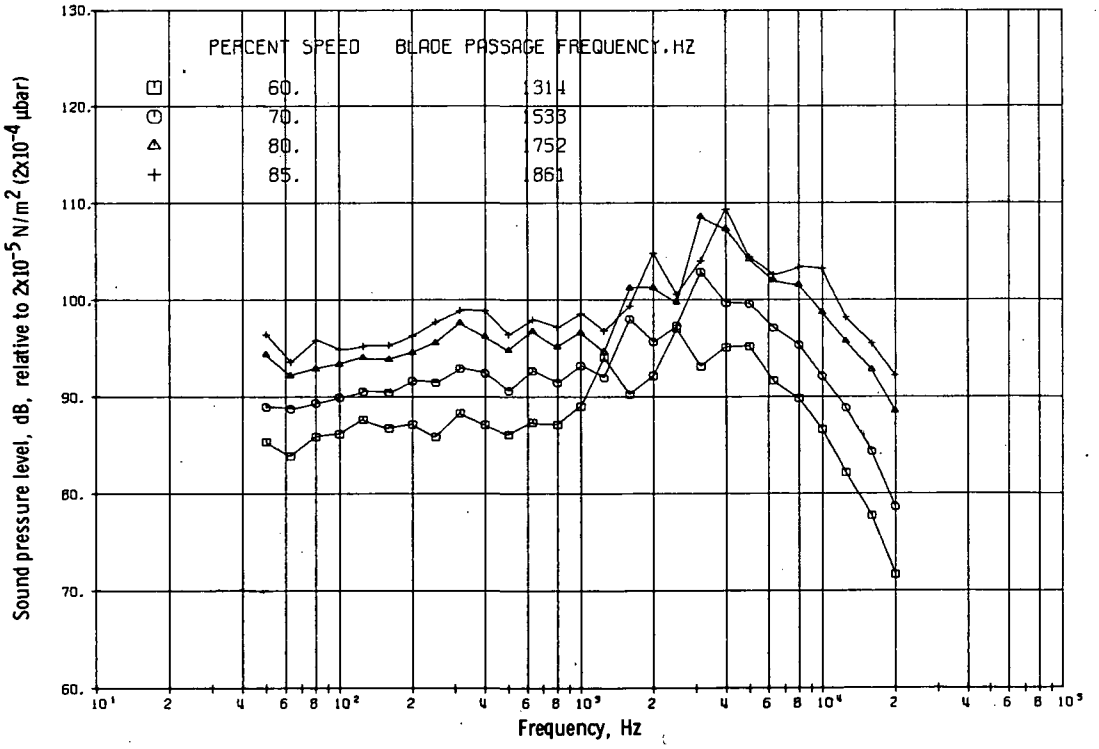

Figure 61. - Sound pressure levels with rotor-to-stator spacing of 1.65 chords, at 30.48-meter (100-ft) radius and 110^0 angular location.

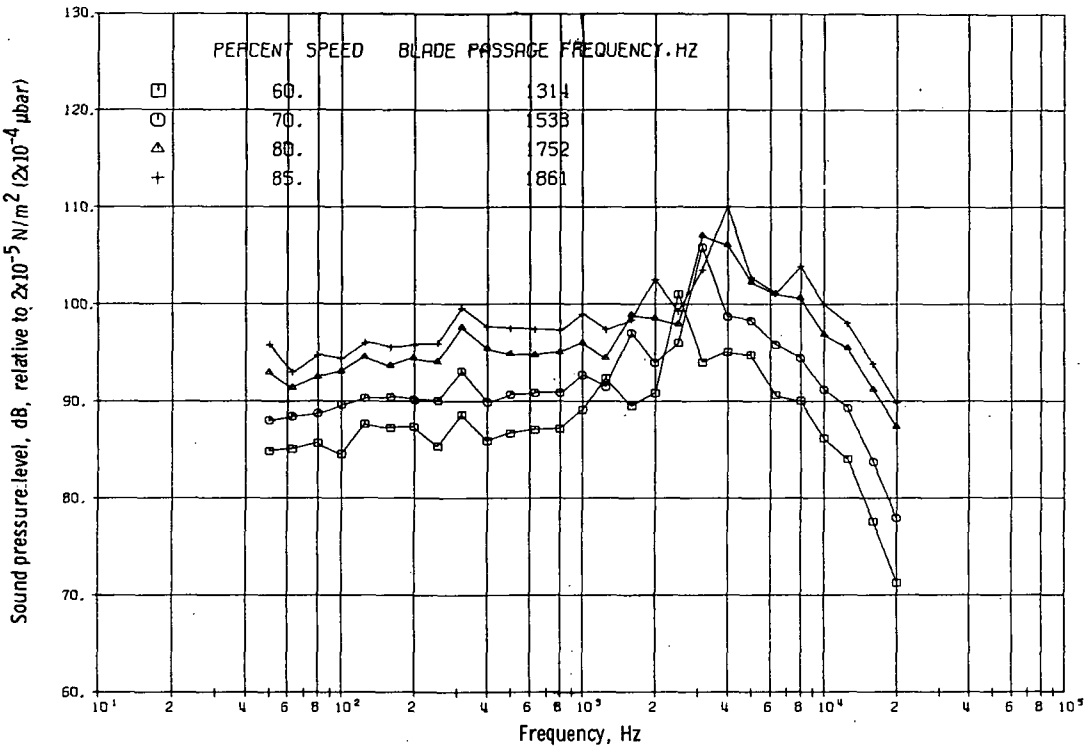

Figure 62. - Sound pressure levels with rotor-to-stator spacing of 1.65 chords, at 30.48-meter (100-ft) radius and 120° angular location.

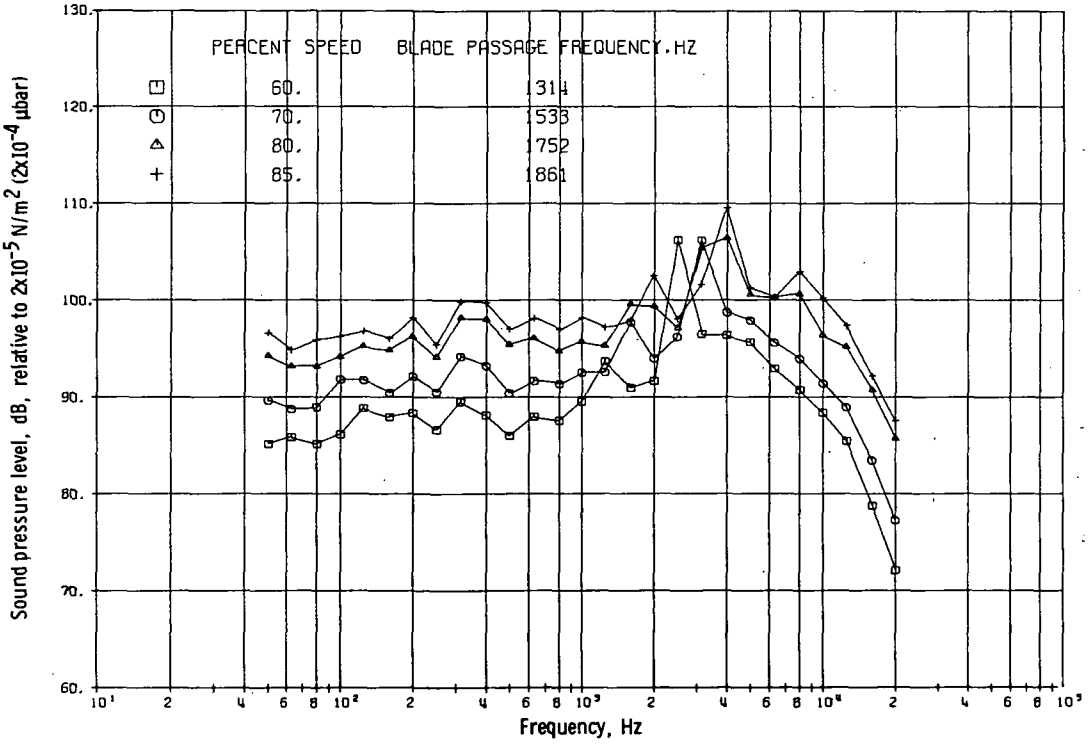

Figure 63. - Sound pressure levels with rotor-to-stator spacing of 1.65 chords, at 30.48-meter (100-ft) radius and 130° angular location.

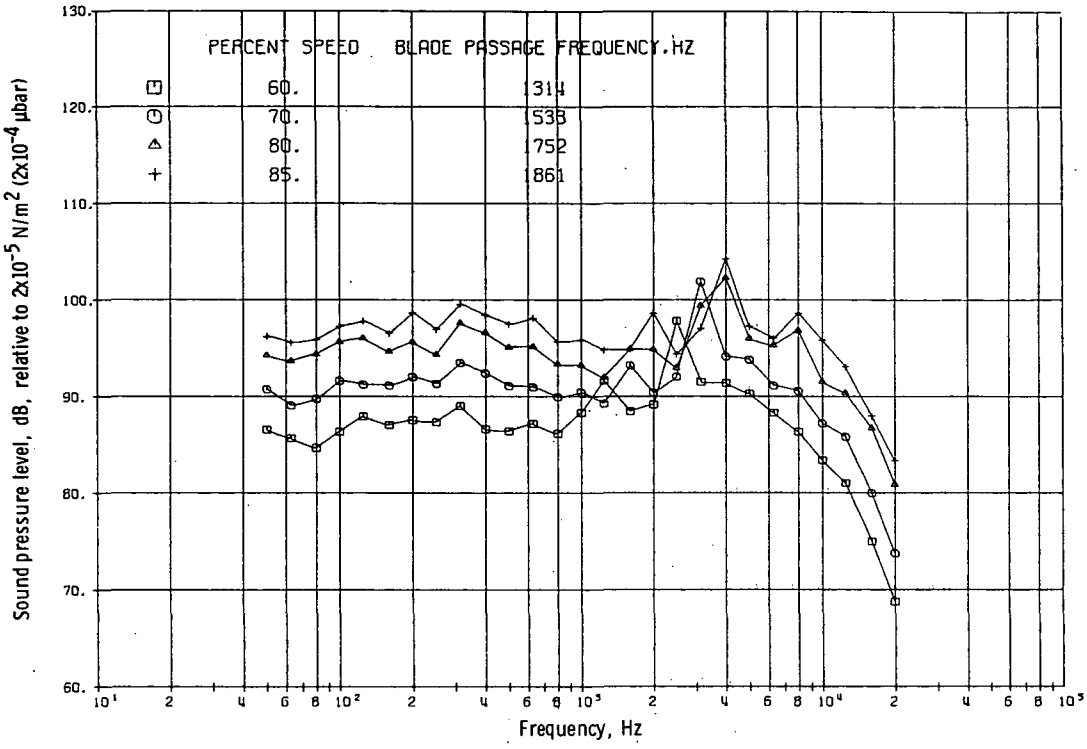

Figure 64. - Sound pressure levels with rotor-to-stator spacing of 1.65 chords, at 30.48-meter (100-ft) radius and 140^0 angular location.

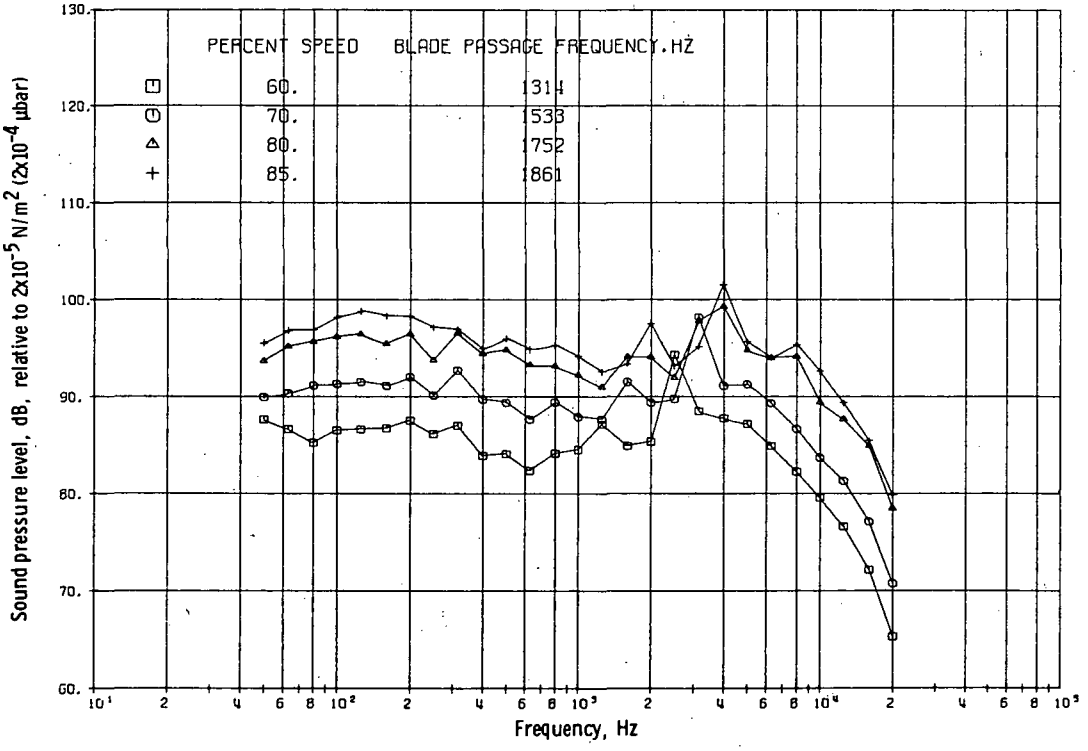

Figure 65. - Sound pressure levels with rotor-to-stator spacing of 1.65 chords, at 30.48-meter (100-ft) radius and 150^0 angular location.

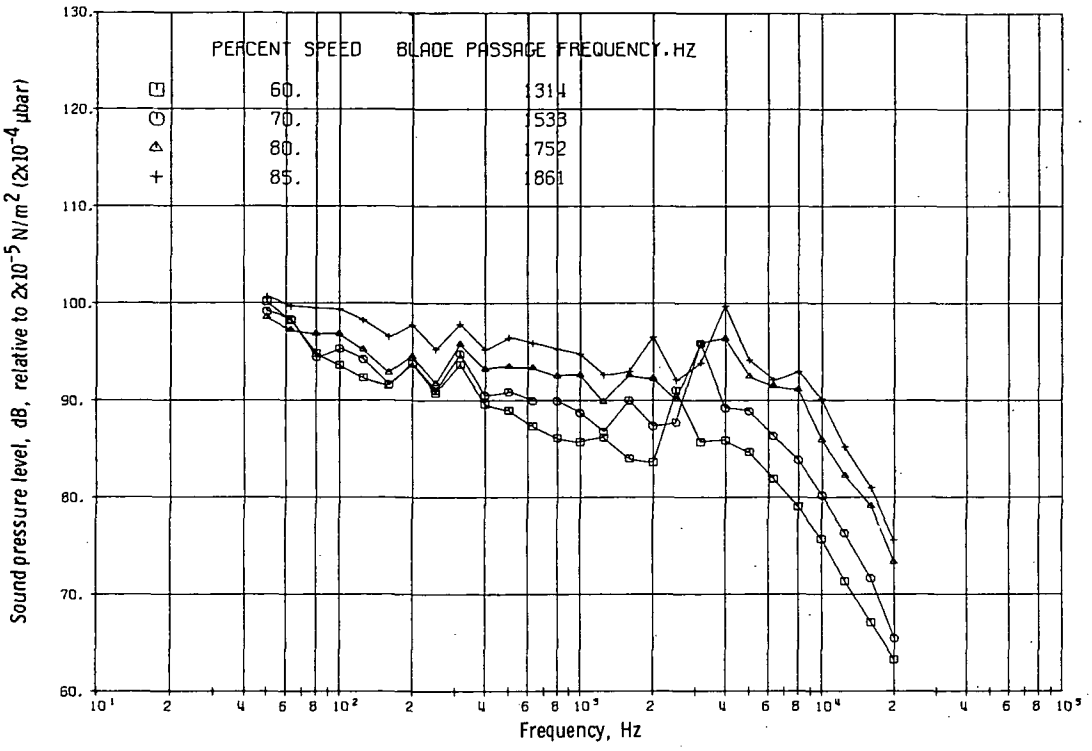

Figure 66. - Sound pressure levels with rotor-to-stator spacing of 1.65 chords, at 30.48-meter (100-ft) radius and 160^0 angular location.

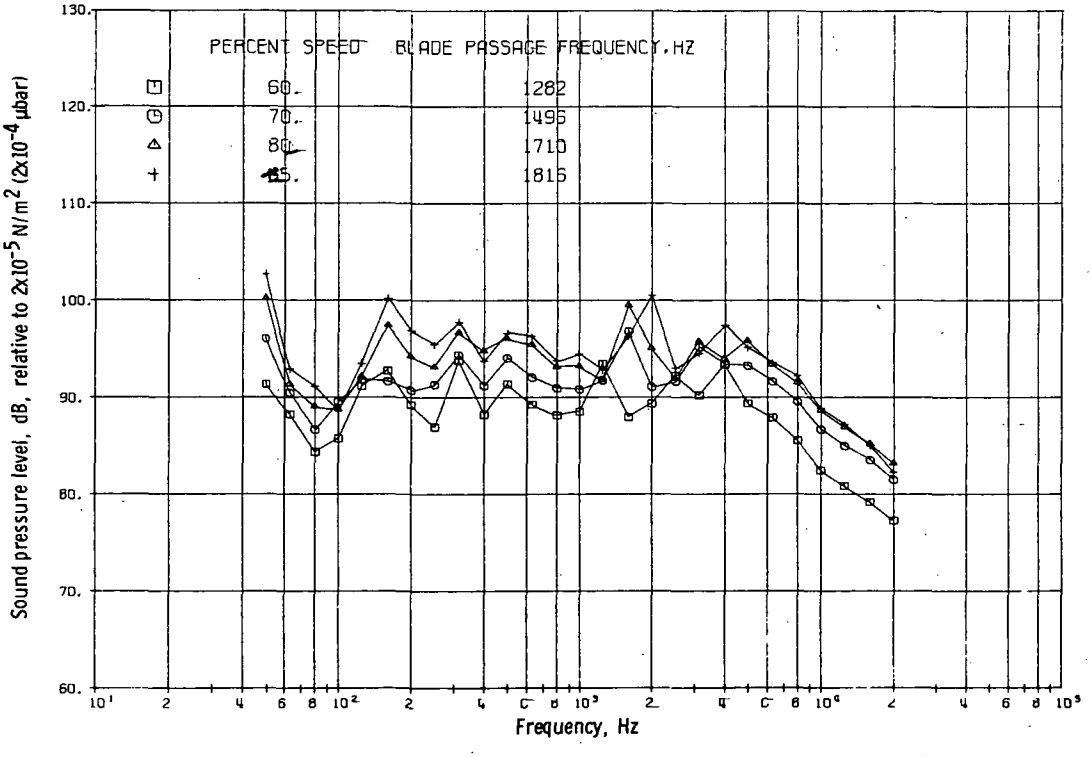

Figure 67. - Sound pressure levels with rotor-to-stator spacing of 2.27 chords, at 30.48-meter (100-ft) radius and 10^0 angular location.

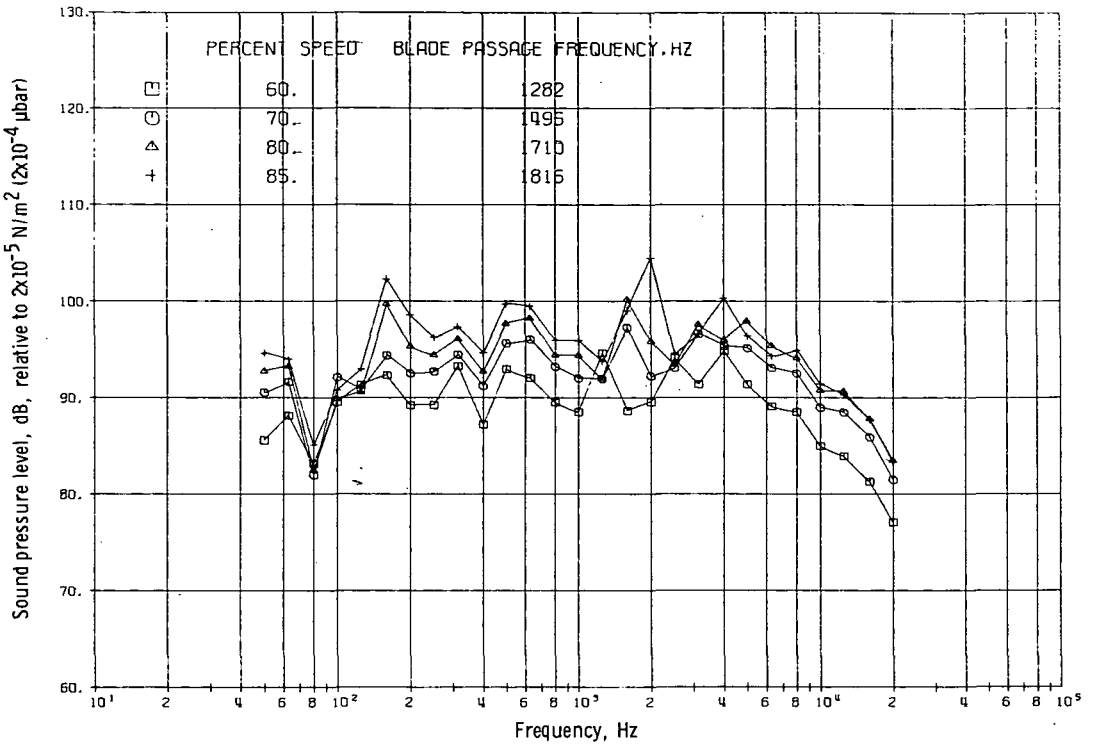

Figure 68. - Sound pressure levels with rotor-to-stator spacing of 2.27 chords, at 30.48-meter (100-ft) radius and 20^0 angular location.

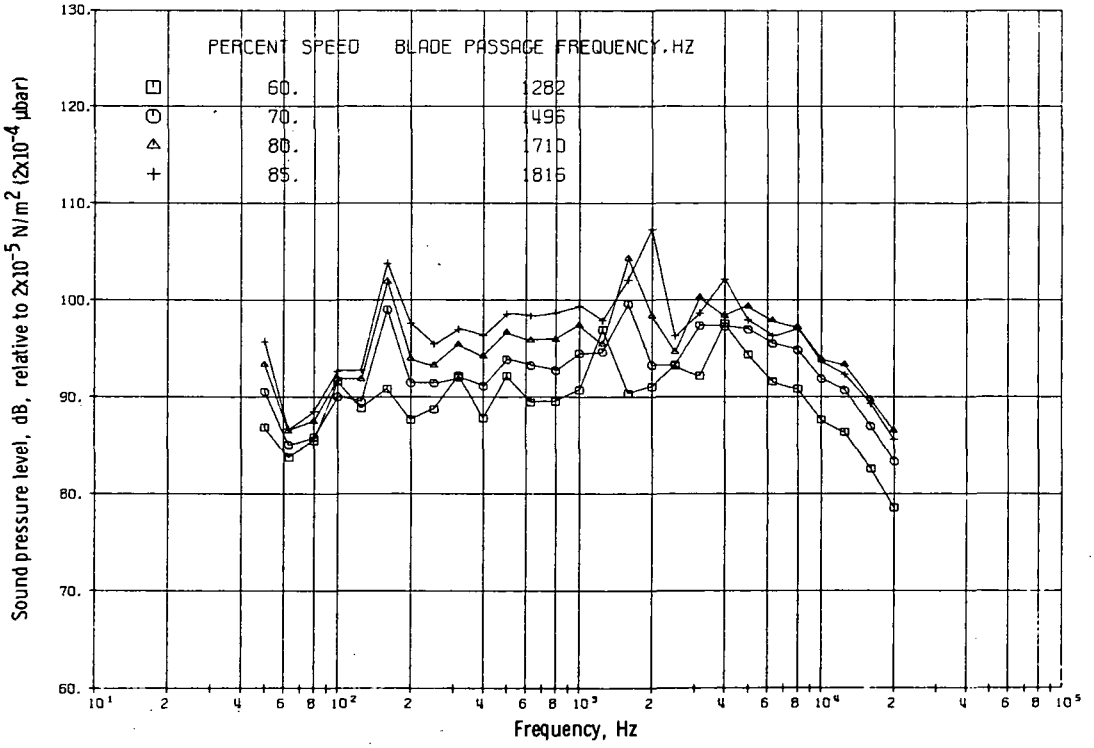

Figure 69. - Sound pressure levels with rotor-to-stator spacing of 2.27 chords, at 30.48-meter (100-ft) radius and 30^0 angular location.

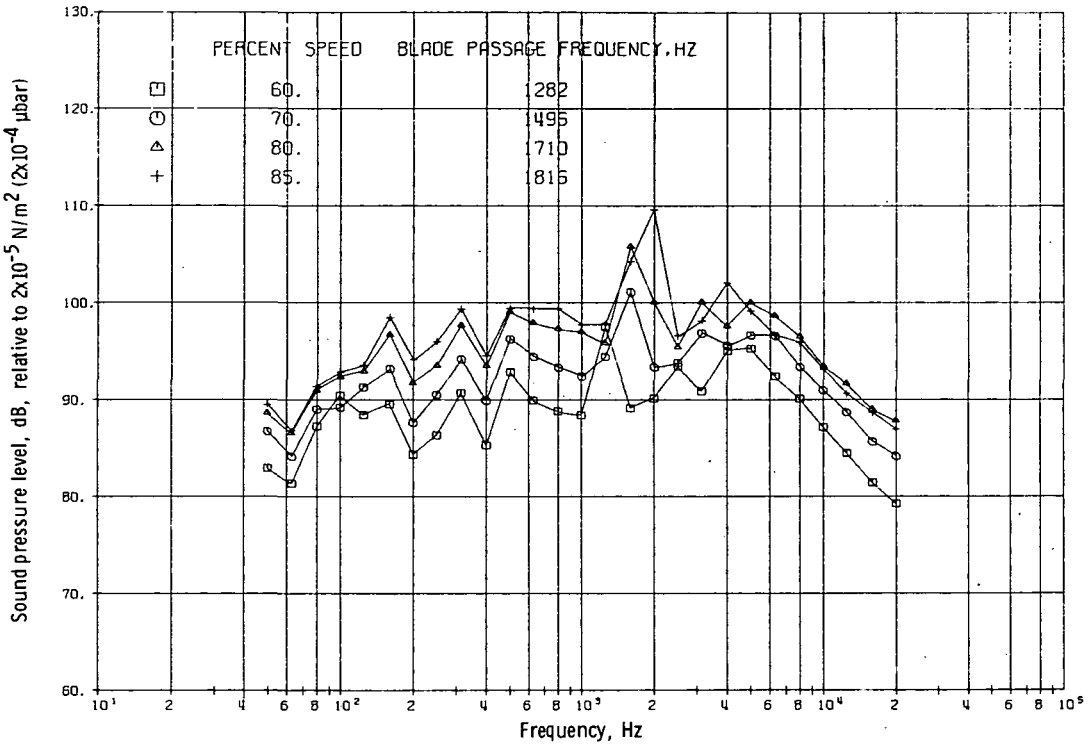

Figure 70. - Sound pressure levels with rotor-to-stator spacing of 2.27 chords, at 30.48-meter (100-ft) radius and 40° angular location.

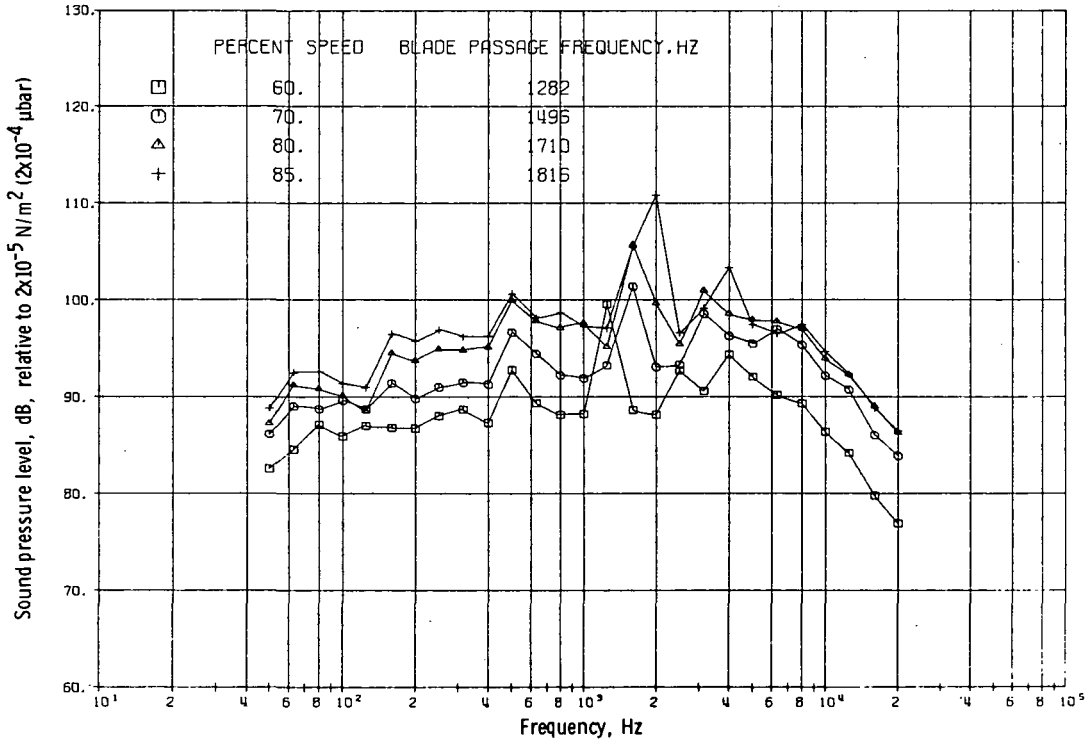

Figure 71. - Sound pressure levels with rotor-to-stator spacing of 2.27 chords, at 30.48-meter (100-ft) radius and 50° angular location.

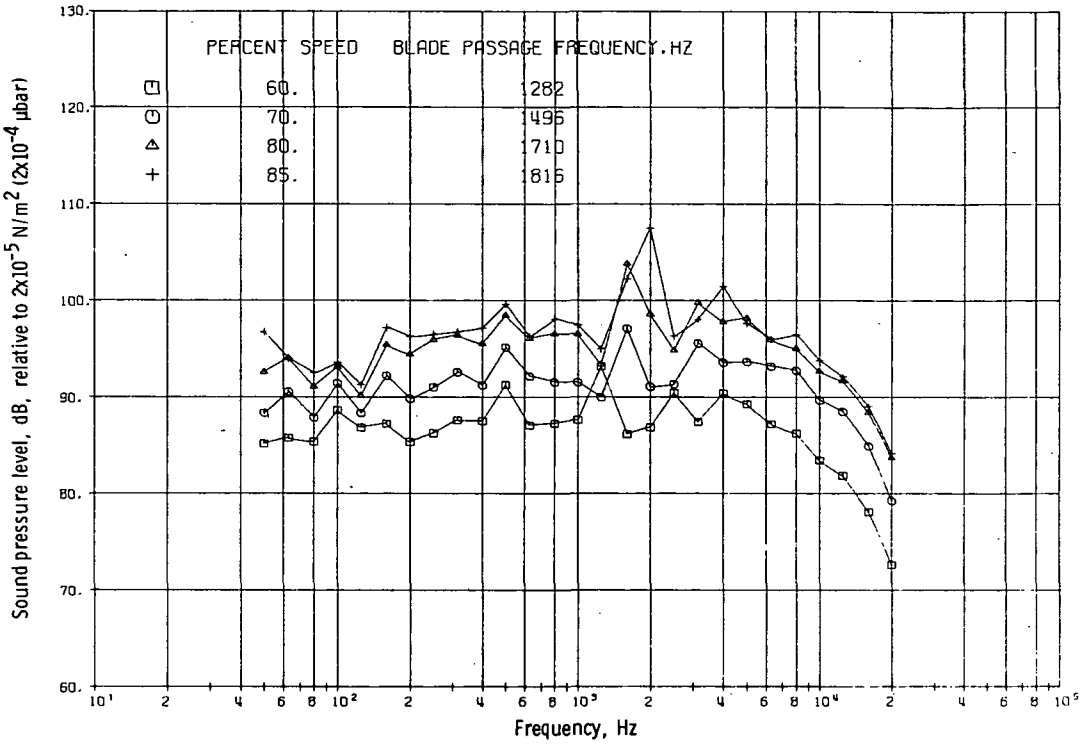

Figure 72. - Sound pressure levels with rotor-to-stator spacing of 2.27 chords, at 30.48-meter (100-ft) radius and 60^0 angular location.

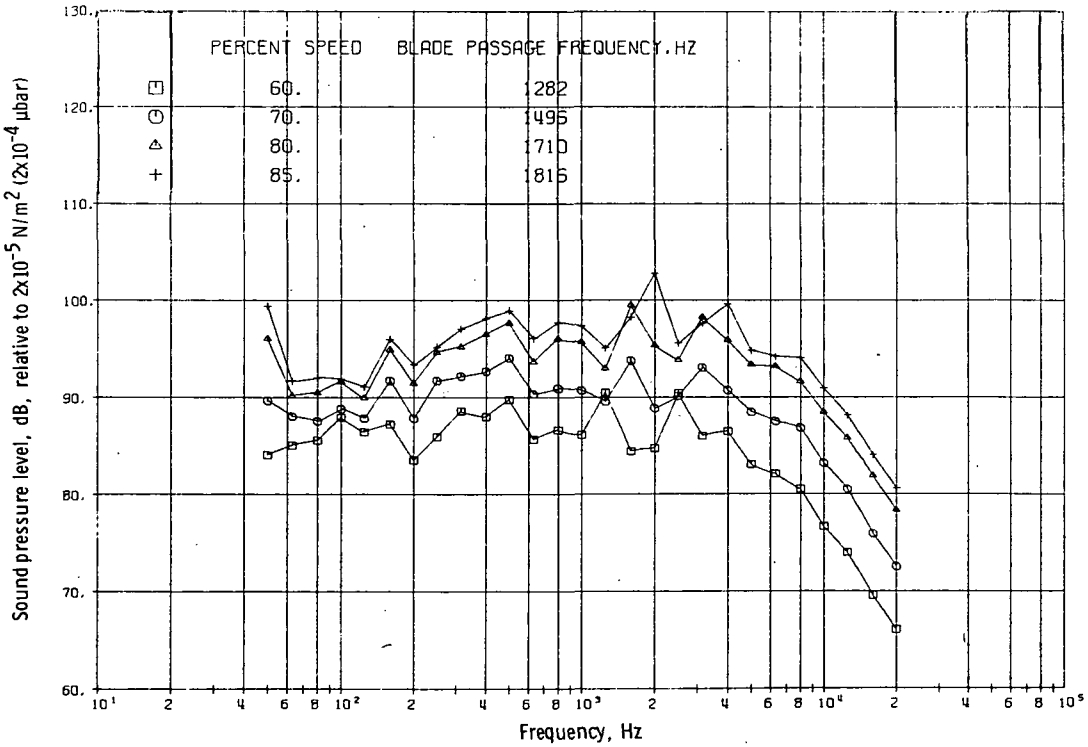

Figure 73. - Sound pressure levels with rotor-to-stator spacing of 2.27 chords, at 30.48-meter (100-ft) radius and 70^0 angular location.

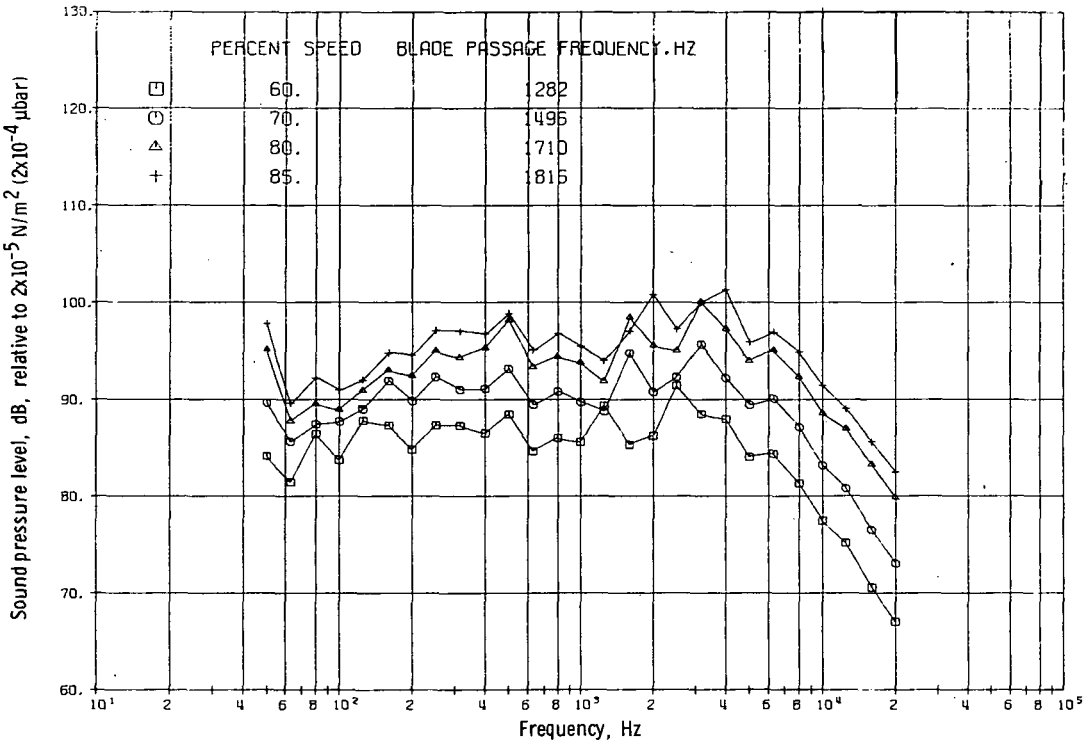

Figure 74. - Sound pressure levels with rotor-to-stator spacing of 2.27 chords, at 30.48-meter (100-ft) radius and 80^0 angular location.

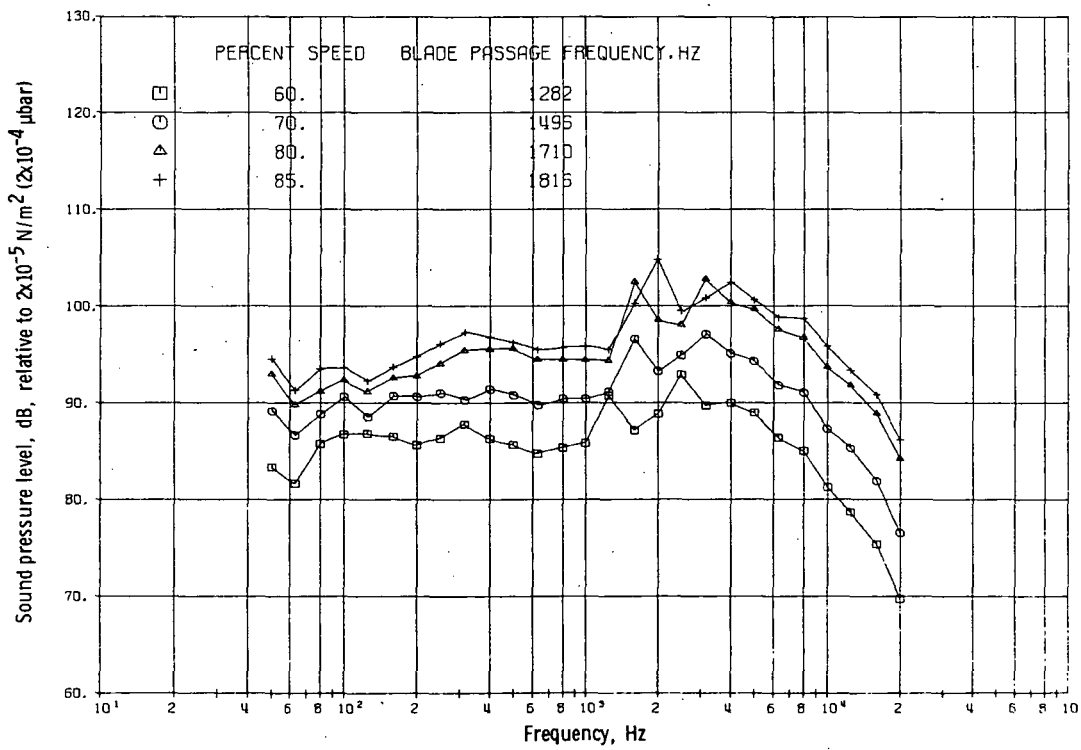

Figure 75. - Sound pressure levels with rotor-to-stator spacing of 2.27 chords, at 30.48-meter (100-ft) radius and 90^0 angular location.

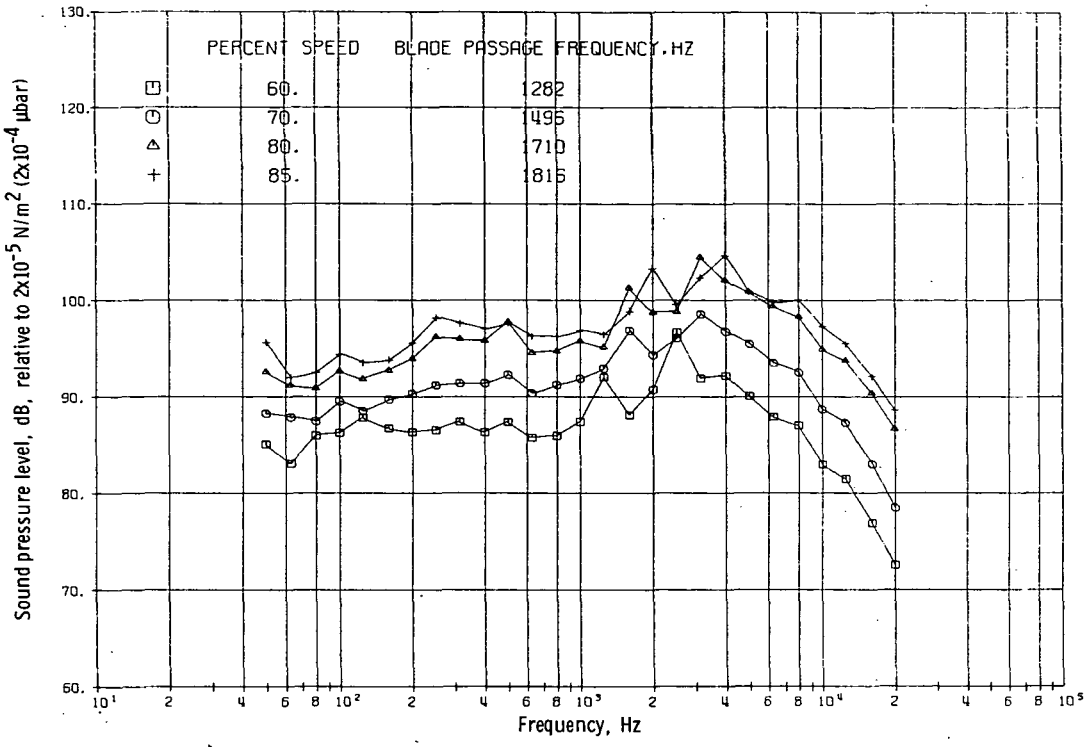

Figure 76. - Sound pressure levels with rotor-to-stator spacing of 2.27 chords, at 30.48-meter (100-ft) radius and 100^0 angular location.

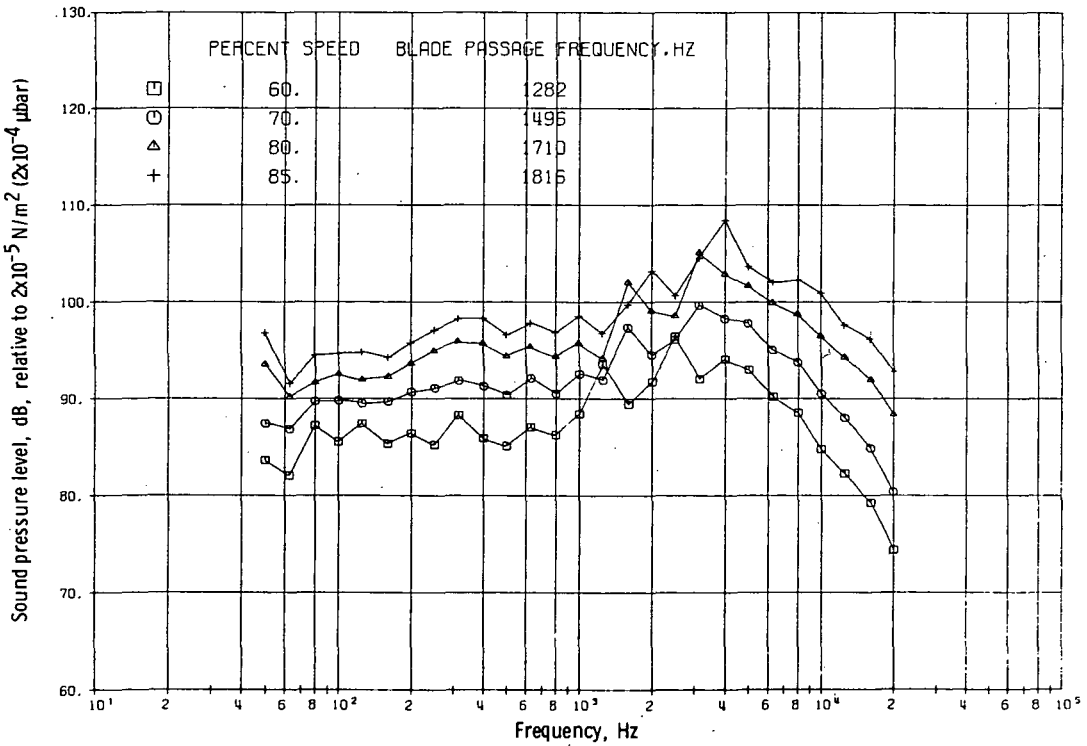

Figure 77. - Sound pressure levels with rotor-to-stator spacing of 2.27 chords, at 30.48-meter (100-ft) radius and 110^0 angular location.

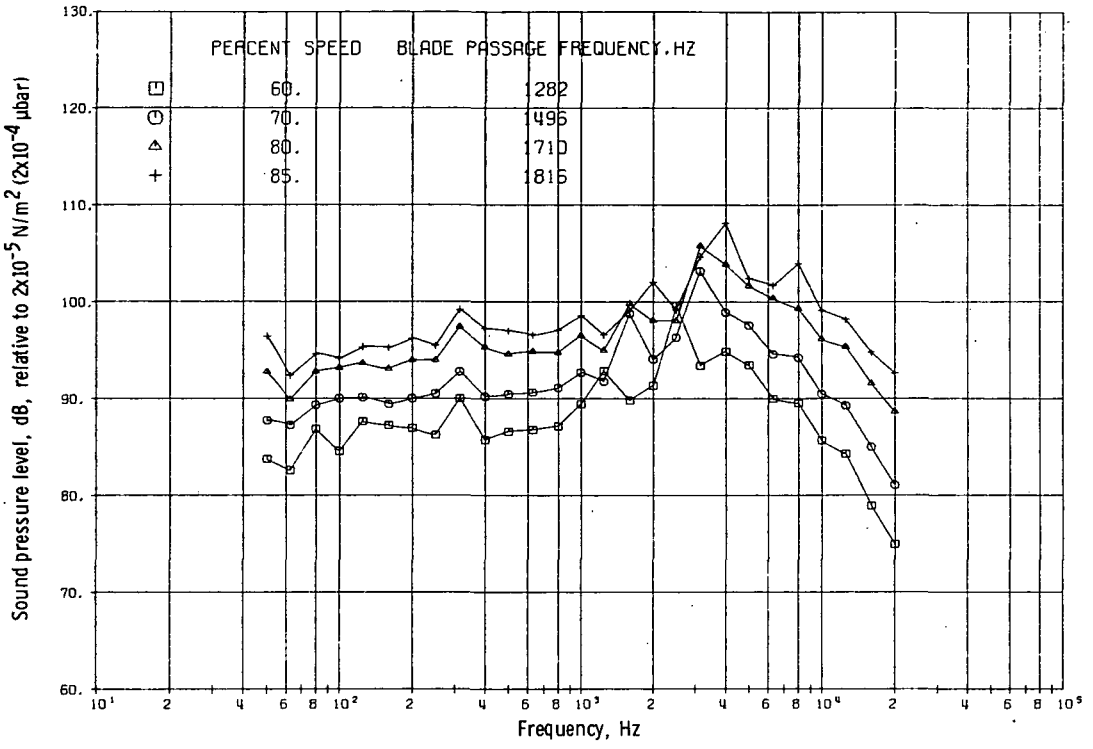

Figure 78. - Sound pressure levels with rotor-to-stator spacing of 2.27 chords, at 30.48-meter (100-ft) radius and 120^0 angular location.

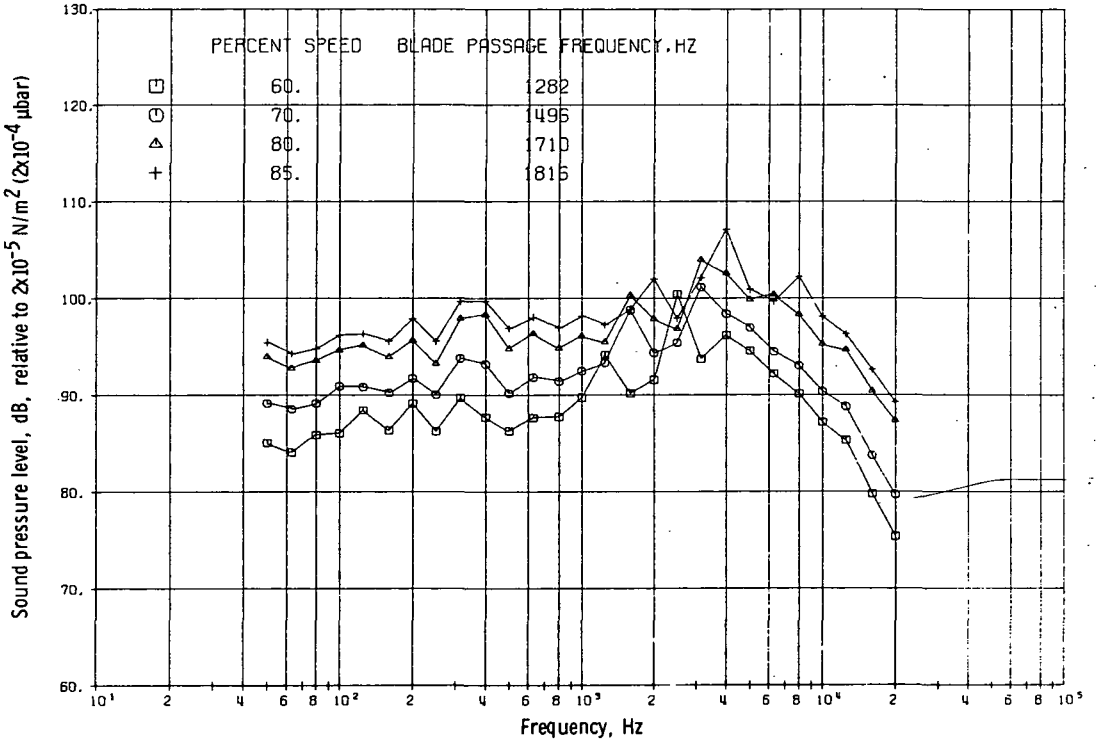

Figure 79. - Sound pressure levels with rotor-to-stator spacing of 2.27 chords, at 30.48-meter (100-ft) radius and 130^0 angular location.

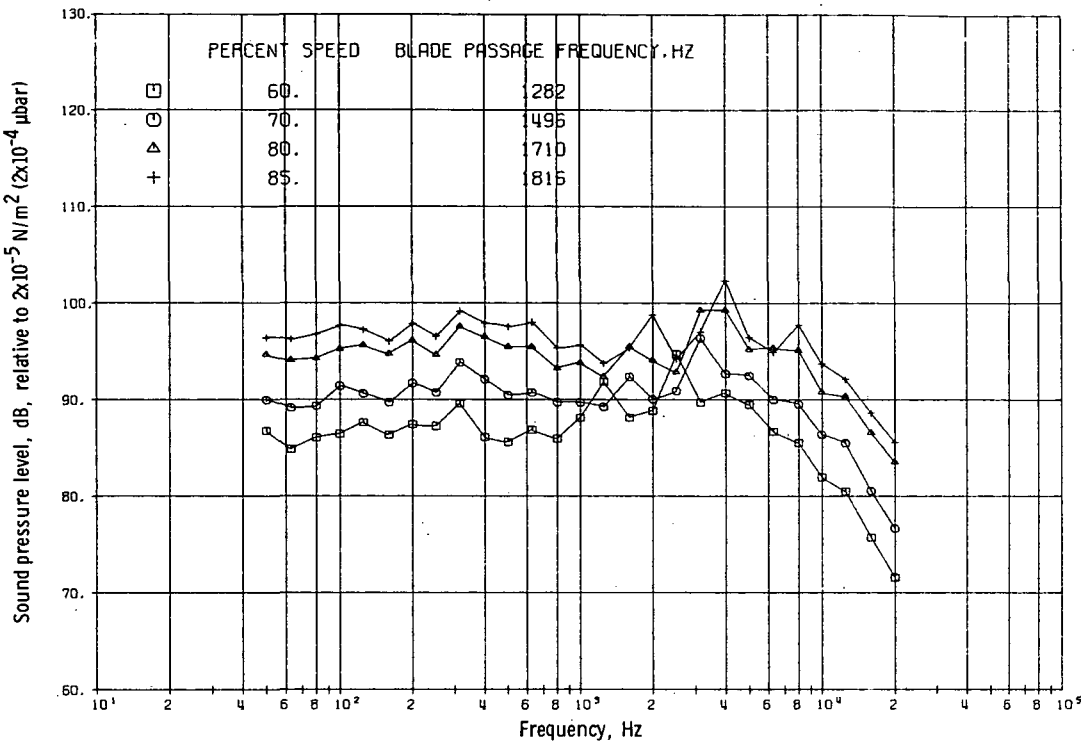

Figure 80. - Sound pressure levels with rotor-to-stator spacing of 2.27 chords, at 30.48-meter (100-ft) radius and 140^0 angular location.

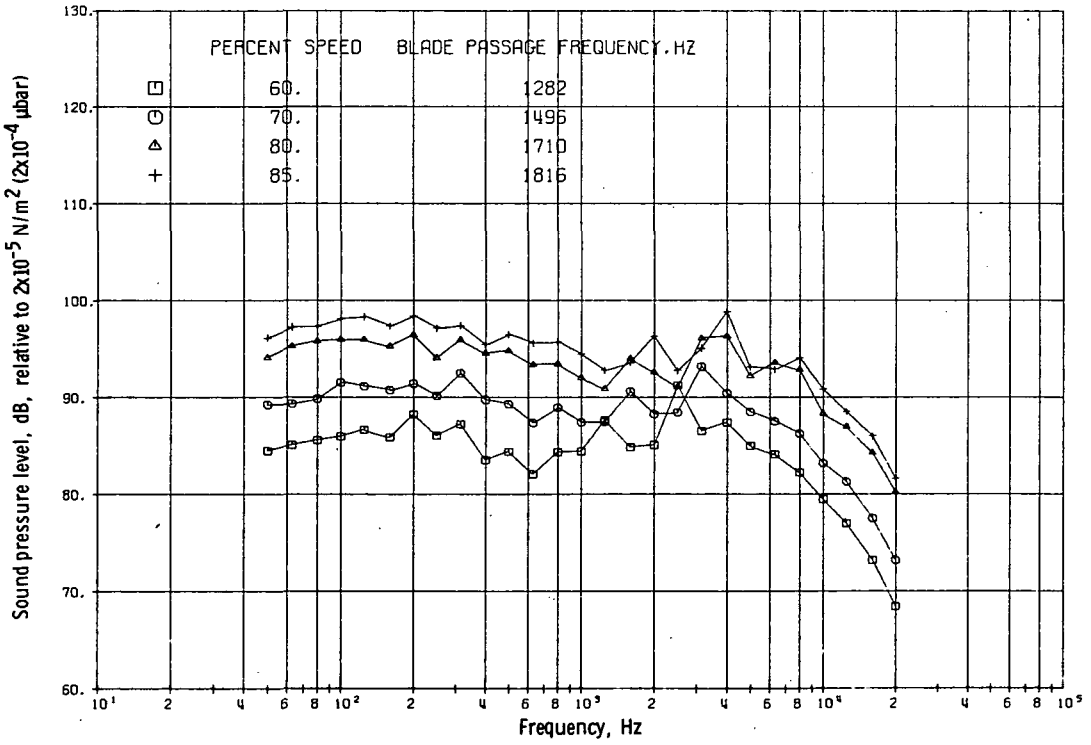

Figure 81. - Sound pressure levels with rotor-to-stator spacing of 2.27 chords, at 30.48-meter (100-ft) radius and 150^0 angular location.

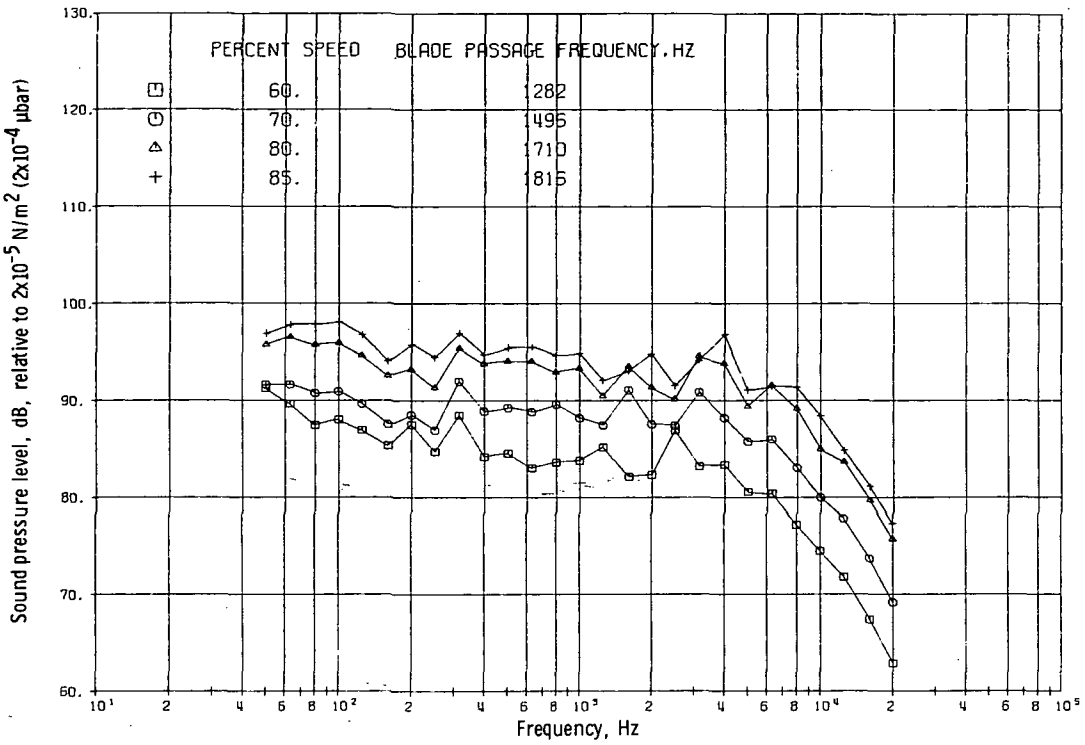

Figure 82. - Sound pressure levels with rotor-to-stator spacing of 2.27 chords, at 30.48-meter (100-ft) radius and 160° angular location.

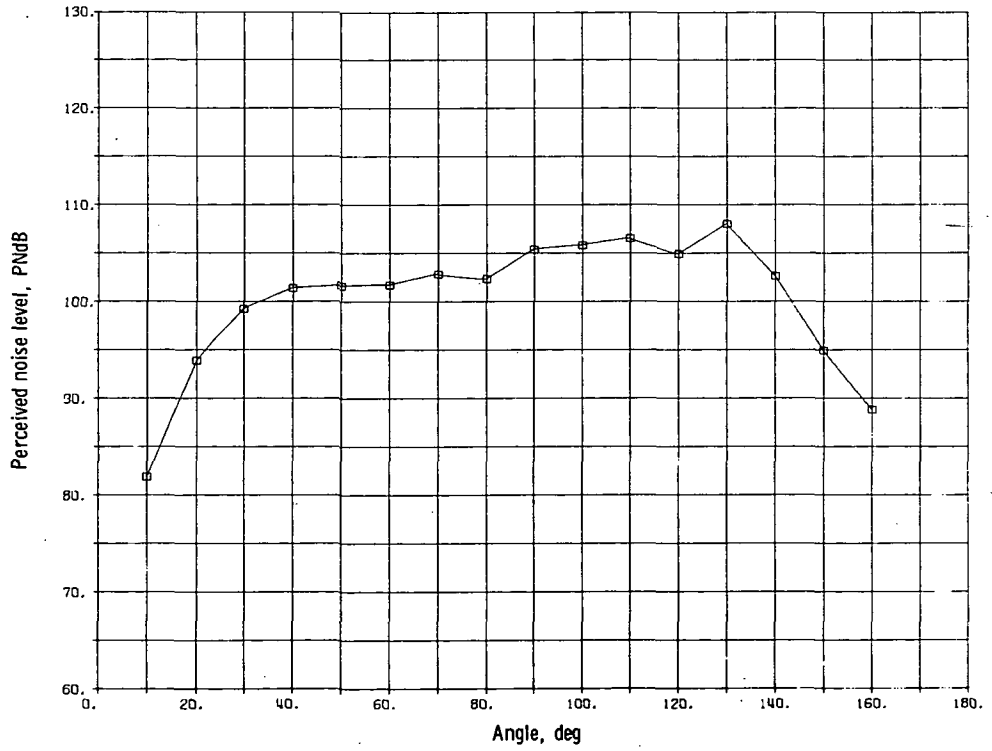

Figure 83. - Perceived noise level on 114.3-meter (375-ft) sideline. Rotor-to-stator spacing, 1.14 chords; speed, 60 percent; blade passage frequency, 1310 hertz.

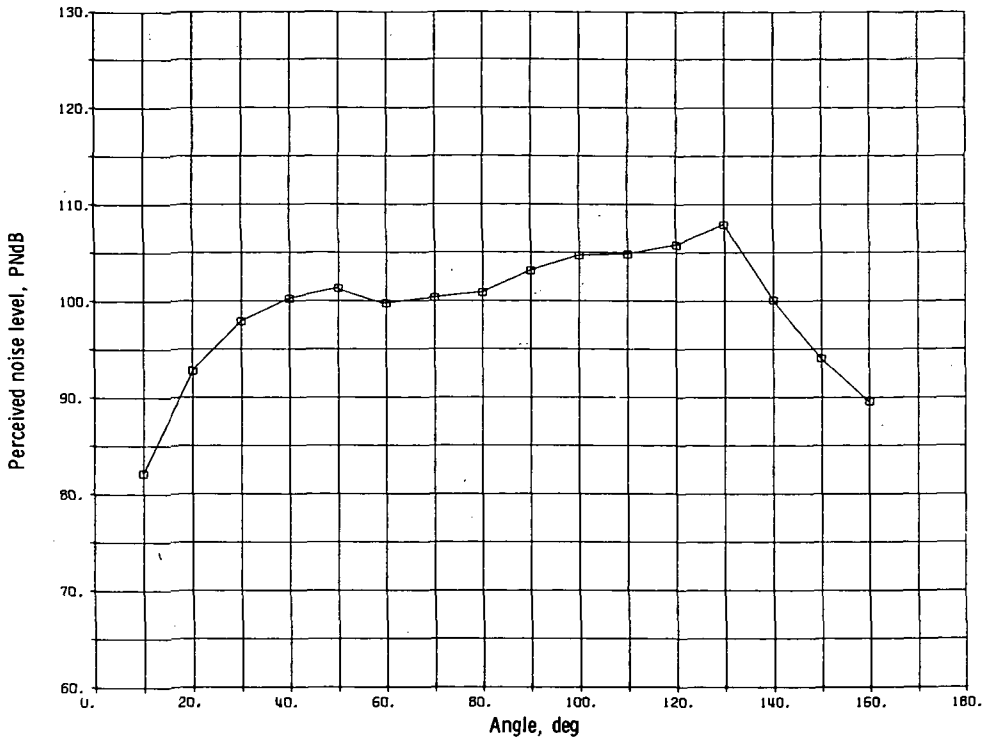

Figure 84. - Perceived noise level on 114.3-meter (375-ft) sideline. Rotor-to-stator spacing, 1.65 chords; speed, 60 percent; blade passage frequency, 1314 hertz.

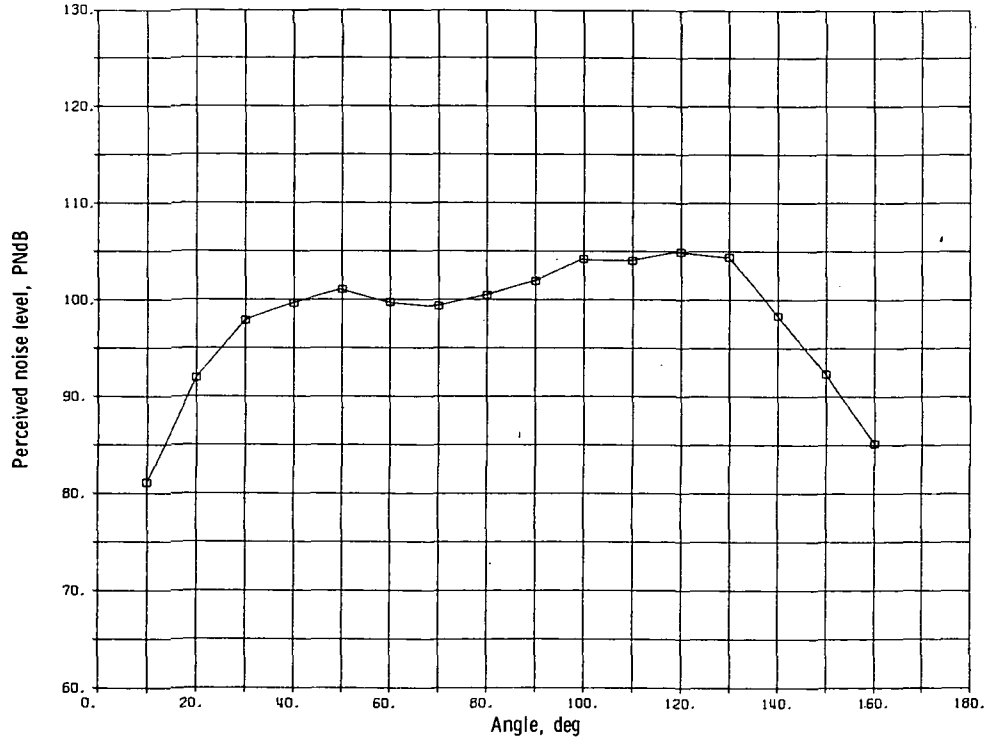

Figure 85. - Perceived noise level on 114.3-meter (375-ft) sideline. Rotor-to-stator spacing, 2.27 chords; speed, 60 percent; blade passage frequency, 1282 hertz.

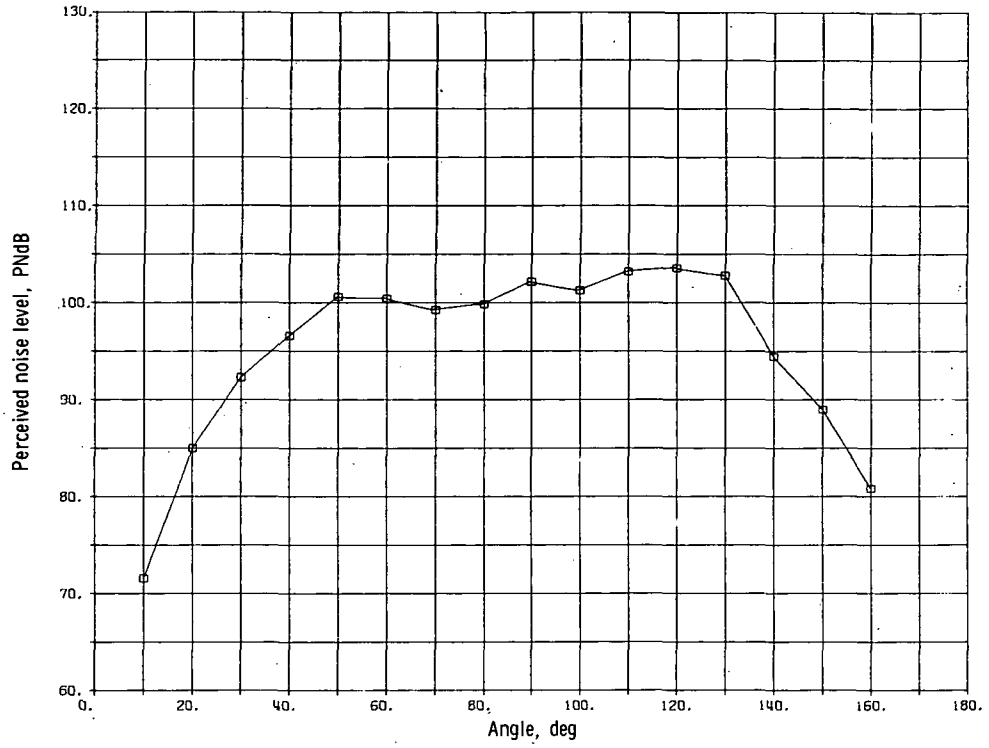

Figure 86. - Perceived noise level on 304.8-meter (1000-ft) sideline. Rotor-to-stator spacing, 1.14 chords; speed, 85 percent; blade passage frequency, 1856 hertz.

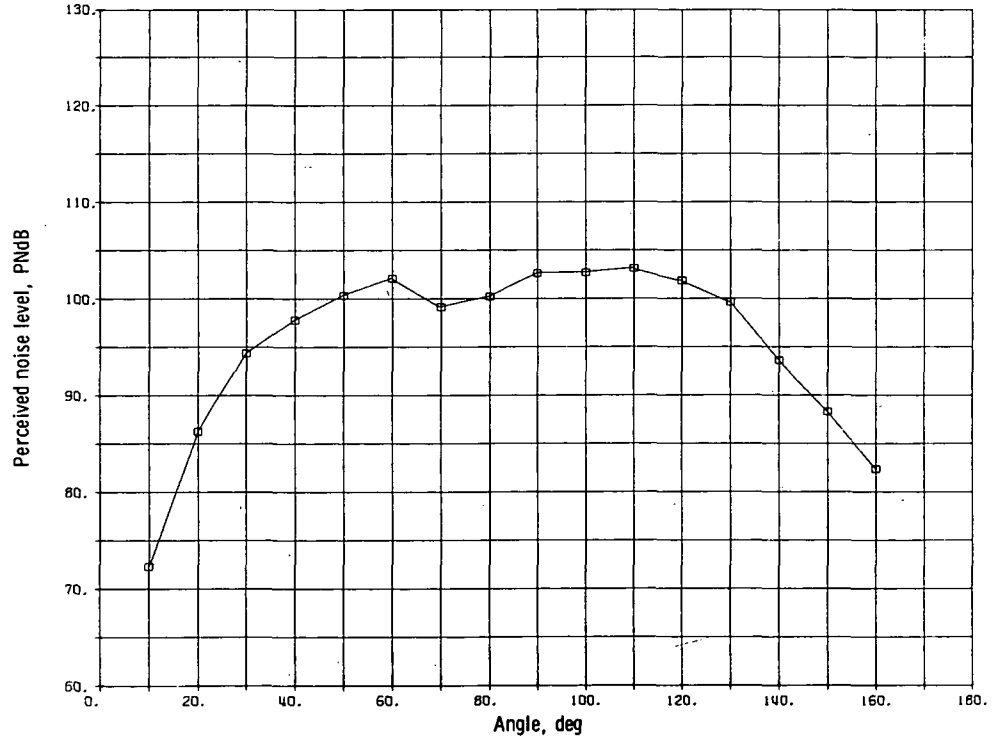

Figure 87. - Perceived noise level on 304.8-meter (1000-ft) sideline. Rotor-to-stator spacing, 1.65 chords; speed, 85 percent; blade passage frequency, 1861.

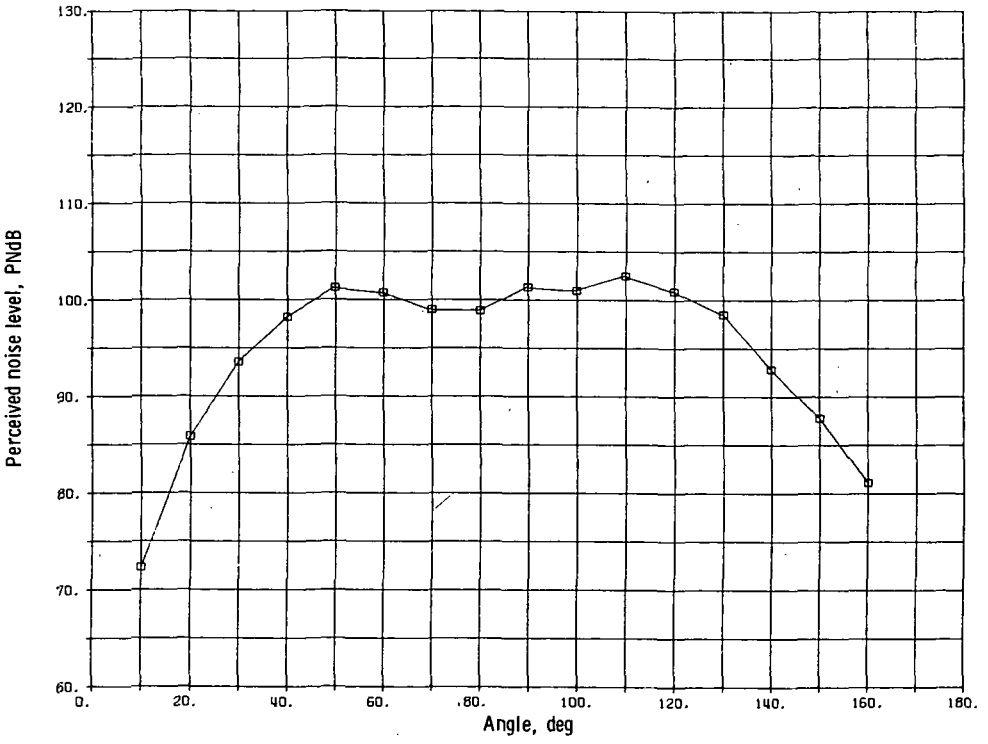

Figure 88. - Perceived noise level on 304.8-meter (1000-ft) sideline. Rotor-to-stator spacing, 2.27 chords; speed, 85 percent; blade passage frequency, 1816 hertz.

"The aeronautical and space activities of the United States shall be conducted so as to contribute . . . to the expansion of human knowledge of phenomena in the atmosphere and space. The Administration shall provide for the widest practicable and appropriate dissemination of information concerning its activities and the results thereof."

—NATIONAL AERONAUTICS AND SPACE ACT OF 1958

NASA SCIENTIFIC AND TECHNICAL PUBLICATIONS

TECHNICAL REPORTS: Scientific and technical information considered important, complete, and a lasting contribution to existing knowledge.

TECHNICAL NOTES: Information less broad in scope but nevertheless of importance as a contribution to existing knowledge.

TECHNICAL MEMORANDUMS: Information receiving limited distribution because of preliminary data, security classification, or other reasons. Also includes conference proceedings with either limited or unlimited distribution.

CONTRACTOR REPORTS: Scientific and technical information generated under a NASA contract or grant and considered an important contribution to existing knowledge.

TECHNICAL TRANSLATIONS: Information published in a foreign language considered to merit NASA distribution in English.

SPECIAL PUBLICATIONS: Information derived from or of value to NASA activities. Publications include final reports of major projects, monographs, data compilations, handbooks, sourcebooks, and special bibliographies.

TECHNOLOGY UTILIZATION PUBLICATIONS: Information on technology used by NASA that may be of particular interest in commercial and other non-aerospace applications. Publications include Tech Briefs, Technology Utilization Reports and Technology Surveys.

Details on the availability of these publications may be obtained from:

SCIENTIFIC AND TECHNICAL INFORMATION OFFICE

NATIONAL AERONAUTICS AND SPACE ADMINISTRATION

Washington, D.C. 20546